Search for supersymmetry in final states with disappearing tracks in proton-proton collisions at $\sqrt{s} = 13$ TeV

A. Hayrapetyan *et al.*[*]
(CMS Collaboration)

(Received 28 September 2023; accepted 14 February 2024; published 17 April 2024)

A search is presented for charged, long-lived supersymmetric particles in final states with one or more disappearing tracks. The search is based on data from proton-proton collisions at a center-of-mass energy of 13 TeV collected with the CMS detector at the CERN LHC between 2016 and 2018, corresponding to an integrated luminosity of 137 fb^{-1}. The search is performed over final states characterized by varying numbers of jets, *b*-tagged jets, electrons, and muons. The length of signal-candidate tracks in the plane perpendicular to the beam axis is used to characterize the lifetimes of wino- and Higgsino-like charginos produced in the context of the minimal supersymmetric standard model. The $\mathrm{d}E/\mathrm{d}x$ energy loss of signal-candidate tracks is used to increase the sensitivity to charginos with a large mass and thus a small Lorentz boost. The observed results are found to be statistically consistent with the background-only hypothesis. Limits on the pair-production cross section of gluinos and squarks are presented in the framework of simplified models of supersymmetric particle production and decay, and for electroweakino production based on models of wino and Higgsino dark matter. The limits presented are the most stringent to date for scenarios with light third-generation squarks and a wino- or Higgsino-like dark matter candidate capable of explaining the observed dark matter relic density.

DOI: 10.1103/PhysRevD.109.072007

I. INTRODUCTION

Supersymmetry (SUSY) [1–9], a well-motivated extension of the standard model (SM) of particle physics, addresses open questions of the SM such as dark matter (DM) [10,11] and the fine-tuning [12–14] of the electroweak sector. Studies from the ATLAS [15] and CMS [16] Collaborations at the CERN LHC have placed significant constraints on the minimal supersymmetric SM (MSSM), with no direct evidence as yet for the existence of SUSY particles. Nonetheless, important regions of the MSSM parameter space remain unexplored, such as regions with a nearly pure wino- or Higgsino-like lightest supersymmetric particle (LSP) that are consistent with the observed DM relic density [17].

A DM candidate can arise in SUSY if the LSP is stable, as occurs in models with *R*-parity [7,18] conservation. In viable realizations of the *R*-parity conserving MSSM, the LSP is a stable neutralino $\tilde{\chi}_1^0$, namely, an electroweakino mass eigenstate composed of a mixture of bino, wino, and Higgsino states. To be consistent with the observed DM relic density, a nearly pure wino (Higgsino) LSP must have a mass of approximately 2 (1) TeV in such realizations [19]. The constraint arises from the value of the coannihilation cross section required to sufficiently reduce the DM content of the early Universe before thermal freeze-out [20,21]. The coannihilation cross section depends on the masses of the LSP and its coannihilation partner. For a pure wino- or Higgsino-like LSP, this partner is a chargino $\tilde{\chi}_1^\pm$ that is nearly degenerate in mass with the LSP, having a mass only a few hundred MeV larger. Because of the limited kinematic phase space in $\tilde{\chi}_1^\pm \to \tilde{\chi}_1^0 \pi^\pm$ decays, the $\tilde{\chi}_1^\pm$ then has a macroscopic lifetime, with a decay length at the LHC on the order of several centimeters or more.

Long-lived charginos associated with pure wino or Higgsino DM give rise to the distinctive experimental signature known as a disappearing track (DTk). In $\tilde{\chi}_1^\pm \to \tilde{\chi}_1^0 \pi^\pm$ decays, the resulting pion has a momentum of only a few hundred MeV, too low, in general, for it to be reconstructed. The $\tilde{\chi}_1^0$ in these decays escapes undetected with most of the momentum. The chargino is reconstructed as a track with hits up to its point of decay, beyond which no hits or associated signals are recorded. This leads to the DTk signature in which a reconstructed track emanating from the beam collision region ends abruptly within the sensitive tracking volume, with a continuation that has "disappeared." The DTk signature has been used in recent searches to set the most stringent chargino mass limits to

[*]Full author list given at the end of the article.

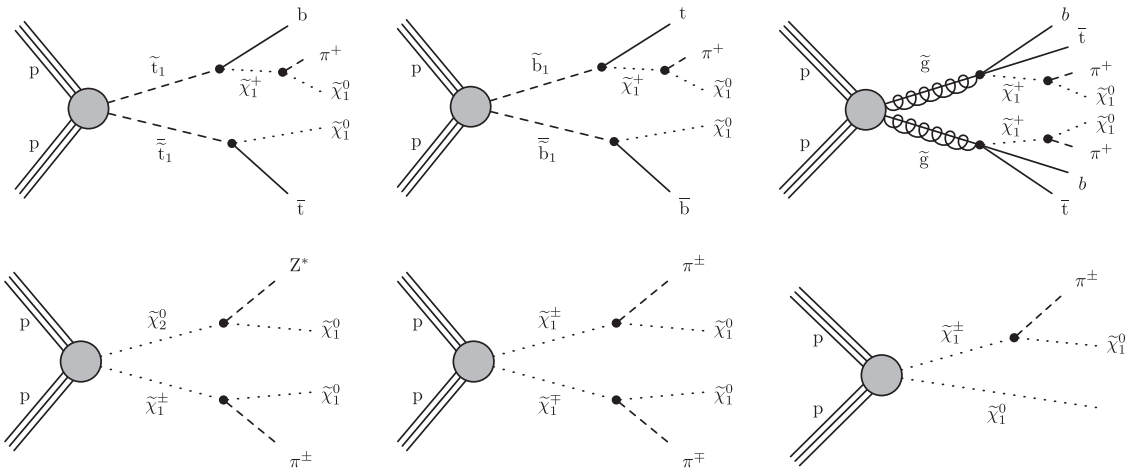

FIG. 1. Representative diagrams for the simplified models considered in this analysis. From left to right: T6btLL, T6tbLL, and T5btbtLL (upper); and TChiWZ, TChiWW, and TChiW (lower). The shaded circles at the production vertices represent a sum over perturbative terms.

date for certain scenarios, e.g., wino or Higgsino LSP scenarios with minimal neutralino mixing [22–24].

This paper presents a search for long-lived charginos, probing a comprehensive set of final states relevant to the R-parity conserving MSSM. The analysis is based on a sample of proton-proton (pp) collision events collected at center-of-mass energy $\sqrt{s} = 13$ TeV with the CMS detector in 2016–2018, corresponding to an integrated luminosity of 137 fb^{-1}. It expands on previous searches [22,23] by introducing electron + DTk and muon + DTk channels, by reanalyzing the fully hadronic channel, and by making use of a machine-learning-based track classification method to improve the DTk selection efficiency and background rejection. The addition of the electron + DTk and muon + DTk channels increases sensitivity to new-physics scenarios with leptonic final states. Additional sensitivity to high-mass LSP states is achieved by employing a measure of the $\mathrm{d}E/\mathrm{d}x$ ionization energy loss of signal-candidate tracks, which takes large values for candidates with a small Lorentz boost. The analysis targets both the electroweak and strong production mechanisms, making use of jet and b-tagged jet multiplicities to distinguish between different production modes and decay chains. The incorporation of new final states and observables improves the sensitivity to relatively unexplored regions of the MSSM, including scenarios with pure wino or Higgsino DM with masses of 1 TeV or larger, or with light third-generation squarks that yield leptons in the final state.

This paper is structured as follows. The signal models considered for the analysis are presented in Sec. II. The CMS detector is described in Sec. III and the event reconstruction in Sec. IV. Section V discusses the simulated event samples used in the study. The DTk selection procedure is presented in Sec. VI and the definition of the search regions (SRs) in Sec. VII. The methods used to estimate SM backgrounds are presented in Sec. VIII. Systematic uncertainties are discussed in Sec. IX. The results and summary are presented in Secs. X and XI, respectively. Tabulated results for the study are provided in the HEPData record for this analysis [25].

II. SIMPLIFIED SIGNAL MODELS

A number of simplified models of SUSY [26–28] are used to survey and characterize the sensitivity of the search. These models, depicted by representative production diagrams in Fig. 1 and summarized in Table I, are effective-Lagrangian descriptions defined by the SUSY particle

TABLE I. Overview of the simplified models of supersymmetry considered in this analysis.

Model name	Description	Processes
T6btLL	Top squark associated $\tilde{\chi}_1^\pm$ production	$\tilde{t}\bar{\tilde{t}}$; $\tilde{t} \to t\tilde{\chi}_1^0$, $\tilde{t} \to b\tilde{\chi}_1^\pm$
T6tbLL	Bottom squark associated $\tilde{\chi}_1^\pm$ production	$\tilde{b}\bar{\tilde{b}}$; $\tilde{b} \to b\tilde{\chi}_1^0$, $\tilde{b} \to t\tilde{\chi}_1^\pm$
T5btbtLL	Gluino associated $\tilde{\chi}_1^\pm$ production	$\tilde{g}\tilde{g}$; $\tilde{g} \to b\bar{b}\tilde{\chi}_1^0$, $t\bar{t}\tilde{\chi}_1^0$, $tb\tilde{\chi}_1^-$, $\bar{t}b\tilde{\chi}_1^+$
TChiWZ	Electroweakino production for wino or Higgsino LSP	$\tilde{\chi}_2^0\tilde{\chi}_1^\pm$; $\tilde{\chi}_2^0 \to Z^*\tilde{\chi}_1^0$, $\tilde{\chi}_1^\pm \to \tilde{\chi}_1^0\pi^\pm$
TChiWW		$\tilde{\chi}_1^+\tilde{\chi}_1^-$; $\tilde{\chi}_1^\pm \to \tilde{\chi}_1^0\pi^\pm$
TChiW		$\tilde{\chi}_1^\pm\tilde{\chi}_1^0$; $\tilde{\chi}_1^\pm \to \tilde{\chi}_1^0\pi^\pm$, $\tilde{\chi}_1^0$

masses and the production and decay processes. A simplified model focuses on a specific small set of particles and interactions, with all other new-physics particles considered to be irrelevant to that particular process. One model, denoted T6btLL, features top squark pair production in which the top squark decays as $\tilde{t} \to t\tilde{\chi}_1^0$ and $\tilde{t} \to b\tilde{\chi}_1^{\pm}$, each with 50% probability. An analogous model with bottom squark production is labeled T6tbLL. A third model, denoted T5btbtLL, features gluino pair production in which the gluino decays as $\tilde{g} \to b\bar{b}\tilde{\chi}_1^0$, $t\bar{t}\tilde{\chi}_1^0$, $tb\tilde{\chi}_1^-$, or $tb\tilde{\chi}_1^+$, each with 25% probability. Various proper decay lengths $c\tau$ of the chargino are considered. For the models with gluino and squark pair production, we focus on a benchmark model with $c\tau = 10$ cm, corresponding roughly to pure wino and Higgsino-like states. We also consider a model with $c\tau = 200$ cm, which can be realized in a scenario with a binolike LSP and a wino coannihilation partner. The chargino and LSP are required to be mass degenerate within a few hundred MeV. We set this mass difference to 180 MeV. This choice has no direct impact on the acceptance because the decay products of the chargino are not reconstructed.

Sensitivity to the direct production of either a nearly pure wino DM candidate or a nearly pure Higgsino DM candidate is considered through the topologies denoted TChiWZ, TChiWW, and TChiW. The $\tilde{\chi}_2^0$ particle depicted for the TChiWZ diagram [Fig. 1 (lower left)] is the second lightest neutralino, only present in the Higgsino scenario. Relationships among the electroweakino masses, the $\tilde{\chi}_1^{\pm}$ lifetime, and the $\tilde{\chi}_1^{\pm}$ decay width are constrained by radiative corrections that account for a large difference between the LSP mass and the SUSY-breaking scale. They are characterized in Refs. [29,30] for the wino scenario and in Refs. [31,32] for the Higgsino scenario. The mass difference $\Delta m^0 = \Delta m(\tilde{\chi}_2^0, \tilde{\chi}_1^0)$ between the two neutral states is taken to be twice the mass difference $\Delta m^{\pm} = \Delta m(\tilde{\chi}_1^{\pm}, \tilde{\chi}_1^0)$ between the charged and lightest states. This choice corresponds to large $\tan\beta$, where $\tan\beta$ is the ratio of the vacuum expectation values of the neutral components of the two Higgs doublets in the MSSM [33]. The lifetime of the $\tilde{\chi}_2^0$, while not directly relevant for this study, is taken from a tree-level calculation based on the program SUSYHIT 1.5a [34]. The free parameters of the model are $\Delta m^{\pm}$ and the chargino mass $m_{\tilde{\chi}_1^{\pm}}$.

III. THE CMS DETECTOR AND ANALYSIS TRIGGERS

The CMS detector is structured around a cylindrical superconducting solenoid with an inner diameter of 6 m. The solenoid provides a nearly uniform 3.8 T magnetic field within its volume. This volume contains a number of nested particle detectors: from the innermost region outward, a silicon pixel and strip tracking detector, a lead tungstate crystal electromagnetic calorimeter (ECAL), and a brass and scintillator hadron calorimeter (HCAL). The ECAL and HCAL, each composed of a barrel and two end cap sections, cover the pseudorapidity range $|\eta| < 3.0$. Forward calorimeters extend the coverage to $3.0 < |\eta| < 5.2$. Muons are measured with gas-ionization detectors embedded in a steel flux-return yoke outside the solenoid, allowing muon reconstruction within $|\eta| < 2.4$. The CMS components taken together provide a nearly hermetic detector, permitting accurate measurements of the missing transverse momentum $p_{\mathrm{T}}^{\mathrm{miss}}$.

The tracking detector is of special importance for this analysis. The tracker consists of an inner pixel detector and an outer strip detector. The tracker used for the 2016 data-taking period, referred to as the "phase-0" tracker, measured particles within $|\eta| < 2.5$. At the beginning of 2017, an upgraded pixel detector was installed [35]. The upgraded tracker is referred to as the "phase-1" tracker. The phase-1 tracker, used for the 2017 and 2018 data-taking periods, measured particles within $|\eta| < 3.0$. Tracks traversing the tracker system encounter 3 (4) pixel layers within a radius of 102 (160) mm in the phase-0 (phase-1) tracker. They encounter up to around 10 layers in the strip detector within a radius of 1.2 m. Compared to the phase-0 tracker, the phase-1 tracker provides improved tracking and vertex resolution, enhanced b-tagging performance, and a better measurement of the $\mathrm{d}E/\mathrm{d}x$ track energy loss [35].

Events of interest are selected using a two-tiered trigger system [36]. The first level (L1), composed of custom hardware processors, uses information from the calorimeters and muon detectors to select events at a rate of around 100 kHz within a fixed latency of about 4 μs [37]. The second level, known as the high-level trigger, consists of a farm of processors running a version of the full event reconstruction software optimized for fast processing and reduces the event rate to around 1 kHz before data storage [36]. For the hadronic DTk channel, signal event candidates were recorded by requiring $p_{\mathrm{T}}^{\mathrm{miss}}$ at the trigger level to exceed a threshold that varied between 100 and 120 GeV, depending on the LHC instantaneous luminosity. For the electron + DTk (muon + DTk) channel, signal event candidates were recorded by requiring an electron (muon) candidate with $p_{\mathrm{T}} > 27$ (24) GeV at the trigger level, where p_{T} is the transverse momentum. The trigger efficiencies are measured in data using independent cross triggers and are found to exceed 97% for events in the hadronic DTk channel and 80 (90)% for $p_{\mathrm{T}} > 40$ GeV in the electron + DTk (muon + DTk) channel, for events that satisfy the selection criteria given below in Sec. VII.

A detailed description of the CMS detector, along with definitions of the coordinate system and kinematic variables, is given in Ref. [16].

IV. EVENT RECONSTRUCTION

Individual particles are reconstructed as particle-flow (PF) objects with the CMS PF algorithm [38], which

identifies them as photons, charged hadrons, neutral hadrons, electrons, or muons. To improve the quality of the electron reconstruction, additional criteria (beyond those of the PF algorithm) are imposed on the $\sigma_{i\eta i\eta}$ variable [39], which is a measure of the width of the ECAL shower shape in the η coordinate, and on the ratio H/E of energies associated with the electron candidate in the HCAL and ECAL [39]. Specifically, small values of $\sigma_{i\eta i\eta}$ and H/E are required, with the criteria optimized separately for the barrel and end caps [39]. For muon candidates, additional criteria are imposed on the matching between track segments reconstructed in the silicon tracker and muon detector [40]. Electron and muon candidates are required to have $p_{\mathrm{T}} > 40$ GeV and $|\eta| < 2.4$.

The primary vertex (PV) is taken to be the vertex corresponding to the hardest scattering in the event, evaluated using tracking information alone as described in Sec. 9.4.1 of Ref. [41]. Charged-particle tracks associated with vertices other than the PV are removed from further consideration. The PV is required to lie within 24 cm of the center of the detector in the direction along the beam axis and within 2 cm in the plane transverse to that axis.

Jets are defined by clustering PF candidates using the anti-k_{T} jet algorithm [42,43] with a distance parameter of 0.4. Jet quality criteria [44,45] are imposed to eliminate jets from spurious sources such as electronics noise. The jet energies are corrected for the nonlinear response of the detector [46] and to account for the expected contributions of neutral particles from extraneous pp interactions (pileup) [47]. Jets are required to have $p_{\mathrm{T}} > 30$ GeV, $|\eta| < 2.4$, and to not overlap with an identified lepton within a cone of radius $\Delta R \equiv \sqrt{(\Delta\phi)^2 + (\Delta\eta)^2} = 0.4$ around the jet direction, where ϕ is the azimuthal angle. The number of selected jets in an event is denoted N_{jet}.

The identification of b jets is performed by applying a version of the combined secondary vertex algorithm based on deep neural networks (DeepCSV)[48] to the selected jet sample. The medium working point of this algorithm is used. The tagging efficiency for b jets with $p_{\mathrm{T}} \approx 30$ GeV is 65%. The corresponding misidentification probability for gluon and light-quark (u, d, s) jets is 1.6%, while that for charm quark jets is 13%. The number of identified b jets in an event is denoted $N_{b\text{-jet}}$.

To suppress the contributions of jets erroneously identified as leptons as well as those due to genuine leptons from hadron decays, electron and muon candidates are subjected to a lepton-isolation requirement. This isolation criterion is based on the variable I, which is the sum of the scalar p_{T} of charged hadron, neutral hadron, and photon PF candidates within a cone of radius ΔR around the lepton direction, divided by the lepton p_{T}. The expected contributions to this sum of neutral particles from pileup are subtracted [47]. The radius ΔR of the cone is 0.2 for lepton $p_{\mathrm{T}} < 50$ GeV, $10\ \mathrm{GeV}/p_{\mathrm{T}}$ for $50 < p_{\mathrm{T}} < 200$ GeV, and 0.05 for $p_{\mathrm{T}} > 200$ GeV. The decrease in ΔR with increasing lepton p_{T} accounts for the increased collimation of the decay products from the lepton's parent particle as the Lorentz boost of the parent particle increases [49]. The isolation requirement is $I < 0.1$ (0.2) for electrons (muons).

The analysis uses a measure of the missing transverse momentum called the "hard $p_{\mathrm{T}}^{\mathrm{miss}}$" $p_{\mathrm{T,hard}}^{\mathrm{miss}}$, defined as the magnitude of the vector sum of $\vec{p}_{\mathrm{T}}$ over all PF jets with $p_{\mathrm{T}} > 30$ GeV and $|\eta| < 5.0$, where the PF jets are defined as outlined above but are clustered inclusively, meaning that isolated leptons and photons are included as "jets." The lepton-isolation and jet-lepton overlap rejection criteria described above are not applied to jets used to compute $p_{\mathrm{T,hard}}^{\mathrm{miss}}$. Hard $p_{\mathrm{T}}^{\mathrm{miss}}$ is more robust against pileup and soft radiation than the $p_{\mathrm{T}}^{\mathrm{miss}}$ variable calculated through a sum over individual particles in an event rather than jets.

V. SIMULATED EVENT SAMPLES

Simulated events are used to train boosted decision tree (BDT) multivariate binary classifiers and to estimate the signal acceptance in the SRs. The BDTs are used to help identify DTk candidates, as discussed in Sec. VI.

The SM production of $t\bar{t}$, $W+$jet, and $Z+$jet events, as well as of multijet events produced through quantum chromodynamics (QCD) processes, is simulated at leading order (LO) precision using the MadGraph 5_aMC@NLO 2.2.2 [50,51] event generator. The $t\bar{t}$ events are generated with up to three additional partons in the matrix element calculation. The $W+$jet and $Z+$jet events are generated with up to four additional partons. Single top quark events produced through the s channel, diboson events such as those originating from WW, ZZ, or ZH production (where H is the SM Higgs boson), and rare events such as those from $t\bar{t}W$, $t\bar{t}Z$, and WWZ production, are generated with the MadGraph 5_aMC@NLO generator at next-to-leading order (NLO) [52], with the exception of WW events when both W bosons decay leptonically, which are generated with the POWHEG v2.0 [53–57] generator at NLO. This same POWHEG generator is used to describe single top quark event production through the t and tW channels. Normalization of the simulated background samples is based on the cross section calculations of Refs. [50,56–66], which generally correspond to NLO or next-to-NLO (NNLO) precision. The detector response is based on the Geant4 [67] suite of programs.

With the exception of the pure wino and Higgsino models, simulated signal events are generated at LO using the MadGraph 5_aMC@NLO generator, with up to two additional partons included. The production cross sections are determined with approximate NNLO plus next-to-next-to-leading logarithmic (NNLL) accuracy [68–79]. Events with gluino (squark) pair production are generated for a range

of gluino $m_{\tilde{g}}$ (squark $m_{\tilde{q}}$) and LSP $m_{\tilde{\chi}_1^0}$ mass values, with $m_{\tilde{\chi}_1^0} < m_{\tilde{g}}$ ($m_{\tilde{\chi}_1^0} < m_{\tilde{q}}$). The ranges of mass considered vary according to the model, but are generally from around 600–2500 GeV for $m_{\tilde{g}}$, 200–1700 GeV for $m_{\tilde{q}}$, and 0–1500 GeV for $m_{\tilde{\chi}_1^0}$. The gluinos and squarks decay according to the phase space model of Ref. [80]. For the pure wino and Higgsino models, simulated signal events are generated at LO using the PYTHIA 8.205 generator [80].

To render the computational requirements manageable, the detector response for signal events is based on the CMS fast simulation program [81,82], which yields results that are generally consistent with those from Geant4. To improve the consistency with Geant4, we apply a correction of 1% to the fast simulation samples to account for differences in the efficiency of the jet quality requirements [44,45] and corrections of 5%–12% to account for differences in the b jet tagging efficiency. Additional corrections are applied to account for differences in the efficiency of tagging charginos with the phase-0 and -1 trackers.

Parton showering and hadronization are simulated with the PYTHIA 8.205 generator [80]. For background events, the phase-0 samples use the CUETP8M1 [83] tune while the phase-1 samples use the CP5 [84] tune. For signal events, the CP2 [84] tune is used. Simulated samples generated at LO (NLO) with the CUETP8M1 tune use the NNPDF3.0LO (NNPDF3.0NLO) [85] parton distribution function (PDF). Those generated with the CP2 or CP5 tune use the NNPDF3.1LO (NNPDF3.1NNLO) [86] PDF.

To improve the MadGraph 5_aMC@NLO modeling of the jet multiplicity from initial-state radiation (ISR), we follow the procedure introduced in Refs. [87,88]. A control sample enriched in $t\bar{t}$ events is selected in both data and simulation by requiring two lepton candidates (ee, $\mu\mu$, or $e\mu$) and two tagged b jets. The number of all other jets in an event is denoted $N_{\text{jet}}^{\text{ISR}}$. Reweighting factors are applied to the simulated $t\bar{t}$ events so that the $N_{\text{jet}}^{\text{ISR}}$ distribution in simulation agrees with that in data. The same reweighting factors are also applied to the simulated signal events. The reweighting factors are 0.920, 0.821, 0.715, 0.662, 0.561, and 0.511 for $N_{\text{jet}}^{\text{ISR}} = 1$, 2, 3, 4, 5, and ≥ 6, respectively.

VI. SELECTION OF DISAPPEARING TRACK CANDIDATES

Two categories of DTk are defined: short tracks and long tracks. Short tracks have hits recorded only in the pixel detector. Long tracks have hits in both the pixel and strip detectors. The track p_{T} is required to exceed 25 (40) GeV for the short (long) category. The pseudorapidity is required to satisfy $|\eta| < 2.0$. This latter requirement reduces the background from spurious tracks (Sec. VIII), which appears preferentially in the forward region. To ensure that the tracks are isolated, we calculate the relative isolation I_{rel}, defined by the sum of the scalar p_{T} of other tracks within a cone of radius $\Delta R = 0.3$ around the track direction, divided by the track p_{T}. We require $I_{\text{rel}} < 0.2$. The impact parameter d_{xy} of the track in the transverse plane and the impact parameter d_z in the direction along the beam axis must both be less than 0.1 cm, where d_{xy} and d_z are measured relative to the PV. The track is required to have at least three hits, one of which must be on the innermost pixel layer. Studies of simulated data show that charginos that decay within the tracker are rarely reconstructed as PF candidates. We therefore require the track to lie at least $\Delta R = 0.01$ away from any reconstructed particle and at least $\Delta R = 0.4$ away from any reconstructed jet with $p_{\text{T}} > 15$ GeV.

To select tracks that are consistent with a DTk, long tracks are required to not have hits in the outermost two layers of the strip detector, while short tracks are required to not have any hits whatsoever in the strip detector. In addition, tracks must not be identified as an electron, muon, or hadron. To ensure that DTk candidates are not associated with a large deposit of calorimetric energy, we calculate the quantity E_{dep}, which is the sum of ECAL and HCAL cluster energies deposited within $\Delta R = 0.4$ of the candidate track. Different criteria on E_{dep} and E_{dep}/p (with p the track momentum) are used to define SRs and control regions (CRs) for short and long tracks, respectively, and for the phase-0 and -1 detectors, as indicated in Table II. We use E_{dep}/p for long tracks because the resulting signal distribution peaks near 1, which is convenient for the selection process. However, because the uncertainty in p is larger for short tracks, the E_{dep}/p distribution for short

TABLE II. Selection criteria on the BDT classifier score and on the calorimetric energy E_{dep} associated with a disappearing track candidate for the SR and CR samples discussed in Sec. VIII.

Phase/category	Phase 0/short	Phase 0/long	Phase 1/short	Phase 1/long
BDT for SR samples	>0.1	>0.12	>0.15	>0.08
E_{dep} for SR samples	<15 GeV	$<0.2p$	<15 GeV	$<0.2p$
E_{dep} for $\text{CR}^{\text{genuine}}$ samples	[30, 300] GeV	$[0.3, 1.2]p$	[30, 300] GeV	$[0.3, 1.2]p$
BDT for $\text{CR}^{\text{genuine}}$ samples	>0.1	>0.05	>0.05	>0.08
BDT for $\text{CR}^{\text{spurious}}$ samples	$[-0.10, -0.05]$	$[-0.1, 0.0]$	$[-0.10, 0.05]$	$[-0.1, 0.0]$

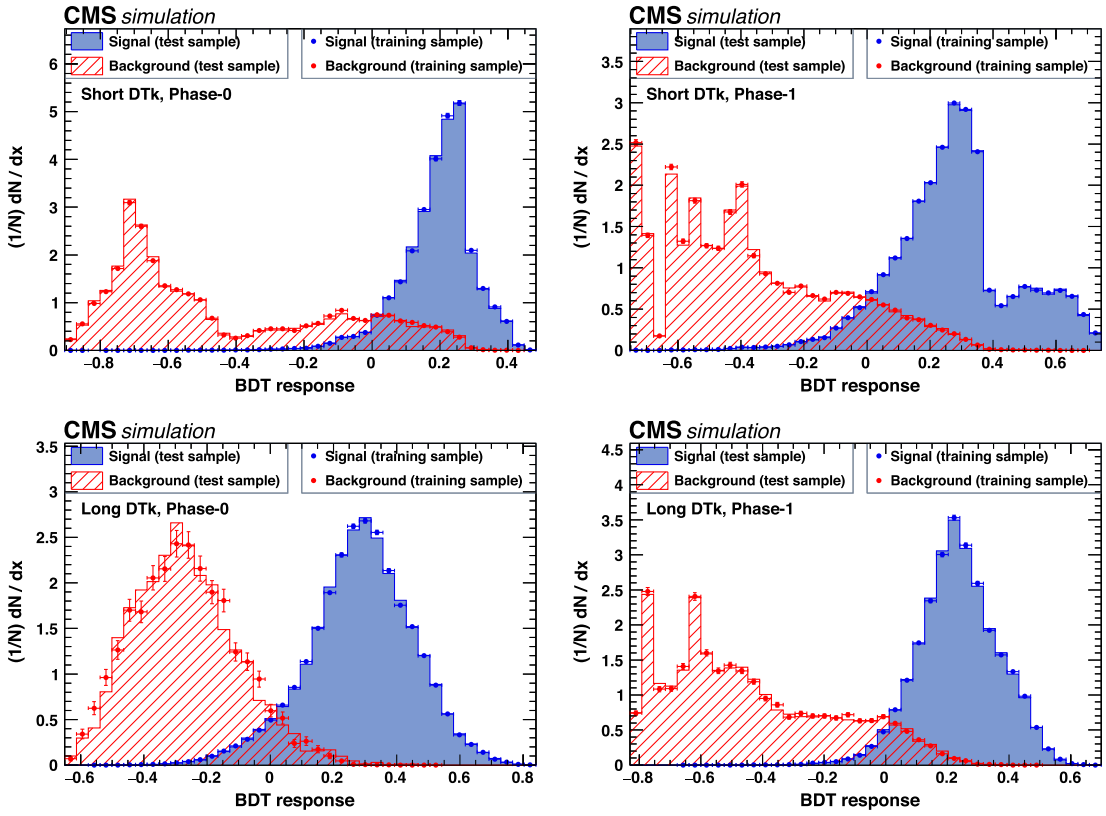

FIG. 2. The distributions of simulated events used to train and validate the BDT classifiers. The left (right) column corresponds to the phase-0 (phase-1) detector and the upper (lower) row to the short-(long) track category. The uncertainty bars shown for the training samples indicate the Poisson uncertainties. No events appear outside of the regions shown.

tracks does not exhibit a clear peak, making it simpler to use E_{dep}. (The momentum resolution for long tracks is 10% or better, while for short tracks it is 20% or worse, depending on the number of hits associated with the track.) To further reduce background from electrons, additional criteria are applied to reject tracks that enter detector regions with an ECAL crystal with anomalously low light yield, a disabled crystal, or a noisy channel. These additional criteria reduce the signal efficiency by less than 2%.

A BDT classifier is used to improve the purity of the DTk candidate sample. For the signal training, chargino-matched tracks from simulated gluino and top squark pair-production events are used. The matching criterion is $\Delta R(\text{track}, \tilde{\chi}^{\pm}_{1,\text{gen}}) < 0.01$, where $\tilde{\chi}^{\pm}_{1,\text{gen}}$ represents a generator-level chargino. For the background training, tracks from all simulated SM processes are used. The input variables to the classifier are d_{xy}, d_z, I_{rel}, $\Delta p_{\text{T}}/p^2_{\text{T}}$, χ^2/n_{d} (with Δp_{T} the uncertainty in the reconstructed p_{T} value and n_{d} the number of degrees of freedom), the number of pixel hits, and, for long tracks, the number of strip hits and the number of missing outer strip hits, where this latter quantity is the number of strip layers between the outermost strip hit and the outermost strip layer for which no hit is recorded. Separate BDTs are trained for the short- and long-track categories and for the phase-0 and -1 detectors. Distributions of the BDT output scores for these categories are shown in Fig. 2. Thresholds on the classifier output values are applied in defining SRs and CRs for the phase-0 and -1 detectors, as indicated in Table II. The classifier significantly improves the selection performance compared to so-called "cut-based" approaches, increasing the signal efficiency for short tracks by a factor ranging from 2 to 4, depending on the data-taking period, and of long tracks by around 50%, for an equivalent background rejection.

These requirements select 45%–55% of charginos that decay after the second tracker layer and before the penultimate one, depending on the length of the track.

A novel technique is used to validate the DTk selection efficiency. First, well reconstructed, isolated muons are selected from both data and simulation. Tracker hits associated with the muon are iteratively removed from the event one by one, starting with the outermost hit and working inward, until only three tracker hits remain. These shortened track segments are used as a proxy for long-lived charged particles. After each step in the process, the complete event reconstruction procedure is reapplied and the efficiency for the tracking algorithm and DTk

classifier to identify the shortened segments as a DTk candidate is determined. This efficiency ranges from 45% to 55% depending on the length of the shortened muon track, similar to the reconstruction efficiency for charginos mentioned above. The procedure is applied to samples corresponding to the various data-taking periods. Comparisons of the results between data and simulation are used to derive scale factors that are applied to the DTk selection efficiencies from simulation. The scale factors are consistent with unity with uncertainties, of statistical origin, that vary between 10% and 17%.

The DTk candidates are further classified on the basis of their $\mathrm{d}E/\mathrm{d}x$ energy loss value in the pixel detector. As the measure of the $\mathrm{d}E/\mathrm{d}x$, we use the so-called "harmonic-2" hit-weighted average I_h [89,90], which is an estimate of the linear stopping power of a particle that is robust with respect to outlier measurements. The I_h variable is defined by

$$I_\mathrm{h} = \left(\frac{1}{N}\sum_{i=1}^{N}(\Delta E/\Delta x)_i^{-2}\right)^{-1/2}, \tag{1}$$

where ΔE is the energy loss estimated from the charge collected by a pixel hit, Δx is the length of the track segment corresponding to that hit, and N is the number of pixel hits on the track. We define two intervals in I_h: $I_\mathrm{h} < 4.0$ and $I_\mathrm{h} > 4.0$ MeV/cm. In the following, the term "$\mathrm{d}E/\mathrm{d}x$" refers to the I_h value.

Time-dependent calibration of the $\mathrm{d}E/\mathrm{d}x$ measurement is performed in data using the position of the center of a Gaussian fit to the minimum-ionizing-particle peak of well-reconstructed muons, separately for the barrel and end cap regions. The $\mathrm{d}E/\mathrm{d}x$ values from all data-taking periods are scaled to be consistent with the result from simulation, with a fit mean of 2.87 MeV/cm.

The $\mathrm{d}E/\mathrm{d}x$ value can further be used to estimate the mass of the DTk, through the relation (with m the charged-particle mass)

$$\mathrm{d}E/\mathrm{d}x = K\frac{m^2}{p^2} + C, \tag{2}$$

which is valid for singly charged particles [89]. The constants K and C are determined as described in Ref. [90] to be 2.684 ± 0.001 and 3.375 ± 0.001 MeV/cm, respectively. We refer to the DTk mass value determined in this manner as $m_{\mathrm{DTk};\mathrm{d}E/\mathrm{d}x}$. We do not use the $m_{\mathrm{DTk};\mathrm{d}E/\mathrm{d}x}$ variable for quantitative purposes but merely examine its distribution in Sec. X.

VII. EVENT SELECTION AND SEARCH REGIONS

The number of DTk candidates in an event is denoted N_DTk. Signal events are required to have $N_\mathrm{DTk} \geq 1$, $N_\mathrm{jet} \geq 1$, and $p_\mathrm{T,hard}^\mathrm{miss} > 30$ GeV. At least one DTk candidate must satisfy $m_\mathrm{T}(\mathrm{DTk}, p_\mathrm{T,hard}^\mathrm{miss}) > 20$ GeV, where m_T is the transverse mass [91] formed from the two quantities in parentheses. For $N_\mathrm{DTk} = 1$, the search is performed inclusively in the hadronic DTk, electron + DTk, and muon + DTk channels. We also search in a channel with $N_\mathrm{DTk} \geq 2$. For this latter channel, events are required to satisfy the hadronic trigger requirements in the case of zero leptons or the trigger requirements for the electron (muon) channel in the case of $N_e \geq 1$ ($N_\mu \geq 1$), where N_e (N_μ) is the number of electron (muon) candidates in an event. The different search channels are defined as follows.

(1) Hadronic channel:
   (a) $N_\mathrm{DTk} = 1$,
   (b) $N_e = N_\mu = 0$,
   (c) $p_\mathrm{T,hard}^\mathrm{miss} > 150$ GeV.
(2) Muon channel:
   (a) $N_\mathrm{DTk} = 1$,
   (b) $N_e = 0$,
   (c) $N_\mu \geq 1$,
   (d) $m_{\mathrm{DTk},\mu} > 120$ GeV,
   (e) $m_\mathrm{T}(\mu, p_\mathrm{T,hard}^\mathrm{miss}) > 110$ GeV.
(3) Electron channel:
   (a) $N_\mathrm{DTk} = 1$,
   (b) $N_e \geq 1$,
   (c) $m_{\mathrm{DTk},e} > 120$ GeV,
   (d) $m_\mathrm{T}(e, p_\mathrm{T,hard}^\mathrm{miss}) > 110$ GeV.
(4) $N_\mathrm{DTk} \geq 2$ channel:
   (a) Satisfies the criteria given above for either the hadronic, muon, or electron channel, except for the N_DTk requirement,
   (b) $N_\mathrm{DTk} \geq 2$.

The invariant mass $m_{\mathrm{DTk},\ell}$ is formed from the DTk and the highest p_T electron or muon candidate in the event. The $m_{\mathrm{DTk},\ell}$ and m_T requirements suppress the Drell-Yan (DY) and W + jet backgrounds, respectively. For the $m_{\mathrm{DTk},\ell}$ calculation, the mass of the DTk is assumed to be zero. Note that we require $N_e = 0$ for the muon channel in order to render it orthogonal to the electron channel, but do not require $N_\mu = 0$ for the electron channel because it is unnecessary for the analysis.

The above requirements define the global SR, referred to as the "baseline" region. Events in the baseline region are divided into nonoverlapping SRs as follows. Events with $N_\mathrm{DTk} = 1$ are sorted into 48 SRs based on the DTk length category, the $\mathrm{d}E/\mathrm{d}x$ interval, and the values of N_jet, $N_{b\text{-jet}}$, and $p_\mathrm{T,hard}^\mathrm{miss}$. The choice of binning is designed to provide sensitivity to a wide range of scenarios, covering strong and electroweak production and the presence of all three generations of fermions. Events with $N_\mathrm{DTk} \geq 2$ are grouped into a single SR, bringing the total number of SRs to 49. The definition of the SRs is given in Tables III and IV.

VIII. BACKGROUND ESTIMATION

Disappearing track signatures are rare in the SM but can occasionally arise because of an instrumental effect, either

TABLE III. Definition of the search regions for the hadronic channel.

Hadronic channel ($N_{\mathrm{DTk}} = 1$, $N_\mu = 0$, $N_e = 0$)						
$p_{\mathrm{T,hard}}^{\mathrm{miss}}$ (GeV)	$N_{b\text{-jet}}$	N_{jet}	N_{short}	N_{long}	$\mathrm{d}E/\mathrm{d}x$ (MeV/cm)	SR
150–300	0	1–2	0	1	<4.0	1
					>4.0	2
			1	0	<4.0	3
					>4.0	4
		≥3	0	1	<4.0	5
					>4.0	6
			1	0	<4.0	7
					>4.0	8
	≥1	1–2	0	1	<4.0	9
					>4.0	10
			1	0	<4.0	11
					>4.0	12
		≥3	0	1	<4.0	13
					>4.0	14
			1	0	<4.0	15
					>4.0	16
>300	Any	1–2	0	1	<4.0	17
					>4.0	18
			1	0	<4.0	19
					>4.0	20
		≥3	0	1	<4.0	21
					>4.0	22
			1	0	<4.0	23
					>4.0	24

TABLE IV. Definition of the search regions for the muon, electron, and $N_{\mathrm{DTk}} \geq 2$ channels.

Muon channel ($N_{\mathrm{DTk}} = 1$, $N_\mu \geq 1$, $N_e = 0$)						
$p_{\mathrm{T,hard}}^{\mathrm{miss}}$ (GeV)	$N_{b\text{-jet}}$	N_{jet}	N_{short}	N_{long}	$\mathrm{d}E/\mathrm{d}x$ (MeV/cm)	SR
30–100	0	≥1	0	1	<4.0	25
					>4.0	26
			1	0	<4.0	27
					>4.0	28
	≥1		0	1	<4.0	29
					>4.0	30
			1	0	<4.0	31
					>4.0	32
>100	Any		0	1	<4.0	33
					>4.0	34
			1	0	<4.0	35
					>4.0	36
Electron channel ($N_{\mathrm{DTk}} = 1$, $N_e \geq 1$)						
30–100	0	≥1	0	1	<4.0	37
					>4.0	38
			1	0	<4.0	39
					>4.0	40
	≥1		0	1	<4.0	41
					>4.0	42
			1	0	<4.0	43
					>4.0	44
>100	Any		0	1	<4.0	45
					>4.0	46
			1	0	<4.0	47
					>4.0	48
$N_{\mathrm{DTk}} \geq 2$ channel						
>30	Any	≥1	Any			49

from the misreconstruction of a charged particle or from the coincidental alignment of hits from different tracks. We refer to these backgrounds as the "genuine-particle" background and the "spurious-particle" background, respectively. We use methods based entirely on data to evaluate these backgrounds, as described below. These methods employ the so-called "ABCD" technique, for which a basic description is given in Ref. [92].

A. Genuine-particle background

In a typical case, genuine-particle background might arise from a track that showers in a crack between ECAL crystals or into a crystal with anomalously low light yield, yielding a significantly undermeasured deposited energy that degrades the consistency between the measured track p_{T} and associated calorimetric energy, leading to a failure in the PF particle reconstruction. In other cases, a particle might emit a highly energetic photon, causing a recoil that similarly degrades this consistency. Concomitantly, the two outermost layers of the silicon tracker may not have hits associated with the track, which can arise through rare inefficiencies or from misassociation of hits in the strip detector. We refer to this type of background as the "genuine-particle showering" background. Less often, genuine-particle background can arise from a muon if there is a large or otherwise anomalous occupancy in the muon system or as a result of a rare misalignment between the track segment in the tracker with that in the muon system, again in conjunction with missing hits in the two outermost layers of the silicon tracker. We refer to this background as the "genuine-particle muon" background. These genuine-particle backgrounds represent the dominant background for the long-track category of DTks.

The genuine-particle showering background is evaluated using sideband control regions $\mathrm{CR}^{\mathrm{genuine}}$, one for each SR, and a separate "DY measurement" CR of Drell-Yan events. The $\mathrm{CR}^{\mathrm{genuine}}$ samples are defined by the intervals in E_{dep} and the BDT classifier listed in the third and fourth rows of Table II. These criteria yield a high purity for genuine-particle showering events and thus negligible contamination. The $\mathrm{CR}^{\mathrm{genuine}}$ samples are selected using a loosened

TABLE V. The transfer factors $\kappa^{\text{low}}_{\text{high}}$ and $\kappa^{\mu\text{ veto}}_{\mu\text{ match}}$ used for the evaluation of the genuine-particle backgrounds. The "Genuine shower" columns refer to the $\kappa^{\text{low}}_{\text{high}}$ factors, while the "Genuine muon" columns refer to the $\kappa^{\mu\text{ veto}}_{\mu\text{ match}}$ factors. The genuine-particle muon background is negligible for the short category of DTks. The uncertainties are statistical only.

	Phase 0		Phase 1		Combined phase 0 and 1	
$\kappa^{\text{low}}_{\text{high}}$, $\kappa^{\mu\text{ veto}}_{\mu\text{ match}}$:	Genuine shower	Genuine muon	Genuine shower	Genuine muon	Genuine shower	Genuine muon
Short	0.65 ± 0.11	⋯	0.435 ± 0.049	⋯	0.492 ± 0.046	⋯
Long	0.247 ± 0.020	0.00099 ± 0.00017	0.389 ± 0.032	0.00047 ± 0.00012	0.307 ± 0.018	0.00074 ± 0.00011

isolation requirement on the DTks compared to the SRs. Specifically, the DTk candidate must only lie at least $\Delta R = 0.1$ away from any reconstructed jet with $p_{\text{T}} > 15$ GeV, rather than at least $\Delta R = 0.4$ as in Sec. VI. The reason for this loosened restriction is to increase the statistical precision of the background estimate. Other than these differences, the criteria used to select the $\text{CR}^{\text{genuine}}$ samples are the same as for the SR samples.

The DY measurement CR is selected by requiring events to contain an electron and a DTk candidate of opposite charge. The DTk candidate must satisfy the selection criteria for either the SR or $\text{CR}^{\text{genuine}}$ samples. The invariant mass $m(\text{DTk}, e)$ formed from the DTk and electron must be consistent with a Z boson, namely lie in a range from 65 to 110 GeV. For this calculation, the DTk is assigned a mass of zero. To improve the purity, we require $m_{\text{T}}(e, p^{\text{miss}}_{\text{T,hard}}) < 100$ GeV and that there be a relatively small difference $\Delta\phi$ in the azimuthal angle between the DTk and $p^{\text{miss}}_{\text{T,hard}}$: $\Delta\phi < \pi/2$ for long tracks and $\Delta\phi < \pi/4$ for short tracks. The $\Delta\phi$ requirement is imposed because genuine-particle DTks correspond to particles that are not reconstructed, which can lead to significant $p^{\text{miss}}_{\text{T,hard}}$ along the direction of the DTk.

A transfer factor $\kappa^{\text{low}}_{\text{high}}$ is derived from the DY measurement CR, given by the ratio of the number of events with small and large values of the f_{dep} variable,

$$\kappa^{\text{low}}_{\text{high}} = N^{\text{DY}}_{f^{\text{low}}_{\text{dep}}} / N^{\text{DY}}_{f^{\text{high}}_{\text{dep}}}, \tag{3}$$

where $f_{\text{dep}} = E_{\text{dep}}/p$ for long tracks and $f_{\text{dep}} = E_{\text{dep}}$ for short tracks. The E_{dep} requirements for the $f^{\text{low}}_{\text{dep}}$ ($f^{\text{high}}_{\text{dep}}$) region are the same as those listed for the SR ($\text{CR}^{\text{genuine}}$) samples in Table II. The transfer factor is determined separately for short and long tracks and for the phase-0 and -1 detectors. The DY measurement CR is nearly 100% pure in genuine-particle showering events except for the short-track category at low f_{dep}, where approximately 50% of the events arise from spurious tracks. The spurious-track contamination in this sample is evaluated using the method described in Sec. VIII B and is then subtracted before the $\kappa^{\text{low}}_{\text{high}}$ factors are calculated, with an associated systematic uncertainty evaluated as described in Sec. IX. The values of the $\kappa^{\text{low}}_{\text{high}}$ factors are reported in the genuine shower columns of Table V.

The estimate $N^{\text{genuine}}_{\text{SR}_i}$ of the number of genuine-particle showering background events in the ith SR is

$$N^{\text{genuine}}_{\text{SR}_i} = \kappa^{\text{low}}_{\text{high}} N_{\text{CR}^{\text{genuine}}_i}, \tag{4}$$

with $N_{\text{CR}^{\text{genuine}}_i}$ the number of events in the ith $\text{CR}^{\text{genuine}}$ sample.

An analogous procedure is employed to evaluate the much smaller genuine-particle muon background, making use of sideband control regions $\text{CR}^{\text{genuine-}\mu}$ defined analogously to the SRs but inverting the requirement from Sec. VI that the DTk not be identified as a PF muon, namely the track *must* be identified as a muon. We call this track a "DTk-proxy" track. A DY measurement CR is defined in the same manner as described above for the genuine-particle showering background except with the Z boson candidate formed from a muon and the DTk-proxy track. The $\text{CR}^{\text{genuine-}\mu}$ and this DY measurement CR are essentially 100% pure in genuine-particle muon events and thus have negligible contamination. A transfer factor $\kappa^{\mu\text{ veto}}_{\mu\text{ match}}$ is derived from the DY measurement CR as the ratio of the number of events with the muon veto of Sec. VI applied to the corresponding number with the veto inverted. The values of the transfer factors $\kappa^{\mu\text{ veto}}_{\mu\text{ match}}$ are listed in the genuine muon columns of Table V. Note that this background is negligible for short tracks because of the high efficiency of the combined strip tracker and muon systems.

The estimate $N^{\text{genuine-}\mu}_{\text{SR}_i}$ of the number of genuine-particle muon background events in the ith SR is

$$N^{\text{genuine-}\mu}_{\text{SR}_i} = \kappa^{\mu\text{ veto}}_{\mu\text{ match}} N_{\text{CR}^{\text{genuine-}\mu}_i}, \tag{5}$$

with $N_{\text{CR}^{\text{genuine-}\mu}_i}$ the number of events in the ith $\text{CR}^{\text{genuine-}\mu}$ sample.

We study the dependence of the transfer factors $\kappa^{\text{low}}_{\text{high}}$ and $\kappa^{\mu\text{ veto}}_{\mu\text{ match}}$ on the kinematic properties of the tracks. It is found that the p_{T} spectra of DTks in the DY measurement CRs are predicted reasonably well, with statistically significant deviations within 20% for the showering background

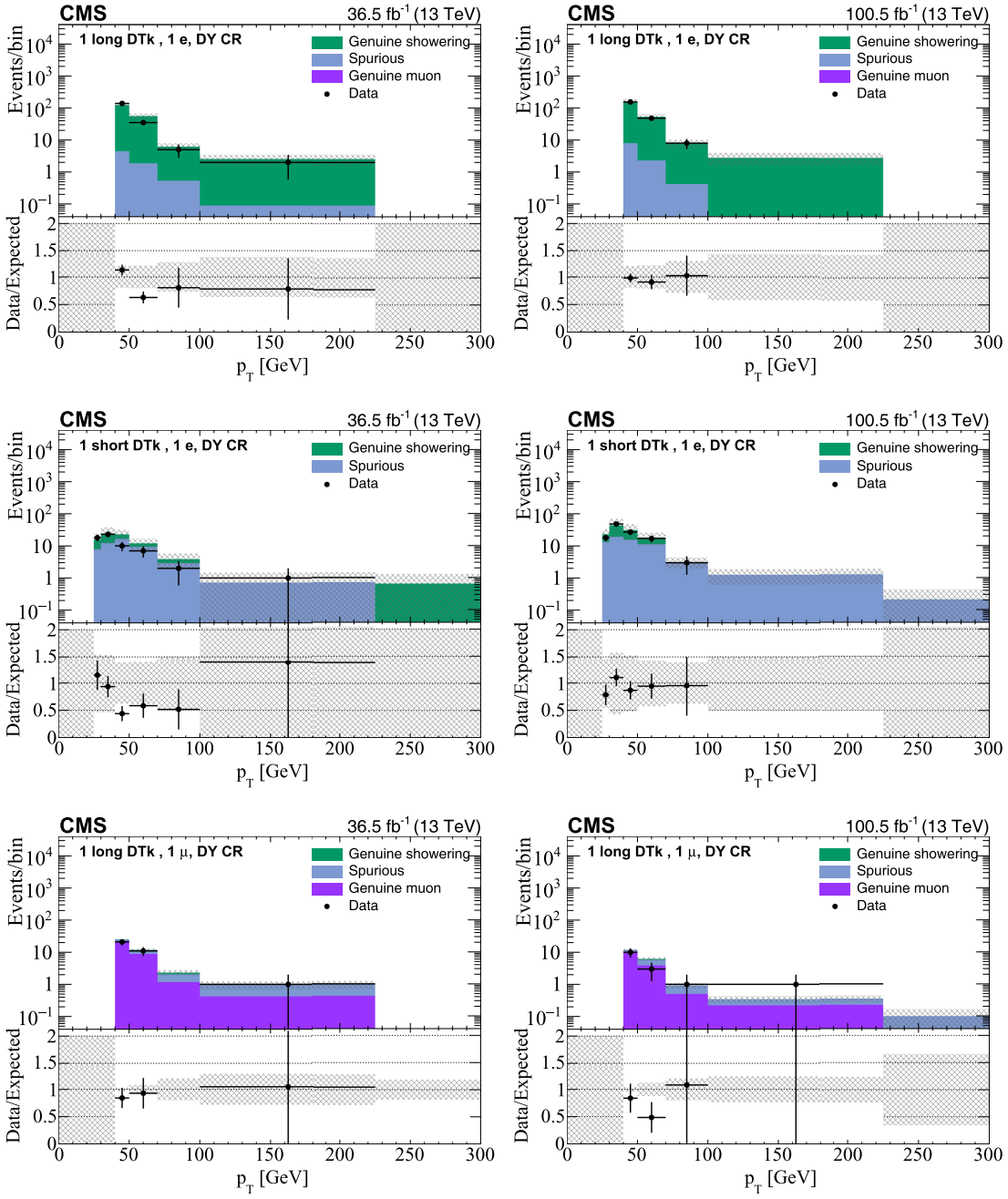

FIG. 3. Comparison of the p_T distributions of DTks in the $\kappa^{\text{low}}_{\text{high}}$ DY measurement control region for the data and background prediction for long (upper) and short (middle) showering tracks and in the $\kappa^{\mu\ \text{veto}}_{\mu\ \text{match}}$ DY measurement control region for long muon tracks (lower). The left (right) column corresponds to the phase-0 (phase-1) detector. The uncertainty bars on the ratios in the lower panels indicate the fractional Poisson uncertainties in the observed counts. The gray bands show the fractional Poisson uncertainties in the sideband region counts, added in quadrature with the systematic uncertainties. The leftmost (rightmost) bin includes underflow (overflow).

tracks. Comparisons between the predicted and observed p_T spectra of the tracks in the two DY measurement CRs are presented in Fig. 3. Tests of the method are performed in high-m_T validation regions defined in the same manner as the corresponding DY measurement CR but with the inverted requirement $m_T > 110$ GeV. The results in the validation regions are shown in Fig. 4 and indicate agreement between the predicted and observed results to within the statistical and systematic uncertainties.

B. Spurious-particle background

The spurious-particle background arises when hits in the silicon tracker from two or more particles align to form a

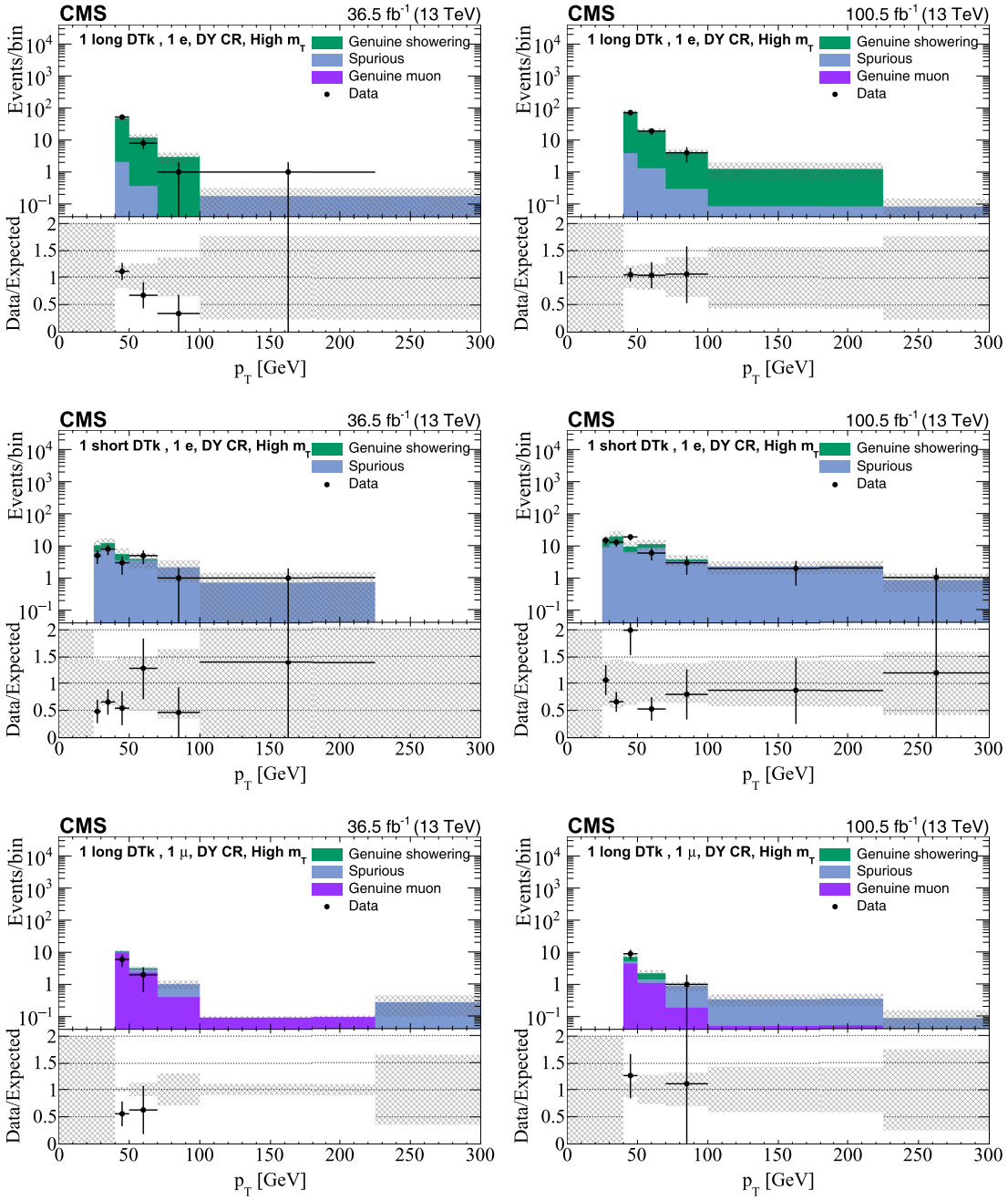

FIG. 4. Comparison of the p_T distributions of DTks in the high-m_T validation region for the data and background prediction for long (upper) and short (middle) showering tracks and for long muon tracks (lower). The left (right) column corresponds to the phase-0 (phase-1) detector. The uncertainty bars on the ratios in the lower panels indicate the fractional Poisson uncertainties in the observed counts. The gray bands show the fractional Poisson uncertainties in the sideband region counts, added in quadrature with the systematic uncertainties. The leftmost (rightmost) bin includes underflow (overflow).

pattern that mimics the signature of a single particle. Such combinatoric patterns typically do not have associated calorimetric or muon system activity. They thereby can satisfy the selection criteria for DTks and appear as background in our search. The spurious-particle background depends primarily on the level of activity in an event, particularly the occupancy of the tracker. It forms the dominant background for the short-track category of DTks.

The spurious-particle background is evaluated using sideband control regions $CR^{spurious}$, one for each SR, and a "QCD measurement CR" enhanced in QCD multijet events. The $CR^{spurious}$ samples are selected using the same

TABLE VI. The transfer factor $\theta_{\text{low}}^{\text{high}}$ used for the evaluation of the spurious-particle background. The uncertainties are statistical only.

	Spurious particle		
$\theta_{\text{low}}^{\text{high}}$:	Phase 0	Phase 1	Combined phase 0 and 1
Short	0.722 ± 0.079	0.210 ± 0.020	0.346 ± 0.025
Long	0.089 ± 0.015	0.042 ± 0.021	0.080 ± 0.013

criteria as for the corresponding SRs except with lower ranges in the BDT variable. These ranges are listed in the last row of Table II. The ranges are chosen so as to yield sufficiently populated samples, a high purity of spurious tracks, and a phase space similar to the SRs.

The QCD measurement CR is selected by requiring $N_e = N_\mu = N_{b\text{-jet}} = 0$ and $30 < p_{\text{T,hard}}^{\text{miss}} < 60$ GeV. It is essentially 100% pure in spurious-track events, with negligible contamination. A transfer factor $\theta_{\text{low}}^{\text{high}}$ is derived from the QCD measurement CR sample as

$$\theta_{\text{low}}^{\text{high}} = N_{\text{BDT}^{\text{high}}}^{\text{QCD}} / N_{\text{BDT}^{\text{low}}}^{\text{QCD}}, \tag{6}$$

with $N_{\text{BDT}^{\text{high}}}^{\text{QCD}}$ and $N_{\text{BDT}^{\text{low}}}^{\text{QCD}}$ the number of events satisfying the BDT selection criteria in Table II for the SR and $\text{CR}^{\text{spurious}}$ selections, respectively. The values of the transfer factors $\theta_{\text{low}}^{\text{high}}$ are listed in Table VI.

The estimate $N_{\text{SR}_i}^{\text{spurious}}$ of the number of spurious-particle background events in the ith SR is

$$N_{\text{SR}_i}^{\text{spurious}} = \theta_{\text{low}}^{\text{high}} N_{\text{CR}_i^{\text{spurious}}}, \tag{7}$$

with $N_{\text{CR}_i^{\text{spurious}}}$ the number of events in the ith $\text{CR}^{\text{spurious}}$ event sample.

Because of the limited size of the data sample, six SRs in the large $\mathrm{d}E/\mathrm{d}x$ category have no events in the corresponding $\text{CR}^{\text{spurious}}$ sample: these are bins 18, 22, 34, 42, 44, and 46 (see Tables III and IV). To obtain a prediction for these bins, an extrapolation is made based on the predicted spurious-track background in the adjacent SR, namely, the

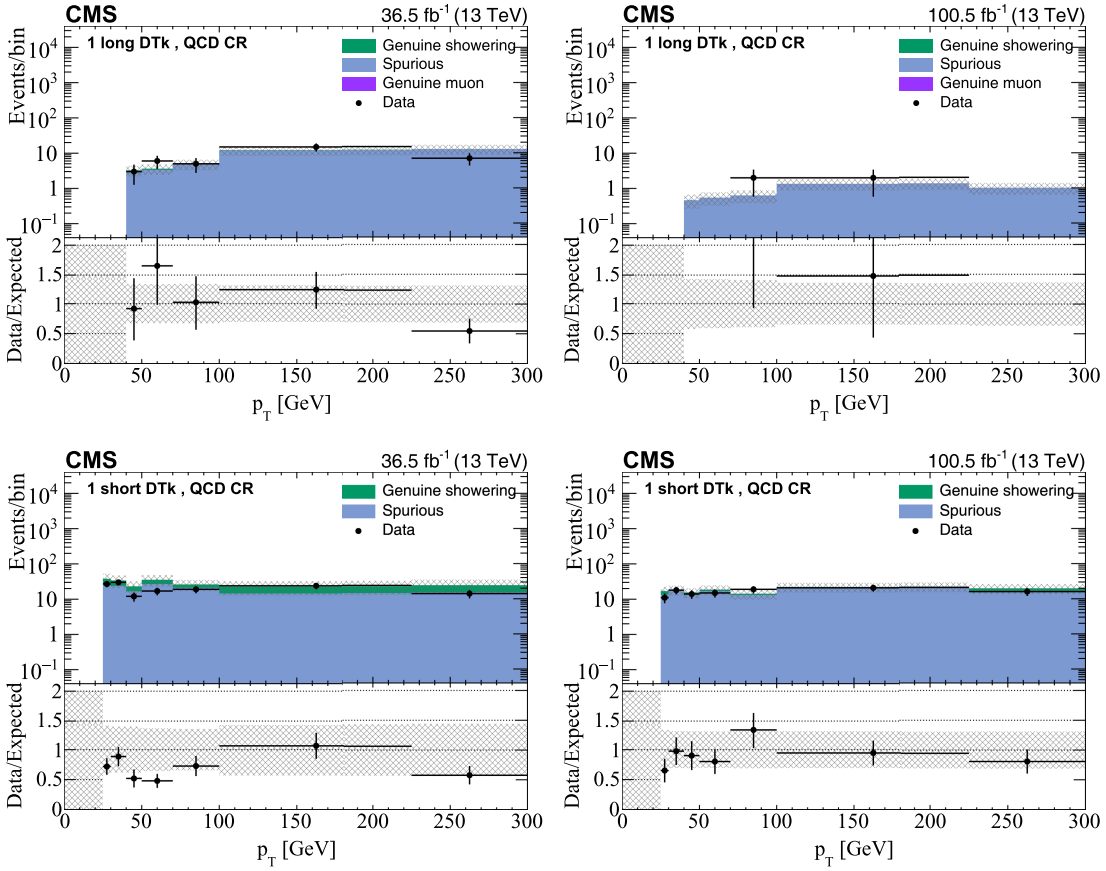

FIG. 5. Comparison of the p_{T} distributions of DTks in the $\theta_{\text{low}}^{\text{high}}$ QCD measurement control region for the data and background prediction for long (upper) and short (lower) tracks. The left (right) column corresponds to the phase-0 (phase-1) detector. The uncertainty bars on the ratios in the lower panels indicate the fractional Poisson uncertainties in the observed counts. The gray bands show the fractional Poisson uncertainties in the control region counts, added in quadrature with the systematic uncertainties. The leftmost (rightmost) bin includes underflow (overflow).

equivalent SR in the low $\mathrm{d}E/\mathrm{d}x$ category. The prediction is made as

$$(N_{\mathrm{SR}_i}^{\mathrm{spurious}})_{\mathrm{d}E/\mathrm{d}x\text{-high}} = \phi_{\mathrm{low}}^{\mathrm{high}} (N_{\mathrm{SR}_i}^{\mathrm{spurious}})_{\mathrm{d}E/\mathrm{d}x\text{-low}}, \quad (8)$$

where the transfer factor $\phi_{\mathrm{low}}^{\mathrm{high}}$ is studied in various CRs and is found to be 0.18 ± 0.05 for both long and short tracks, independent of any analysis variable. Relative systematic uncertainties associated with the extrapolated counts are taken from the bin from which the value is extrapolated, in addition to the uncertainty in $\phi_{\mathrm{low}}^{\mathrm{high}}$.

Comparisons between the predicted and observed p_{T} spectra of DTk candidates in the QCD measurement CR are shown in Fig. 5. The spectra are seen to be reasonably well modeled, with statistically significant deviations below around 30%, within the total uncertainty. Tests of the spurious-particle background evaluation procedure are performed in a validation region defined by requiring the presence of one electron and one DTk, with the restrictions $m_{\mathrm{T}} < 110$ GeV and $m_{\mathrm{DTk},e} \notin [65, 110]$ GeV. Note that this validation region also accounts for genuine-particle background that might be present in the spurious-particle sample. The results, shown in Fig. 6, again demonstrate general agreement within the uncertainties.

IX. SYSTEMATIC UNCERTAINTIES

We consider the following sources of systematic uncertainty in the signal event yields. Nuisance parameters associated with systematic uncertainties are treated as correlated across all search bins.

(i) DTk selection efficiency: The uncertainty in the DTk selection efficiency is taken to be the uncertainty in the DTk selection efficiency scale factors mentioned in Sec. VI.

(ii) Integrated luminosity: The systematic uncertainty in the determination of the integrated luminosity is 1.6% [93–96].

(iii) Jet energy scale and resolution: Uncertainties in the jet energy scale and resolution are evaluated as a function of jet p_{T} and η and propagated to higher level quantities such as N_{jet} and $p_{\mathrm{T,hard}}^{\mathrm{miss}}$ [45,46,97].

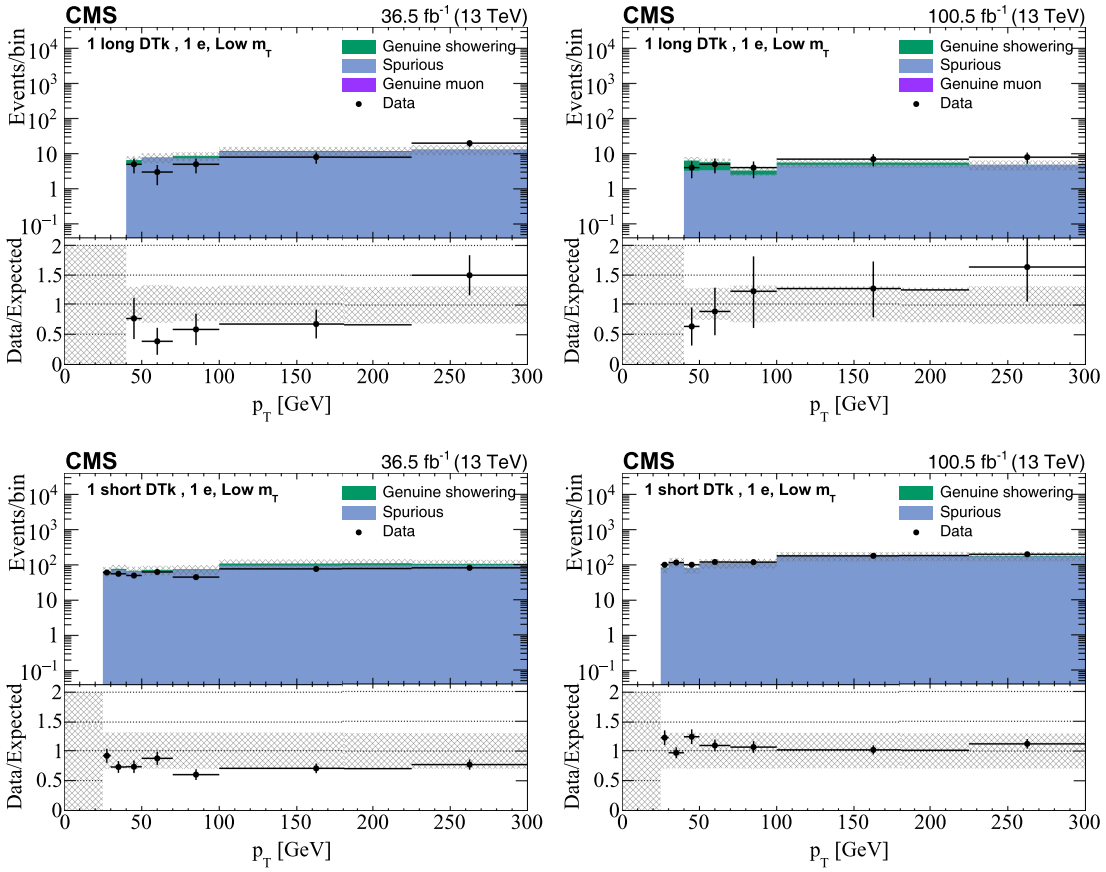

FIG. 6. Comparison of the p_{T} distributions of DTks in events with one electron and one DTk, in a validation region with $m_{\mathrm{T}} < 110$ GeV and $m_{\mathrm{DTk},e} \notin [65, 110]$ GeV, for the data and background prediction for long (upper) and short (lower) tracks. The left (right) column corresponds to the phase-0 (phase-1) detector. The uncertainty bars on the ratios in the lower panels indicate the fractional Poisson uncertainties in the observed counts. The gray bands show the fractional Poisson uncertainties in the control region counts, added in quadrature with the systematic uncertainties. The leftmost (rightmost) bin includes underflow (overflow).

(iv) b jet tagging efficiency and mistagging: p_{T}, η, and flavor-dependent uncertainties in the b jet tagging and light-quark jet mistagging scale factors, accounting both for data-versus-Geant4-simulation differences and for Geant4-versus-fast-simulation differences, are derived from control samples of $t\bar{t}$ and QCD multijet events.

(v) Renormalization and factorization scales: Uncertainties associated with the renormalization (μ_{R}) and factorization (μ_{F}) scales are evaluated by independently varying μ_{R} and μ_{F} by a factor of 2.0 and 0.5 [98–100].

(vi) Initial-state radiation: The uncertainty in the modeling of initial-state radiation is taken to be one half of the deviation from unity in the ISR reweighting factors presented in Sec. V.

(vii) Pileup modeling: The uncertainty associated with pileup reweighting is evaluated by varying the value of the total inelastic cross section by 4.6% [101] from its nominal value of 69.2 mb.

(viii) Trigger efficiency: The uncertainty in the trigger efficiency of the hadronic channel is assessed from its observed dependence on jet multiplicity and of the leptonic channels from the observed difference relative to an alternative trigger. In addition, the 2016 and 2017 data-taking periods were affected by an erroneous "prefiring" of the L1 trigger on the previous bunch crossing, prohibiting the triggering of some fraction of potential signal events. We evaluate the resulting uncertainty in the trigger efficiency using a preliminary L1 prefiring efficiency map based on the end of the 2017 data-taking period, representing a worst case scenario.

(ix) $\mathrm{d}E/\mathrm{d}x$ calibration: A time-dependent calibration of the $\mathrm{d}E/\mathrm{d}x$ measurement is performed using tracks associated with a muon, with the $\mathrm{d}E/\mathrm{d}x$ value extracted from a Gaussian fit around the peak of the $\mathrm{d}E/\mathrm{d}x$ distribution. A similar set of calibration factors is derived using low-p_{T} protons from Λ baryon decays. The difference in the calibration factors derived from the muons and protons is used to determine a systematic uncertainty in the $\mathrm{d}E/\mathrm{d}x$ calibration.

The following systematic uncertainties are evaluated for the estimates of the number of background events.

(i) Spurious-particle contamination: An uncertainty of 100% is assigned to the estimated number of genuine-particle short-track background events to account for the presence of spurious-particle contamination in the DY CR used to calculate the $\kappa^{\mathrm{low}}_{\mathrm{high}}$ transfer factors for this category. A 100% uncertainty is assigned because the measurement region for short tracks is dominated by spurious tracks and, after the subtraction, this is the order of how well the transfer factor is known. This uncertainty does not impact the sensitivity because this background is nearly negligible in the short-track SRs.

(ii) Residual p_{T} dependence: Differences in the predicted and observed p_{T} spectra of DTks in the transfer factor CRs are used to assess uncertainties of 30% and 20% in the number of spurious-particle long-track and genuine-particle long-track background events, respectively.

Statistical uncertainties in the SRs and CRs are accounted for in the fit described in Sec. X.

The sources of systematic uncertainty and their assessed ranges across the 49 SRs are summarized in Table VII.

TABLE VII. The considered sources of systematic uncertainty in the predicted signal yield and the corresponding range of values over the 49 search regions (a value of 0 is reported when the relative uncertainty is determined to be less than 0.5%) and the ranges for the total prefit uncertainty in the predicted background counts with respect to the respective background contribution.

Uncertainty source	Relative uncertainty in yield (%)
Signal	
DTk selection efficiency	10–17
Integrated luminosity	1.6
Jet energy scale and resolution	0–24
b jet tagging	0–4
Renormalization and factorization scales	0–2
Initial-state radiation	0–3
Pileup modeling	0–2
Trigger efficiency	0–4
$\mathrm{d}E/\mathrm{d}x$ calibration	3–8
Background	
Genuine particle showering long	20–28
Genuine particle showering short	100–104
Genuine particle muon long	25–38
Spurious particle long	5–52
Spurious particle short	6–28

X. RESULTS AND INTERPRETATION

Figures 7 and 8 show a comparison in the baseline region between the data and prefit background prediction for the N_{jet}, $N_{b\text{-jet}}$, $p^{\mathrm{miss}}_{\mathrm{T,hard}}$, N_e, N_μ, and $m_{\mathrm{DTk};\mathrm{d}E/\mathrm{d}x}$ distributions. The results for long tracks are shown in Fig. 7 and for short tracks in Fig. 8. Figure 9 presents the prefit (left) and postfit (right) background predictions in comparison to the data in the 49 individual SRs. The corresponding numerical results for the prefit predictions are given in Table VIII. For purposes of illustration, these figures and table include example results for the T6tbLL and T5btbtLL models, with choices for squark (or gluino) mass, LSP mass, and chargino $c\tau$ value as indicated in the legends or table header. The data are found to be consistent with the background-only hypothesis, and therefore no evidence

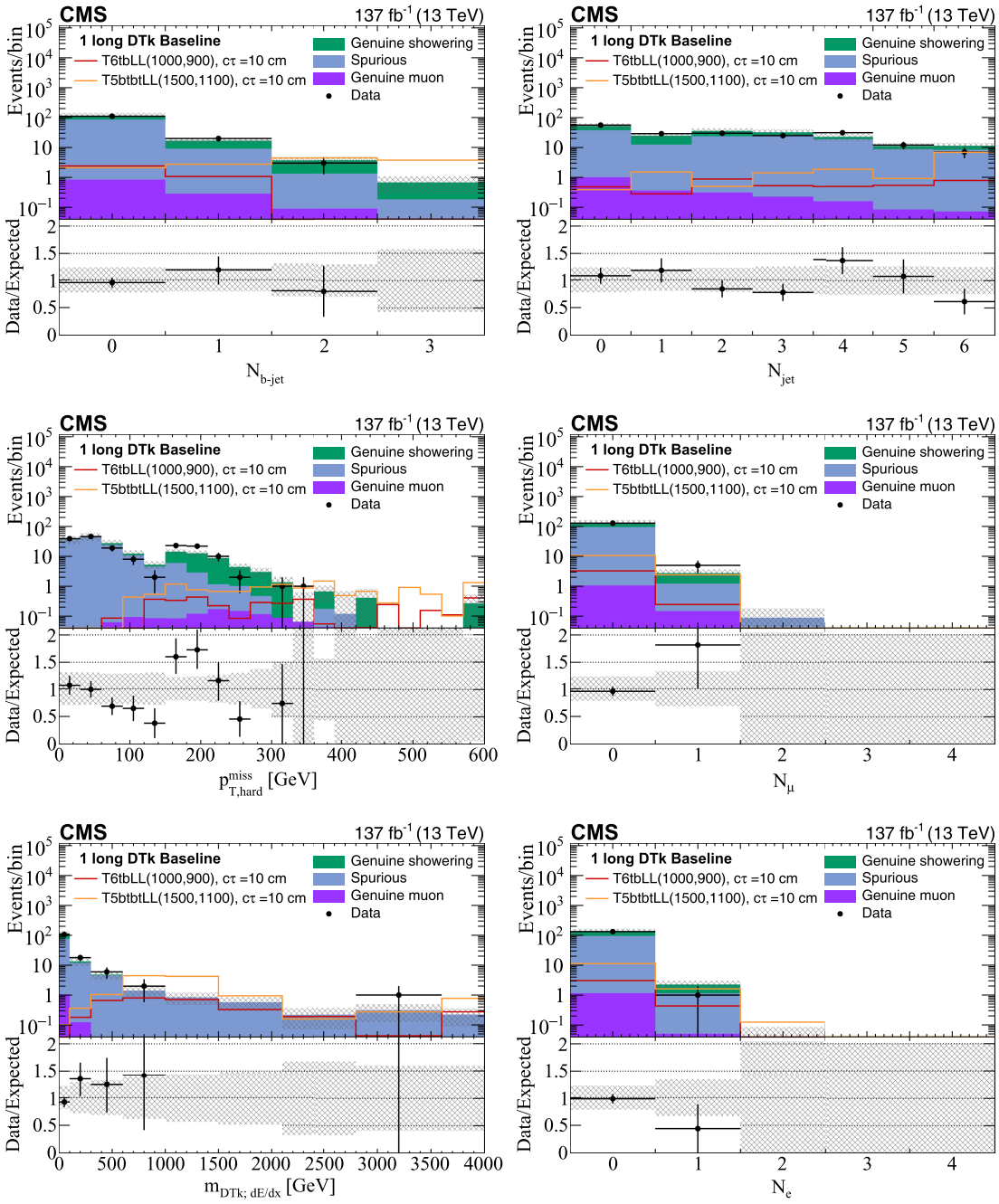

FIG. 7. Comparison in the baseline region for the long-track DTk category between the data and prefit predicted SM background for the N_{jet} (upper left), $N_{b\text{-jet}}$ (upper right), $p_{\text{T,hard}}^{\text{miss}}$ (middle left), N_e (middle right), N_μ (lower left), and $m_{\text{DTk;d}E/\text{d}x}$ (lower right) distributions. The uncertainty bars on the ratios in the lower panels indicate the fractional Poisson uncertainties in the observed counts. The gray bands show the fractional Poisson uncertainties in the control region counts, added in quadrature with the systematic uncertainties. The leftmost (rightmost) bin includes underflow (overflow). For purposes of illustration, results from the T6tbLL and T5btbtLL models are shown, where the first and second numbers in parentheses indicate the squark (or gluino) mass and the LSP mass, respectively, in GeV.

for new physics is observed. A slight systematic overprediction is seen in the short-track category, consistent with the presence of spurious-particle contamination in the showering background sidebands. The background uncertainty model accounts for this effect via a nuisance parameter that reduces the total genuine-particle background yield for short-track bins to nearly zero.

Upper limits on the production cross sections of the considered simplified models are computed using a maximum likelihood fit. The likelihood is a product of Poisson

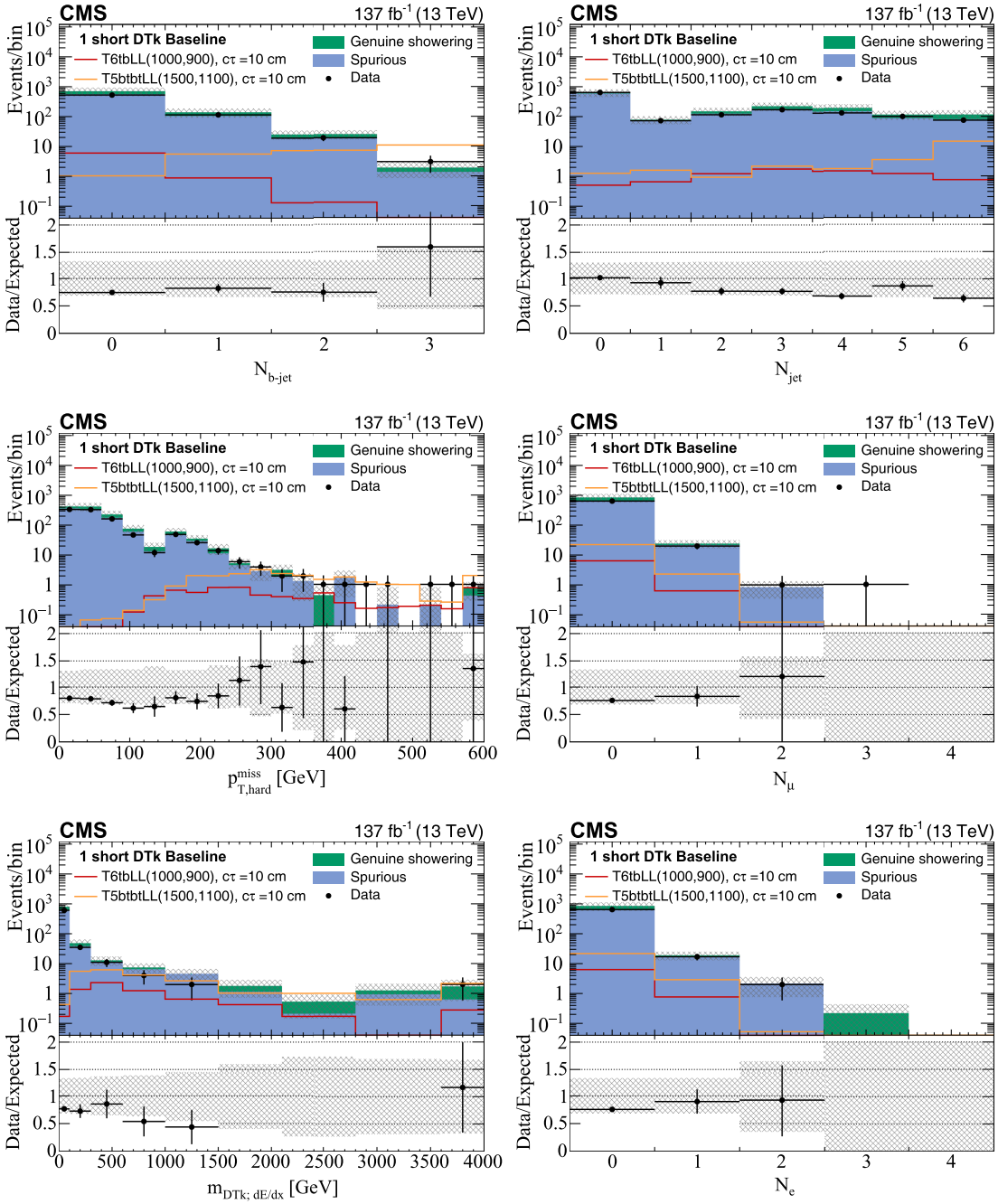

FIG. 8. Comparison in the baseline region for the short-track DTk category between the data and prefit predicted SM background for the N_{jet} (upper left), $N_{b\text{-jet}}$ (upper right), $p_{\text{T,hard}}^{\text{miss}}$ (middle left), N_e (middle right), N_μ (lower left), and $m_{\text{DTk;d}E/\text{d}x}$ (lower right) distributions. The uncertainty bars on the ratios in the lower panels indicate the fractional Poisson uncertainties in the observed counts. The gray bands show the fractional Poisson uncertainties in the control region counts, added in quadrature with the systematic uncertainties. The leftmost (rightmost) bin includes underflow (overflow). For purposes of illustration, results from the T6tbLL and T5btbtLL models are shown, where the first and second numbers in parentheses indicate the squark (or gluino) mass and the LSP mass, respectively, in GeV.

functions, one for each SR, accounting for the expected yields and evaluated using the observed event counts. The mean expected background and signal yields are constrained using γ functions that account for the observed event counts in each sideband control region and for the simulated signal event counts. Other sources of uncertainty are accounted for using log-normal functions, with one nuisance parameter per source of uncertainty. Limits are determined under the asymptotic approximation [102] of the CL_s criterion described in Refs. [103,104]. All 49 SRs

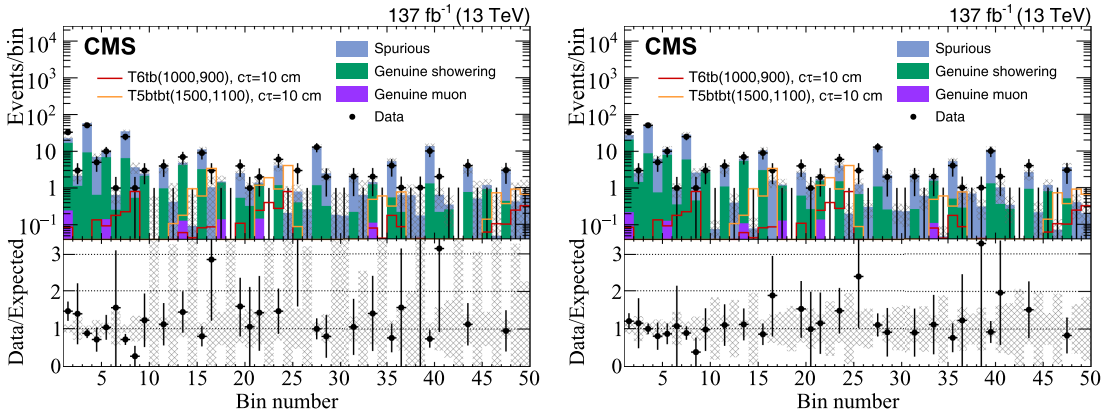

FIG. 9. Comparison between the data and SM background predictions for the 49 search regions. The left (right) plot shows the prefit (postfit) background predictions. The uncertainty bars on the ratios in the lower panels, shown for bins with nonzero entries, indicate the fractional Poisson uncertainties in the observed counts. The gray bands show the fractional Poisson uncertainties in the control region counts, added in quadrature with the systematic uncertainties. For purposes of illustration, results from the T6tbLL and T5btbtLL models are shown, where the first and second numbers in parentheses indicate the squark (or gluino) mass and the LSP mass, respectively, in GeV.

TABLE VIII. Predicted prefit background and uncertainties in the 49 search regions. Statistical and binwise systematic uncertainties are added in quadrature. The control region counts corresponding to each background category are given in the column to the left of the respective column. The numbers in parentheses for the signal points indicate the squark (or gluino) mass in GeV, the LSP mass in GeV, and $c\tau$ for the chargino in centimeters, respectively.

SR no.	CR	Spurious	CR	Showering	CR	Muon	Total bkg.	T6tbLL (1000, 900, 200)	T5btbtLL (1500, 1100, 10)	Observed
1	80	6.40 ± 0.72	56	17.2 ± 2.3	313	0.23 ± 0.01	23.9 ± 2.4	0.10 ± 0.06	0.00 ± 0.00	33
2	14	1.12 ± 0.30	4	1.23 ± 0.61	17	0.01 ± 0.01	2.36 ± 0.68	0.80 ± 0.17	0.00 ± 0.00	3
3	170	58.9 ± 4.5	33	8.1 ± 1.4	0	0.00 ± 0.00	67.0 ± 4.7	0.04 ± 0.03	0.00 ± 0.00	51
4	23	8.0 ± 1.7	3	0.74 ± 0.43	0	0.00 ± 0.00	8.7 ± 1.7	0.17 ± 0.07	0.00 ± 0.00	5
5	44	3.52 ± 0.53	24	7.4 ± 1.5	183	0.13 ± 0.01	11.0 ± 1.6	0.77 ± 0.16	0.03 ± 0.03	10
6	7	0.56 ± 0.21	1	0.31 ± 0.31	9	0.01 ± 0.01	0.87 ± 0.37	4.86 ± 0.38	0.00 ± 0.00	1
7	92	31.9 ± 3.3	23	5.7 ± 1.2	0	0.00 ± 0.00	37.5 ± 3.5	0.19 ± 0.07	0.00 ± 0.00	25
8	10	3.5 ± 1.1	2	0.49 ± 0.35	0	0.00 ± 0.00	4.0 ± 1.2	1.02 ± 0.15	0.03 ± 0.02	1
9	4	0.32 ± 0.16	8	2.46 ± 0.87	37	0.03 ± 0.03	2.81 ± 0.88	0.00 ± 0.00	0.00 ± 0.00	3
10	1	0.08 ± 0.08	0	$0.00^{+0.57}_{-0.00}$	0	0.00 ± 0.00	$0.08^{+0.57}_{-0.08}$	0.06 ± 0.04	0.00 ± 0.00	0
11	10	3.5 ± 1.1	4	0.98 ± 0.49	0	0.00 ± 0.00	4.5 ± 1.2	0.00 ± 0.00	0.00 ± 0.00	4
12	2	0.69 ± 0.49	0	$0.00^{+0.90}_{-0.00}$	0	0.00 ± 0.00	$0.7^{+1.0}_{-0.7}$	0.00 ± 0.00	0.11 ± 0.11	0
13	10	0.80 ± 0.25	15	4.6 ± 1.2	157	0.12 ± 0.01	5.5 ± 1.2	0.14 ± 0.07	0.18 ± 0.10	7
14	1	0.08 ± 0.08	0	$0.00^{+0.57}_{-0.00}$	5	0.00 ± 0.00	$0.08^{+0.57}_{-0.08}$	1.19 ± 0.18	0.96 ± 0.27	0
15	31	10.7 ± 1.9	12	2.95 ± 0.85	0	0.00 ± 0.00	13.7 ± 2.1	0.03 ± 0.02	0.61 ± 0.17	9
16	5	1.73 ± 0.77	0	$0.00^{+0.90}_{-0.00}$	0	0.00 ± 0.00	1.7 ± 1.2	0.18 ± 0.06	3.41 ± 0.42	3
17	1	0.08 ± 0.08	4	1.23 ± 0.61	186	0.14 ± 0.01	1.45 ± 0.62	0.07 ± 0.05	0.00 ± 0.00	0
18	0	0.01 ± 0.01	0	$0.00^{+0.57}_{-0.00}$	12	0.01 ± 0.01	$0.02^{+0.57}_{-0.02}$	0.67 ± 0.18	0.00 ± 0.00	0
19	7	2.42 ± 0.92	2	0.49 ± 0.35	0	0.00 ± 0.00	2.92 ± 0.98	0.00 ± 0.00	0.00 ± 0.00	4
20	3	1.04 ± 0.60	1	0.25 ± 0.25	0	0.00 ± 0.00	1.28 ± 0.65	0.07 ± 0.04	0.00 ± 0.00	1
21	2	0.16 ± 0.11	4	1.23 ± 0.61	198	0.15 ± 0.01	1.54 ± 0.63	0.61 ± 0.14	1.19 ± 0.35	2
22	0	0.03 ± 0.03	0	$0.00^{+0.57}_{-0.00}$	10	0.01 ± 0.01	$0.04^{+0.57}_{-0.04}$	4.81 ± 0.40	1.91 ± 0.40	0
23	9	3.1 ± 1.0	5	1.23 ± 0.55	0	0.00 ± 0.00	4.4 ± 1.2	0.10 ± 0.05	0.94 ± 0.16	6
24	1	0.35 ± 0.35	0	$0.00^{+0.90}_{-0.00}$	0	0.00 ± 0.00	$0.35^{+0.97}_{-0.35}$	1.22 ± 0.19	4.10 ± 0.51	0
25	6	0.48 ± 0.20	1	0.31 ± 0.31	23	0.02 ± 0.02	0.80 ± 0.36	0.02 ± 0.02	0.09 ± 0.09	3
26	4	0.32 ± 0.16	0	$0.00^{+0.57}_{-0.00}$	1	0.00 ± 0.00	$0.32^{+0.59}_{-0.32}$	0.08 ± 0.05	0.00 ± 0.00	0
27	42	14.6 ± 2.2	4	0.98 ± 0.49	0	0.00 ± 0.00	15.5 ± 2.3	0.00 ± 0.00	0.00 ± 0.00	13

(Table continued)

TABLE VIII. *(Continued)*

SR no.	CR	Spurious	CR	Showering	CR	Muon	Total bkg.	T6tbLL (1000, 900, 200)	T5btbtLL (1500, 1100, 10)	Observed
28	8	2.77 ± 0.98	1	0.25 ± 0.25	0	0.00 ± 0.00	3.0 ± 1.0	0.02 ± 0.02	0.03 ± 0.03	2
29	3	0.24 ± 0.14	0	$0.00^{+0.57}_{-0.00}$	19	0.01 ± 0.01	$0.25^{+0.58}_{-0.25}$	0.00 ± 0.00	0.00 ± 0.00	0
30	3	0.24 ± 0.14	0	$0.00^{+0.57}_{-0.00}$	0	0.00 ± 0.00	$0.24^{+0.58}_{-0.24}$	0.00 ± 0.00	0.00 ± 0.00	0
31	8	2.77 ± 0.98	1	0.25 ± 0.25	0	0.00 ± 0.00	3.0 ± 1.0	0.00 ± 0.00	0.00 ± 0.00	2
32	3	1.04 ± 0.60	0	$0.00^{+0.90}_{-0.00}$	0	0.00 ± 0.00	$1.0^{+1.1}_{-1.0}$	0.00 ± 0.00	0.03 ± 0.02	0
33	3	0.24 ± 0.14	4	1.23 ± 0.61	155	0.11 ± 0.01	1.58 ± 0.63	0.06 ± 0.04	0.48 ± 0.25	2
34	0	0.04 ± 0.04	0	$0.00^{+0.57}_{-0.00}$	6	0.00 ± 0.00	$0.05^{+0.57}_{-0.05}$	0.71 ± 0.16	0.59 ± 0.27	0
35	20	6.9 ± 1.6	2	0.49 ± 0.35	0	0.00 ± 0.00	7.4 ± 1.6	0.00 ± 0.00	0.31 ± 0.18	4
36	2	0.69 ± 0.49	1	0.25 ± 0.25	0	0.00 ± 0.00	0.94 ± 0.55	0.12 ± 0.06	0.76 ± 0.22	1
37	9	0.72 ± 0.24	0	$0.00^{+0.57}_{-0.00}$	7	0.01 ± 0.01	0.73 ± 0.61	0.03 ± 0.03	0.00 ± 0.00	0
38	3	0.24 ± 0.14	0	$0.00^{+0.57}_{-0.00}$	1	0.00 ± 0.00	$0.24^{+0.58}_{-0.24}$	0.04 ± 0.04	0.01 ± 0.01	1
39	39	13.5 ± 2.2	5	1.23 ± 0.55	0	0.00 ± 0.00	14.7 ± 2.2	0.00 ± 0.00	0.00 ± 0.00	10
40	2	0.69 ± 0.49	1	0.25 ± 0.25	0	0.00 ± 0.00	0.94 ± 0.55	0.00 ± 0.00	0.00 ± 0.00	2
41	1	0.08 ± 0.08	1	0.31 ± 0.31	12	0.01 ± 0.01	0.40 ± 0.32	0.00 ± 0.00	0.00 ± 0.00	0
42	0	0.01 ± 0.01	0	$0.00^{+0.57}_{-0.00}$	0	0.00 ± 0.00	$0.01^{+0.57}_{-0.01}$	0.00 ± 0.00	0.00 ± 0.00	0
43	6	2.08 ± 0.85	3	0.74 ± 0.43	0	0.00 ± 0.00	2.82 ± 0.95	0.00 ± 0.00	0.00 ± 0.00	4
44	0	0.37 ± 0.37	0	$0.00^{+0.90}_{-0.00}$	0	0.00 ± 0.00	$0.37^{+0.98}_{-0.37}$	0.00 ± 0.00	0.03 ± 0.02	0
45	5	0.40 ± 0.18	3	0.92 ± 0.53	47	0.03 ± 0.01	1.36 ± 0.56	0.27 ± 0.10	0.14 ± 0.05	0
46	0	0.07 ± 0.07	0	$0.00^{+0.57}_{-0.00}$	3	0.00 ± 0.00	$0.07^{+0.57}_{-0.07}$	1.12 ± 0.22	0.72 ± 0.22	0
47	13	4.5 ± 1.3	2	0.49 ± 0.35	0	0.00 ± 0.00	5.0 ± 1.3	0.00 ± 0.00	0.37 ± 0.14	3
48	2	0.69 ± 0.49	0	$0.00^{+0.90}_{-0.00}$	0	0.00 ± 0.00	$0.7^{+1.0}_{-0.7}$	0.27 ± 0.09	0.91 ± 0.19	0
49	1	0.35 ± 0.35	0	$0.00^{+0.57}_{-0.00}$	1	0.00 ± 0.00	$0.35^{+0.66}_{-0.35}$	4.57 ± 0.39	0.66 ± 0.24	0

are used in evaluating the limits for each signal model point. For the models of gluino pair production and top or bottom squark pair production, limits are derived in the mass plane of the mother particle and the LSP for different choices of chargino $c\tau$. We evaluate 95% confidence level (C.L.) upper limits on the signal cross sections. The approximate NNLO + NNLL cross section is used to determine corresponding mass exclusion curves. Expected limits are computed using the background-only hypothesis in place of the observed numbers of events.

For the strong production models, the sensitivity of our results depends on the mass difference $\Delta m_{(\tilde{g},\tilde{q})\text{–LSP}}$ between the gluino or squark and the LSP. The limits weaken when $\Delta m_{(\tilde{g},\tilde{q})\text{–LSP}}$ is small because of the resulting small boost (and thus short decay length) of the chargino in the detector frame. The limits also weaken for small LSP masses because of the significant boost of the chargino, which increasingly fails to decay within the tracker volume as $\Delta m_{(\tilde{g},\tilde{q})\text{–LSP}}$ increases. The strongest constraints on the cross section reside at varying intermediate values of $\Delta m_{(\tilde{g},\tilde{q})\text{–LSP}}$, depending on the chargino $c\tau$.

Upper limits on the cross section for the T6tbLL and T6btLL models are presented in Fig. 10. For the T6tbLL model, we exclude bottom squarks below a mass of 900–1540 GeV, depending on the LSP mass and chargino lifetime. Charginos and LSPs, taken to be essentially mass degenerate in our study, are excluded up to a mass of 850 (1210) GeV for chargino $c\tau = 10$ (200) cm, depending on the bottom squark mass. The analogous limits for the T6btLL model are 1100–1590 GeV for the top squark mass and 1050 (1400) GeV for the chargino and LSP mass. These results extend the maximum limit on the LSP mass in the compressed phase space scenario by hundreds of GeV compared to the previous study [22], both for $c\tau = 10$ and 200 cm.

Upper limits on the cross section for the T5btbtLL model are presented in Fig. 11. Gluinos are excluded below a mass of 1450–2300 GeV, depending on LSP mass and chargino lifetime. Charginos and LSPs are excluded up to a maximum of 1950 GeV, depending on the gluino mass and chargino lifetime.

In Figs. 10 and 11, the white bands indicate the regions previously excluded by the CERN LEP experiments [105].

We examined the change in sensitivity introduced by our inclusion of the electron + DTk and muon + DTk channels in the analysis. We find that, compared to using the fully hadronic channel alone, addition of these channels leads to an improvement of around 40 GeV in the top squark mass limit and of around 100 GeV in both the bottom squark and gluino mass limits.

Finally, limits on pure wino [29] and Higgsino [32] DM models are presented in Fig. 12 for the case of a minimal mass splitting $\Delta m^{\pm}$ between the two lightest SUSY states, bounded by two-loop radiative corrections. The chargino lifetime is determined as a function of $\Delta m^{\pm}$, as described in

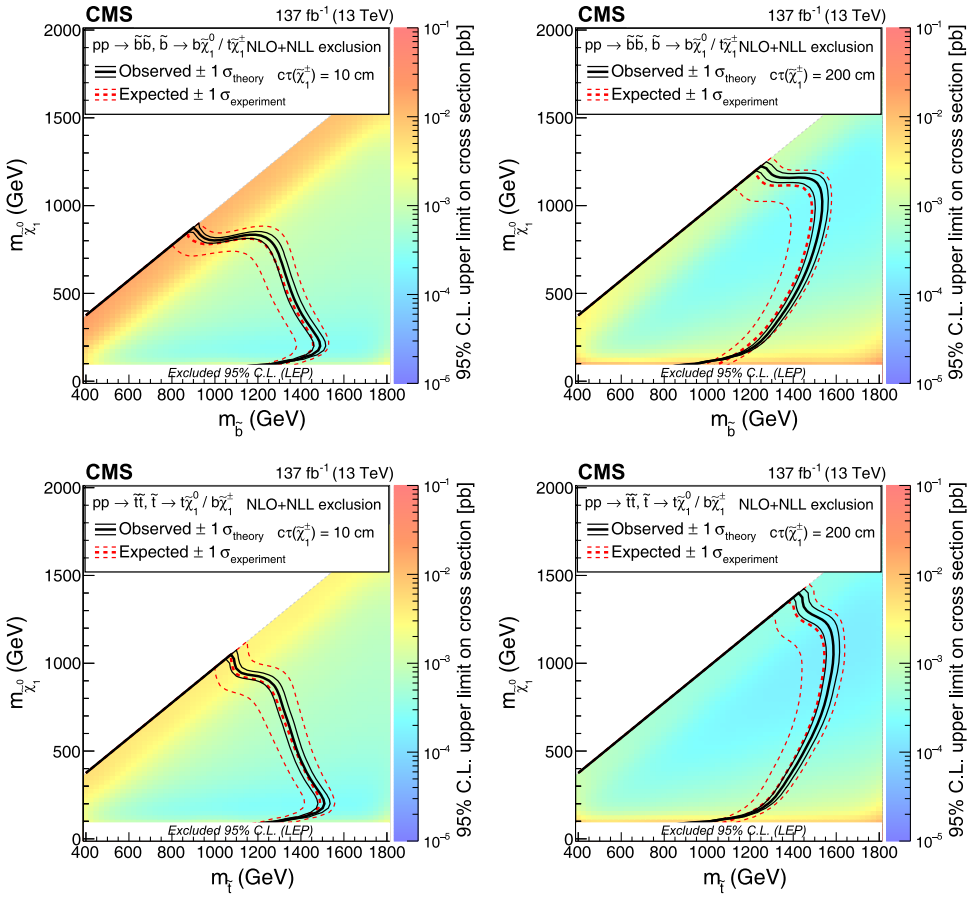

FIG. 10. Observed 95% C.L. upper limits on the signal cross sections (colored area) versus the bottom or top squark and neutralino mass for the T6tbLL (upper) and T6btLL (lower) model for a chargino proper decay length $c\tau$ of 10 (left column) or 200 (right column) cm. Also shown are black (red) contours corresponding to the observed (expected) lower limits, including their uncertainties, on the squark and neutralino masses.

Ref. [30] for the wino case and in Ref. [31] for the Higgsino case. The production scenario accounts for the TChiWZ, TChiWW, and TChiW models taken together, where the first process occurs only in the Higgsino case. The green line indicates the minimum mass splitting required by the radiative corrections. Chargino and LSP masses are excluded up to 650 GeV for the pure wino model and up to 190 GeV for the pure Higgsino model.

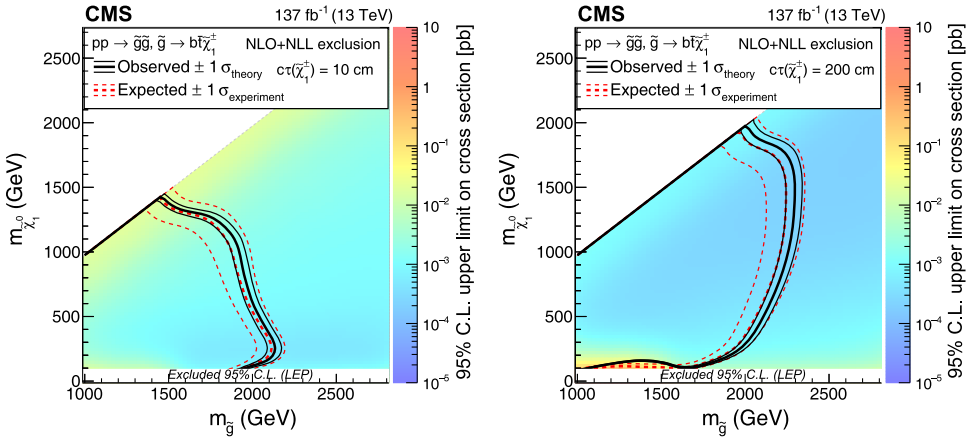

FIG. 11. Observed 95% C.L. upper limits on the signal cross sections (colored area) versus the gluino and neutralino mass for the T5btbtLL model for a chargino proper decay length $c\tau$ of 10 (left column) and 200 (right column) cm. Also shown are black (red) contours corresponding to the observed (expected) lower limits, including their uncertainties, on the gluino and neutralino masses.

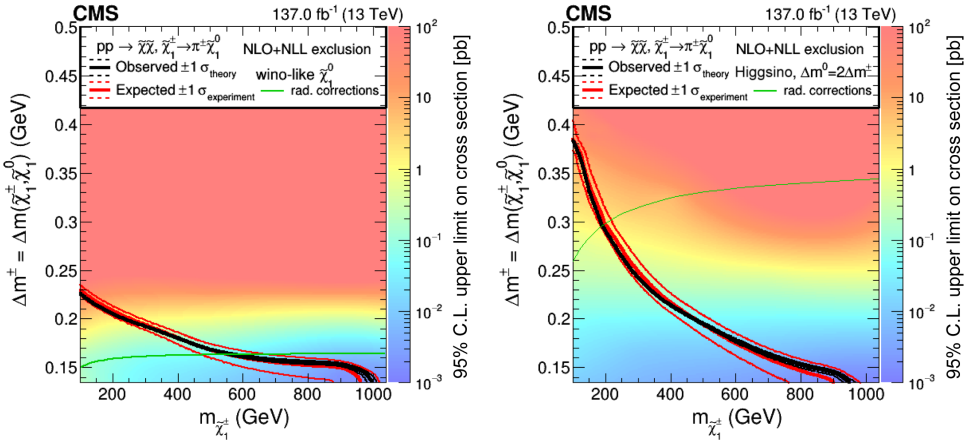

FIG. 12. Observed 95% C.L. upper limits on the signal cross sections (colored area) versus the chargino-LSP mass difference and the mass of the chargino for the wino (left) and Higgsino (right) DM models. The black contours indicate the boundary where the observed upper limit equals the cross section of fully degenerate electroweakino production. The corresponding expected limits are shown by the red contours. The green lines represent the set of model points corresponding to the pure wino and pure Higgsino models where only radiative corrections to the mass splitting are assumed. Chargino lifetimes are based on two-loop calculations.

XI. SUMMARY

A search for long-lived charginos based on data collected in proton-proton collisions at $\sqrt{s} = 13$ TeV, corresponding to an integrated luminosity of 137 fb^{-1}, is presented. Event yields are studied in 49 nonoverlapping search regions defined by the number of electrons, muons, jets, and b-tagged jets, and by the hard missing transverse momentum, in final states with at least one identified disappearing track. Further categorization of the SRs is based on the approximate length of the track and on its dE/dx energy loss in the inner tracking detector. The analysis targets a wide variety of possible production modes appearing in simplified models of R-parity conserving supersymmetry, including gluino, top squark, bottom squark, and electroweakino pair production. A machine-learning-based classifier is employed to optimally select disappearing tracks, while rejecting tracks originating from failures in the reconstruction or from combinatorial effects. Background contributions to the SRs are evaluated based on the observed yields in data control regions. The observed yields in the SRs are found to be consistent with the background-only predictions, and thus no evidence for supersymmetry is found.

In the context of the examined models, bottom squarks, top squarks, and gluinos with masses as large as 1540, 1590, and 2300 GeV, respectively, are excluded. For bottom squark pair production, charginos and the lightest supersymmetric particle, considered to be essentially mass degenerate in our study, are excluded up to a mass of 850 (1210) GeV for a chargino proper decay length $c\tau$ of 10 (200) cm. For top squark pair production, the corresponding limit on the chargino and LSP mass is 1050 (1400) GeV. These results extend the maximum limit on the LSP mass in the compressed phase space scenario by hundreds of GeV compared to the previous study [22] and extend the reach of sensitivity into mass regions where a pure wino- or pure Higgsino-like LSP can account for the observed dark matter relic density. Limits are also determined for a pure wino dark matter model [29] and a pure Higgsino dark matter model [32]. In the context of these two models, charginos and LSPs are excluded up to 650 GeV for the wino model and up to 190 GeV for the Higgsino model.

ACKNOWLEDGMENTS

We congratulate our colleagues in the CERN accelerator departments for the excellent performance of the LHC and thank the technical and administrative staffs at CERN and at other CMS institutes for their contributions to the success of the CMS effort. In addition, we gratefully acknowledge the computing centers and personnel of the Worldwide LHC Computing Grid and other centers for delivering so effectively the computing infrastructure essential to our analyses. Finally, we acknowledge the enduring support for the construction and operation of the LHC, the CMS detector, and the supporting computing infrastructure provided by the following funding agencies: SC (Armenia); BMBWF and FWF (Austria); FNRS and FWO (Belgium); CNPq, CAPES, FAPERJ, FAPERGS, and FAPESP (Brazil); MES and BNSF (Bulgaria); CERN; CAS, MoST, and NSFC (China); MINCIENCIAS (Colombia); MSES and CSF (Croatia); RIF (Cyprus); SENESCYT (Ecuador); MoER, ERC PUT, and ERDF (Estonia); Academy of Finland, MEC, and HIP (Finland); CEA and CNRS/IN2P3 (France); SRNSF (Georgia); BMBF, DFG, and HGF (Germany); GSRI (Greece); NKFIH (Hungary); DAE and DST (India); IPM (Iran); SFI (Ireland); INFN (Italy); MSIP and NRF (Republic of

Korea); MES (Latvia); LAS (Lithuania); MOE and UM (Malaysia); BUAP, CINVESTAV, CONACYT, LNS, SEP, and UASLP-FAI (Mexico); MOS (Montenegro); MBIE (New Zealand); PAEC (Pakistan); MES and NSC (Poland); FCT (Portugal); MESTD (Serbia); MCIN/AEI and PCTI (Spain); MOSTR (Sri Lanka); Swiss Funding Agencies (Switzerland); MST (Taipei); MHESI and NSTDA (Thailand); TUBITAK and TENMAK (Turkey); NASU (Ukraine); STFC (United Kingdom); DOE and NSF (U.S.). Individuals have received support from the Marie-Curie program and the European Research Council and Horizon 2020 Grant, Contracts No. 675440, No. 724704, No. 752730, No. 758316, No. 765710, No. 824093, and COST Action CA16108 (European Union); the Leventis Foundation; the Alfred P. Sloan Foundation; the Alexander von Humboldt Foundation; the Science Committee, Project No. 22rl-037 (Armenia); the Belgian Federal Science Policy Office; the Fonds pour la Formation *à la* Recherche dans l'Industrie et dans l'Agriculture (FRIA-Belgium); the Agentschap voor Innovatie door Wetenschap en Technologie (IWT-Belgium); the F. R. S.-FNRS and FWO (Belgium) under the "Excellence of Science—EOS"—be.h Project No. 30820817; the Beijing Municipal Science and Technology Commission, No. Z191100007219010 and Fundamental Research Funds for the Central Universities (China); the Ministry of Education, Youth, and Sports (MEYS) of the Czech Republic; the Shota Rustaveli National Science Foundation, Grant No. FR-22-985 (Georgia); the Deutsche Forschungsgemeinschaft (DFG), under Germany's Excellence Strategy—EXC 2121 "Quantum Universe"—390833306, and under Project No. 400140256—GRK2497; the Hellenic Foundation for Research and Innovation (HFRI), Project No. 2288 (Greece); the Hungarian Academy of Sciences, the New National Excellence Program—ÚNKP, the NKFIH research Grants No. K 124845, No. K 124850, No. K 128713, No. K 128786, No. K 129058, No. K 131991, No. K 133046, No. K 138136, No. K 143460, No. K 143477, No. 2020-2.2.1-ED-2021-00181, and No. TKP2021-NKTA-64 (Hungary); the Council of Science and Industrial Research, India; the Latvian Council of Science; the Ministry of Education and Science, Project No. 2022/WK/14, and the National Science Center, Contracts Opus 2021/41/B/ST2/01369 and 2021/43/B/ST2/01552 (Poland); the Fundação para a Ciência e a Tecnologia, Grant No. CEECIND/01334/2018 (Portugal); the National Priorities Research Program by Qatar National Research Fund; MCIN/AEI/10.13039/501100011033, ERDF "a way of making Europe," and the Programa Estatal de Fomento de la Investigación Científica y Técnica de Excelencia María de Maeztu, Grant No. MDM-2017-0765 and Programa Severo Ochoa del Principado de Asturias (Spain); the Chulalongkorn Academic into Its Second Century Project Advancement Project, and the National Science, Research and Innovation Fund via the Program Management Unit for Human Resources and Institutional Development, Research and Innovation, Grant No. B05F650021 (Thailand); the Kavli Foundation; the Nvidia Corporation; the SuperMicro Corporation; the Welch Foundation, Contract No. C-1845; and the Weston Havens Foundation (U.S.).

[1] P. Ramond, Dual theory for free fermions, Phys. Rev. D **3**, 2415 (1971).
[2] Yu. A. Gol'fand and E. P. Likhtman, Extension of the algebra of Poincaré group generators and violation of P invariance, JETP Lett. **13**, 323 (1971), http://www.jetpletters.ru/ps/1584/article_24309.pdf.
[3] A. Neveu and J. H. Schwarz, Factorizable dual model of pions, Nucl. Phys. **B31**, 86 (1971).
[4] D. V. Volkov and V. P. Akulov, Possible universal neutrino interaction, JETP Lett. **16**, 438 (1972).
[5] J. Wess and B. Zumino, A Lagrangian model invariant under supergauge transformations, Phys. Lett. **49B**, 52 (1974).
[6] J. Wess and B. Zumino, Supergauge transformations in four dimensions, Nucl. Phys. **B70**, 39 (1974).
[7] P. Fayet, Supergauge invariant extension of the Higgs mechanism and a model for the electron and its neutrino, Nucl. Phys. **B90**, 104 (1975).
[8] P. Fayet and S. Ferrara, Supersymmetry, Phys. Rep. **32**, 249 (1977).
[9] H. P. Nilles, Supersymmetry, supergravity and particle physics, Phys. Rep. **110**, 1 (1984).
[10] F. Zwicky, On the masses of nebulae and of clusters of nebulae, Astrophys. J. **86**, 217 (1937).
[11] V. C. Rubin and W. K. Ford, Jr., Rotation of the Andromeda nebula from a spectroscopic survey of emission regions, Astrophys. J. **159**, 379 (1970).
[12] L. Susskind, Dynamics of spontaneous symmetry breaking in the Weinberg-Salam theory, Phys. Rev. D **20**, 2619 (1979).
[13] G. 't Hooft, Naturalness, chiral symmetry, and spontaneous chiral symmetry breaking, NATO Sci. Ser. B **59**, 135 (1980).
[14] M. J. G. Veltman, The infrared-ultraviolet connection, Acta Phys. Pol. B **12**, 437 (1981), https://www.actaphys.uj.edu.pl/R/12/5/437/pdf.

[15] ATLAS Collaboration, The ATLAS experiment at the CERN Large Hadron Collider, J. Instrum. **3**, S08003 (2008).

[16] CMS Collaboration, The CMS experiment at the CERN LHC, J. Instrum. **3**, S08004 (2008).

[17] N. Aghanim *et al.* (Planck Collaboration), Planck 2018 results. VI. Cosmological parameters, Astron. Astrophys. **641**, A6 (2020); **652**, C4 (2021).

[18] G. R. Farrar and P. Fayet, Phenomenology of the production, decay, and detection of new hadronic states associated with supersymmetry, Phys. Lett. **76B**, 575 (1978).

[19] A. Delgado and M. Quirós, Higgsino dark matter in the MSSM, Phys. Rev. D **103**, 015024 (2021).

[20] K. Griest and D. Seckel, Three exceptions in the calculation of relic abundances, Phys. Rev. D **43**, 3191 (1991).

[21] G. Jungman, M. Kamionkowski, and K. Griest, Supersymmetric dark matter, Phys. Rep. **267**, 195 (1996).

[22] CMS Collaboration, Searches for physics beyond the standard model with the M_{T2} variable in hadronic final states with and without disappearing tracks in proton-proton collisions at $\sqrt{s} = 13$ TeV, Eur. Phys. J. C **80**, 3 (2020).

[23] CMS Collaboration, Search for disappearing tracks in proton-proton collisions at $\sqrt{s} = 13$ TeV, Phys. Lett. B **806**, 135502 (2020).

[24] ATLAS Collaboration, Search for long-lived charginos based on a disappearing-track signature using 136 fb^{-1} of pp collisions at $\sqrt{s} = 13$ TeV with the ATLAS detector, Eur. Phys. J. C **82**, 606 (2022).

[25] HEPData record for this analysis (2023), https://doi.org/10.17182/hepdata.144178.

[26] J. Alwall, P. C. Schuster, and N. Toro, Simplified models for a first characterization of new physics at the LHC, Phys. Rev. D **79**, 075020 (2009).

[27] D. Alves, N. Arkani-Hamed, S. Arora, Y. Bai, M. Baumgart, J. Berger, M. Buckley, B. Butler, S. Chang, H.-C. Cheng, C. Cheung, R. S. Chivukula, W. S. Cho, R. Cotta, M. D'Alfonso *et al.*, Simplified models for LHC new physics searches, J. Phys. G **39**, 105005 (2012).

[28] CMS Collaboration, Interpretation of searches for supersymmetry with simplified models, Phys. Rev. D **88**, 052017 (2013).

[29] M. Ibe, S. Matsumoto, and R. Sato, Mass splitting between charged and neutral winos at two-loop level, Phys. Lett. B **721**, 252 (2013).

[30] M. Ibe, M. Mishima, Y. Nakayama, and S. Shirai, Precise estimate of charged wino decay rate, J. High Energy Phys. 01 (2023) 017.

[31] N. Nagata and S. Shirai, Higgsino dark matter in high-scale supersymmetry, J. High Energy Phys. 01 (2015) 029.

[32] H. Fukuda, N. Nagata, H. Otono, and S. Shirai, Higgsino dark matter or not: Role of disappearing track searches at the LHC and future colliders, Phys. Lett. B **781**, 306 (2018).

[33] S. P. Martin, A supersymmetry primer, Adv. Ser. Dir. High Energy Phys. **18**, 1 (1998).

[34] B. C. Allanach, SOFTSUSY: A program for calculating supersymmetric spectra, Comput. Phys. Commun. **143**, 305 (2002).

[35] W. Adam *et al.* (CMS Tracker Group), The CMS phase-1 pixel detector upgrade, J. Instrum. **16**, P02027 (2021).

[36] CMS Collaboration, The CMS trigger system, J. Instrum. **12**, P01020 (2017).

[37] CMS Collaboration, Performance of the CMS Level-1 trigger in proton-proton collisions at $\sqrt{s} = 13$ TeV, J. Instrum. **15**, P10017 (2020).

[38] CMS Collaboration, Particle-flow reconstruction and global event description with the CMS detector, J. Instrum. **12**, P10003 (2017).

[39] CMS Collaboration, Electron and photon reconstruction and identification with the CMS experiment at the CERN LHC, J. Instrum. **16**, P05014 (2021).

[40] CMS Collaboration, Performance of the CMS muon detector and muon reconstruction with proton-proton collisions at $\sqrt{s} = 13$ TeV, J. Instrum. **13**, P06015 (2018).

[41] CMS Collaboration, Technical proposal for the phase-II upgrade of the compact muon solenoid, CMS Technical Proposal, Reports No. CERN-LHCC-2015-010, No. CMS-TDR-15-02, 2015.

[42] M. Cacciari, G. P. Salam, and G. Soyez, The anti-k_T jet clustering algorithm, J. High Energy Phys. 04 (2008) 063.

[43] M. Cacciari, G. P. Salam, and G. Soyez, FastJet user manual, Eur. Phys. J. C **72**, 1896 (2012).

[44] CMS Collaboration, Jet performance in pp collisions at $\sqrt{s} = 7$ TeV, CMS Physics Analysis Summary, Report No. CMS-PAS-JME-10-003, 2010, https://cds.cern.ch/record/1279362.

[45] CMS Collaboration, Jet algorithms performance in 13 TeV data, CMS Physics Analysis Summary, Report No. CMS-PAS-JME-16-003, 2017, https://cds.cern.ch/record/2256875.

[46] CMS Collaboration, Jet energy scale and resolution in the CMS experiment in pp collisions at 8 TeV, J. Instrum. **12**, P02014 (2017).

[47] M. Cacciari and G. P. Salam, Pileup subtraction using jet areas, Phys. Lett. B **659**, 119 (2008).

[48] CMS Collaboration, Identification of heavy-flavour jets with the CMS detector in pp collisions at 13 TeV, J. Instrum. **13**, P05011 (2018).

[49] K. Rehermann and B. Tweedie, Efficient identification of boosted semileptonic top quarks at the LHC, J. High Energy Phys. 03 (2011) 059.

[50] J. Alwall, R. Frederix, S. Frixione, V. Hirschi, F. Maltoni, O. Mattelaer, H.-S. Shao, T. Stelzer, P. Torrielli, and M. Zaro, The automated computation of tree-level and next-to-leading order differential cross sections, and their matching to parton shower simulations, J. High Energy Phys. 07 (2014) 079.

[51] J. Alwall *et al.*, Comparative study of various algorithms for the merging of parton showers and matrix elements in hadronic collisions, Eur. Phys. J. C **53**, 473 (2008).

[52] R. Frederix and S. Frixione, Merging meets matching in MC@NLO, J. High Energy Phys. 12 (2012) 061.

[53] P. Nason, A new method for combining NLO QCD with shower Monte Carlo algorithms, J. High Energy Phys. 11 (2004) 040.

[54] S. Frixione, P. Nason, and C. Oleari, Matching NLO QCD computations with parton shower simulations: The POWHEG method, J. High Energy Phys. 11 (2007) 070.

[55] S. Alioli, P. Nason, C. Oleari, and E. Re, A general framework for implementing NLO calculations in shower

Monte Carlo programs: The POWHEG BOX, J. High Energy Phys. 06 (2010) 043.
[56] S. Alioli, P. Nason, C. Oleari, and E. Re, NLO single-top production matched with shower in POWHEG: s- and t-channel contributions, J. High Energy Phys. 09 (2009) 111; 02 (2010) 11.
[57] E. Re, Single-top Wt-channel production matched with parton showers using the POWHEG method, Eur. Phys. J. C **71**, 1547 (2011).
[58] T. Melia, P. Nason, R. Rontsch, and G. Zanderighi, W^+W^-, WZ and ZZ production in the POWHEG BOX, J. High Energy Phys. 11 (2011) 078.
[59] M. Beneke, P. Falgari, S. Klein, and C. Schwinn, Hadronic top-quark pair production with NNLL threshold resummation, Nucl. Phys. **B855**, 695 (2012).
[60] M. Cacciari, M. Czakon, M. Mangano, A. Mitov, and P. Nason, Top-pair production at hadron colliders with next-to-next-to-leading logarithmic soft-gluon resummation, Phys. Lett. B **710**, 612 (2012).
[61] P. Bärnreuther, M. Czakon, and A. Mitov, Percent level precision physics at the Tevatron: First genuine NNLO QCD corrections to $q\bar{q} \to t\bar{t} + X$, Phys. Rev. Lett. **109**, 132001 (2012).
[62] M. Czakon and A. Mitov, NNLO corrections to top-pair production at hadron colliders: The all-fermionic scattering channels, J. High Energy Phys. 12 (2012) 054.
[63] M. Czakon and A. Mitov, NNLO corrections to top pair production at hadron colliders: The quark-gluon reaction, J. High Energy Phys. 01 (2013) 080.
[64] M. Czakon, P. Fiedler, and A. Mitov, Total top-quark pair-production cross section at hadron colliders through $O(\alpha_S^4)$, Phys. Rev. Lett. **110**, 252004 (2013).
[65] R. Gavin, Y. Li, F. Petriello, and S. Quackenbush, W physics at the LHC with FEWZ 2.1, Comput. Phys. Commun. **184**, 208 (2013).
[66] R. Gavin, Y. Li, F. Petriello, and S. Quackenbush, FEWZ 2.0: A code for hadronic Z production at next-to-next-to-leading order, Comput. Phys. Commun. **182**, 2388 (2011).
[67] S. Agostinelli *et al.* (Geant4 Collaboration), Geant4—a simulation toolkit, Nucl. Instrum. Methods Phys. Res., Sect. A **506**, 250 (2003).
[68] W. Beenakker, R. Höpker, M. Spira, and P. M. Zerwas, Squark and gluino production at hadron colliders, Nucl. Phys. **B492**, 51 (1997).
[69] A. Kulesza and L. Motyka, Threshold resummation for squark-antisquark and gluino-pair production at the LHC, Phys. Rev. Lett. **102**, 111802 (2009).
[70] A. Kulesza and L. Motyka, Soft gluon resummation for the production of gluino-gluino and squark-antisquark pairs at the LHC, Phys. Rev. D **80**, 095004 (2009).
[71] W. Beenakker, S. Brensing, M. Krämer, A. Kulesza, E. Laenen, and I. Niessen, Soft-gluon resummation for squark and gluino hadroproduction, J. High Energy Phys. 12 (2009) 041.
[72] W. Beenakker, S. Brensing, M. Krämer, A. Kulesza, E. Laenen, L. Motyka, and I. Niessen, Squark and gluino hadroproduction, Int. J. Mod. Phys. A **26**, 2637 (2011).
[73] W. Beenakker, C. Borschensky, M. Kraemer, A. Kulesza, and E. Laenen, NNLL-fast: Predictions for coloured supersymmetric particle production at the LHC with threshold and Coulomb resummation, J. High Energy Phys. 12 (2016) 133.
[74] W. Beenakker, S. Brensing, M. Kramer, A. Kulesza, E. Laenen, and I. Niessen, NNLL resummation for squark-antisquark pair production at the LHC, J. High Energy Phys. 01 (2012) 076.
[75] W. Beenakker, T. Janssen, S. Lepoeter, M. Kraemer, A. Kulesza, E. Laenen, I. Niessen, S. Thewes, and T. Van Daal, Towards NNLL resummation: Hard matching coefficients for squark and gluino hadroproduction, J. High Energy Phys. 10 (2013) 120.
[76] W. Beenakker, C. Borschensky, M. Kraemer, A. Kulesza, E. Laenen, V. Theeuwes, and S. Thewes, NNLL resummation for squark and gluino production at the LHC, J. High Energy Phys. 12 (2014) 023.
[77] W. Beenakker, M. Kramer, T. Plehn, M. Spira, and P. M. Zerwas, Stop production at hadron colliders, Nucl. Phys. **B515**, 3 (1998).
[78] W. Beenakker, S. Brensing, M. Kramer, A. Kulesza, E. Laenen, and I. Niessen, Supersymmetric top and bottom squark production at hadron colliders, J. High Energy Phys. 08 (2010) 098.
[79] W. Beenakker, C. Borschensky, R. Heger, M. Kraemer, A. Kulesza, and E. Laenen, NNLL resummation for stop pair-production at the LHC, J. High Energy Phys. 05 (2016) 153.
[80] T. Sjöstrand, S. Ask, J. R. Christiansen, R. Corke, N. Desai, P. Ilten, S. Mrenna, S. Prestel, C. O. Rasmussen, and P. Z. Skands, An introduction to PYTHIA 8.2, Comput. Phys. Commun. **191**, 159 (2015).
[81] S. Abdullin, P. Azzi, F. Beaudette, P. Janot, and A. Perrotta, The fast simulation of the CMS detector at LHC, J. Phys. Conf. Ser. **331**, 032049 (2011).
[82] A. Giammanco, The fast simulation of the CMS experiment, J. Phys. Conf. Ser. **513**, 022012 (2014).
[83] CMS Collaboration, Event generator tunes obtained from underlying event and multiparton scattering measurements, Eur. Phys. J. C **76**, 155 (2016).
[84] CMS Collaboration, Extraction and validation of a new set of CMS PYTHIA8 tunes from underlying-event measurements, Eur. Phys. J. C **80**, 4 (2020).
[85] R. D. Ball, V. Bertone, S. Carrazza, L. Del Debbio, S. Forte, A. Guffanti, N. P. Hartland, and J. Rojo (NNPDF Collaboration), Parton distributions with QED corrections, Nucl. Phys. **B877**, 290 (2013).
[86] R. D. Ball *et al.* (NNPDF Collaboration), Parton distributions from high-precision collider data, Eur. Phys. J. C **77**, 663 (2017).
[87] CMS Collaboration, Search for supersymmetry in multijet events with missing transverse momentum in proton-proton collisions at 13 TeV, Phys. Rev. D **96**, 032003 (2017).
[88] CMS Collaboration, Search for new phenomena with the M_{T2} variable in the all-hadronic final state produced in proton-proton collisions at $\sqrt{s} = 13$ TeV, Eur. Phys. J. C **77**, 710 (2017).
[89] CMS Collaboration, Search for heavy stable charged particles in pp collisions at $\sqrt{s} = 7$ TeV, J. High Energy Phys. 03 (2011) 024.
[90] CMS Collaboration, Search for long-lived charged particles in proton-proton collisions at $\sqrt{s} = 13$ TeV, Phys. Rev. D **94**, 112004 (2016).

[91] G. Arnison *et al.* (UA1 Collaboration), Experimental observation of isolated large transverse energy electrons with associated missing energy at $\sqrt{s} = 540$ GeV, Phys. Lett. B **122**, 103 (1983).
[92] G. Kasieczka, B. Nachman, M. D. Schwartz, and D. Shih, Automating the ABCD method with machine learning, Phys. Rev. D **103**, 035021 (2021).
[93] CMS Collaboration, Precision luminosity measurement in proton-proton collisions at $\sqrt{s} = 13$ TeV in 2015 and 2016 at CMS, Eur. Phys. J. C **81**, 800 (2021).
[94] CMS Collaboration, CMS luminosity measurement for the 2017 data-taking period at $\sqrt{s} = 13$ TeV, CMS Physics Analysis Summary, Report No. CMS-PAS-LUM-17-004, 2018, https://cds.cern.ch/record/2621960.
[95] CMS Collaboration, CMS luminosity measurement for the 2018 data-taking period at $\sqrt{s} = 13$ TeV, CMS Physics Analysis Summary, Report No. CMS-PAS-LUM-18-002, 2019, https://cds.cern.ch/record/2676164.
[96] A. Giraldi, Precision luminosity measurement with proton-proton collisions at the CMS experiment in run 2, in *Proceedings of the 41st International Conference on High Energy Physics (ICHEP2022)* (2022), p. 638, 10.22323/1.414.0638.
[97] CMS Collaboration, Performance of missing transverse momentum reconstruction in proton-proton collisions at $\sqrt{s} = 13$ TeV using the CMS detector, J. Instrum. **14**, P07004 (2019).
[98] A. Kalogeropoulos and J. Alwall, The SysCalc code: A tool to derive theoretical systematic uncertainties, arXiv:1801.08401.
[99] S. Catani, D. de Florian, M. Grazzini, and P. Nason, Soft gluon resummation for Higgs boson production at hadron colliders, J. High Energy Phys. 07 (2003) 028.
[100] M. Cacciari, S. Frixione, M. L. Mangano, P. Nason, and G. Ridolfi, The $t\bar{t}$ cross-section at 1.8 and 1.96 TeV: A study of the systematics due to parton densities and scale dependence, J. High Energy Phys. 04 (2004) 068.
[101] CMS Collaboration, Pileup mitigation at CMS in 13 TeV data, J. Instrum. **15**, P09018 (2020).
[102] G. Cowan, K. Cranmer, E. Gross, and O. Vitells, Asymptotic formulae for likelihood-based tests of new physics, Eur. Phys. J. C **71**, 1554 (2011); **73**, 2501(E) (2013).
[103] T. Junk, Confidence level computation for combining searches with small statistics, Nucl. Instrum. Methods Phys. Res., Sect. A **434**, 435 (1999).
[104] A. L. Read, Presentation of search results: The CL_s technique, J. Phys. G **28**, 2693 (2002).
[105] LEP2 SUSY Working Group, ALEPH, DELPHI, L3 and OPAL Collaborations, Combined LEP chargino results, up to 208 GeV for low Δm, http://lepsusy.web.cern.ch/lepsusy/www/inoslowdmsummer02/charginolowdm_pub.html (2002).

A. Hayrapetyan,[1] A. Tumasyan,[1,b] W. Adam,[2] J. W. Andrejkovic,[2] T. Bergauer,[2] S. Chatterjee,[2] K. Damanakis,[2] M. Dragicevic,[2] A. Escalante Del Valle,[2] P. S. Hussain,[2] M. Jeitler,[2,c] N. Krammer,[2] D. Liko,[2] I. Mikulec,[2] J. Schieck,[2,c] R. Schöfbeck,[2] D. Schwarz,[2] M. Sonawane,[2] S. Templ,[2] W. Waltenberger,[2] C.-E. Wulz,[2,c] M. R. Darwish,[3,d] T. Janssen,[3] P. Van Mechelen,[3] E. S. Bols,[4] J. D'Hondt,[4] S. Dansana,[4] A. De Moor,[4] M. Delcourt,[4] H. El Faham,[4] S. Lowette,[4] I. Makarenko,[4] D. Müller,[4] A. R. Sahasransu,[4] S. Tavernier,[4] M. Tytgat,[4,e] S. Van Putte,[4] D. Vannerom,[4] B. Clerbaux,[5] G. De Lentdecker,[5] L. Favart,[5] D. Hohov,[5] J. Jaramillo,[5] A. Khalilzadeh,[5] K. Lee,[5] M. Mahdavikhorrami,[5] A. Malara,[5] S. Paredes,[5] L. Pétré,[5] N. Postiau,[5] L. Thomas,[5] M. Vanden Bemden,[5] C. Vander Velde,[5] P. Vanlaer,[5] M. De Coen,[6] D. Dobur,[6] Y. Hong,[6] J. Knolle,[6] L. Lambrecht,[6] G. Mestdach,[6] C. Rendón,[6] A. Samalan,[6] K. Skovpen,[6] N. Van Den Bossche,[6] L. Wezenbeek,[6] A. Benecke,[7] G. Bruno,[7] C. Caputo,[7] C. Delaere,[7] I. S. Donertas,[7] A. Giammanco,[7] K. Jaffel,[7] Sa. Jain,[7] V. Lemaitre,[7] J. Lidrych,[7] P. Mastrapasqua,[7] K. Mondal,[7] T. T. Tran,[7] S. Wertz,[7] G. A. Alves,[8] E. Coelho,[8] C. Hensel,[8] T. Menezes De Oliveira,[8] A. Moraes,[8] P. Rebello Teles,[8] M. Soeiro,[8] W. L. Aldá Júnior,[9] M. Alves Gallo Pereira,[9] M. Barroso Ferreira Filho,[9] H. Brandao Malbouisson,[9] W. Carvalho,[9] J. Chinellato,[9,f] E. M. Da Costa,[9] G. G. Da Silveira,[9,g] D. De Jesus Damiao,[9] S. Fonseca De Souza,[9] J. Martins,[9,h] C. Mora Herrera,[9] K. Mota Amarilo,[9] L. Mundim,[9] H. Nogima,[9] A. Santoro,[9] A. Sznajder,[9] M. Thiel,[9] A. Vilela Pereira,[9] C. A. Bernardes,[10,g] L. Calligaris,[10] T. R. Fernandez Perez Tomei,[10] E. M. Gregores,[10] P. G. Mercadante,[10] S. F. Novaes,[10] B. Orzari,[10] Sandra S. Padula,[10] A. Aleksandrov,[11] G. Antchev,[11] R. Hadjiiska,[11] P. Iaydjiev,[11] M. Misheva,[11] M. Shopova,[11] G. Sultanov,[11] A. Dimitrov,[12] L. Litov,[12] B. Pavlov,[12] P. Petkov,[12] A. Petrov,[12] E. Shumka,[12] S. Keshri,[13] S. Thakur,[13] T. Cheng,[14] Q. Guo,[14] T. Javaid,[14] M. Mittal,[14] L. Yuan,[14] G. Bauer,[15,i,j] Z. Hu,[15] J. Liu,[15] K. Yi,[15,i,k] G. M. Chen,[16,l] H. S. Chen,[16,l] M. Chen,[16,l] F. Iemmi,[16] C. H. Jiang,[16] A. Kapoor,[16,m] H. Liao,[16] Z.-A. Liu,[16,n] F. Monti,[16] M. A. Shahzad,[16,l] R. Sharma,[16,o] J. N. Song,[16,n] J. Tao,[16] C. Wang,[16,l] J. Wang,[16] Z. Wang,[16,l] H. Zhang,[16] A. Agapitos,[17] Y. Ban,[17] A. Levin,[17] C. Li,[17] Q. Li,[17] Y. Mao,[17] S. J. Qian,[17] X. Sun,[17] D. Wang,[17] H. Yang,[17] L. Zhang,[17] C. Zhou,[17] Z. You,[18] N. Lu,[19] X. Gao,[20,p] D. Leggat,[20] H. Okawa,[20] Y. Zhang,[20] Z. Lin,[21] C. Lu,[21] M. Xiao,[21]

C. Avila,[22] D. A. Barbosa Trujillo,[22] A. Cabrera,[22] C. Florez,[22] J. Fraga,[22] J. A. Reyes Vega,[22] J. Mejia Guisao,[23] F. Ramirez,[23] M. Rodriguez,[23] J. D. Ruiz Alvarez,[23] D. Giljanovic,[24] N. Godinovic,[24] D. Lelas,[24] A. Sculac,[24] M. Kovac,[25] T. Sculac,[25] P. Bargassa,[26] V. Brigljevic,[26] B. K. Chitroda,[26] D. Ferencek,[26] S. Mishra,[26] A. Starodumov,[26,q] T. Susa,[26] A. Attikis,[27] K. Christoforou,[27] S. Konstantinou,[27] J. Mousa,[27] C. Nicolaou,[27] F. Ptochos,[27] P. A. Razis,[27] H. Rykaczewski,[27] H. Saka,[27] A. Stepennov,[27] M. Finger,[28] M. Finger Jr.,[28] A. Kveton,[28] E. Ayala,[29] E. Carrera Jarrin,[30] S. Elgammal,[31,r] A. Ellithi Kamel,[31,s] A. Lotfy,[32] Y. Mohammed,[32] R. K. Dewanjee,[33,t] K. Ehataht,[33] M. Kadastik,[33] T. Lange,[33] S. Nandan,[33] C. Nielsen,[33] J. Pata,[33] M. Raidal,[33] L. Tani,[33] C. Veelken,[33] H. Kirschenmann,[34] K. Osterberg,[34] M. Voutilainen,[34] S. Bharthuar,[35] E. Brücken,[35] F. Garcia,[35] J. Havukainen,[35] K. T. S. Kallonen,[35] R. Kinnunen,[35] T. Lampén,[35] K. Lassila-Perini,[35] S. Lehti,[35] T. Lindén,[35] M. Lotti,[35] L. Martikainen,[35] M. Myllymäki,[35] M. m. Rantanen,[35] H. Siikonen,[35] E. Tuominen,[35] J. Tuominiemi,[35] P. Luukka,[36] H. Petrow,[36] T. Tuuva,[36,a] M. Besancon,[37] F. Couderc,[37] M. Dejardin,[37] D. Denegri,[37] J. L. Faure,[37] F. Ferri,[37] S. Ganjour,[37] P. Gras,[37] G. Hamel de Monchenault,[37] V. Lohezic,[37] J. Malcles,[37] J. Rander,[37] A. Rosowsky,[37] M. Ö. Sahin,[37] A. Savoy-Navarro,[37,u] P. Simkina,[37] M. Titov,[37] M. Tornago,[37] C. Baldenegro Barrera,[38] F. Beaudette,[38] A. Buchot Perraguin,[38] P. Busson,[38] A. Cappati,[38] C. Charlot,[38] F. Damas,[38] O. Davignon,[38] A. De Wit,[38] G. Falmagne,[38] B. A. Fontana Santos Alves,[38] S. Ghosh,[38] A. Gilbert,[38] R. Granier de Cassagnac,[38] A. Hakimi,[38] B. Harikrishnan,[38] L. Kalipoliti,[38] G. Liu,[38] J. Motta,[38] M. Nguyen,[38] C. Ochando,[38] L. Portales,[38] R. Salerno,[38] U. Sarkar,[38] J. B. Sauvan,[38] Y. Sirois,[38] A. Tarabini,[38] E. Vernazza,[38] A. Zabi,[38] A. Zghiche,[38] J.-L. Agram,[39,v] J. Andrea,[39] D. Apparu,[39] D. Bloch,[39] J.-M. Brom,[39] E. C. Chabert,[39] C. Collard,[39] S. Falke,[39] U. Goerlach,[39] C. Grimault,[39] R. Haeberle,[39] A.-C. Le Bihan,[39] G. Saha,[39] M. A. Sessini,[39] P. Van Hove,[39] S. Beauceron,[40] B. Blancon,[40] G. Boudoul,[40] N. Chanon,[40] J. Choi,[40] D. Contardo,[40] P. Depasse,[40] C. Dozen,[40,w] H. El Mamouni,[40] J. Fay,[40] S. Gascon,[40] M. Gouzevitch,[40] C. Greenberg,[40] G. Grenier,[40] B. Ille,[40] I. B. Laktineh,[40] M. Lethuillier,[40] L. Mirabito,[40] S. Perries,[40] A. Purohit,[40] M. Vander Donckt,[40] P. Verdier,[40] J. Xiao,[40] A. Khvedelidze,[41,q] I. Lomidze,[41] Z. Tsamalaidze,[41,q] V. Botta,[42] L. Feld,[42] K. Klein,[42] M. Lipinski,[42] D. Meuser,[42] A. Pauls,[42] N. Röwert,[42] M. Teroerde,[42] S. Diekmann,[43] A. Dodonova,[43] N. Eich,[43] D. Eliseev,[43] F. Engelke,[43] M. Erdmann,[43] P. Fackeldey,[43] B. Fischer,[43] T. Hebbeker,[43] K. Hoepfner,[43] F. Ivone,[43] A. Jung,[43] M. y. Lee,[43] L. Mastrolorenzo,[43] M. Merschmeyer,[43] A. Meyer,[43] S. Mukherjee,[43] D. Noll,[43] A. Novak,[43] F. Nowotny,[43] A. Pozdnyakov,[43] Y. Rath,[43] W. Redjeb,[43] F. Rehm,[43] H. Reithler,[43] V. Sarkisovi,[43] A. Schmidt,[43] A. Sharma,[43] J. L. Spah,[43] A. Stein,[43] F. Torres Da Silva De Araujo,[43,x] L. Vigilante,[43] S. Wiedenbeck,[43] S. Zaleski,[43] C. Dziwok,[44] G. Flügge,[44] W. Haj Ahmad,[44,y] T. Kress,[44] A. Nowack,[44] O. Pooth,[44] A. Stahl,[44] T. Ziemons,[44] A. Zotz,[44] H. Aarup Petersen,[45] M. Aldaya Martin,[45] J. Alimena,[45] S. Amoroso,[45] Y. An,[45] S. Baxter,[45] M. Bayatmakou,[45] H. Becerril Gonzalez,[45] O. Behnke,[45] A. Belvedere,[45] S. Bhattacharya,[45] F. Blekman,[45,z] K. Borras,[45,aa] D. Brunner,[45] A. Campbell,[45] A. Cardini,[45] C. Cheng,[45] F. Colombina,[45] S. Consuegra Rodríguez,[45] G. Correia Silva,[45] M. De Silva,[45] G. Eckerlin,[45] D. Eckstein,[45] L. I. Estevez Banos,[45] O. Filatov,[45] E. Gallo,[45,z] A. Geiser,[45] A. Giraldi,[45] G. Greau,[45] V. Guglielmi,[45] M. Guthoff,[45] A. Hinzmann,[45] A. Jafari,[45,bb] L. Jeppe,[45] N. Z. Jomhari,[45] B. Kaech,[45] M. Kasemann,[45] H. Kaveh,[45] C. Kleinwort,[45] R. Kogler,[45] M. Komm,[45] D. Krücker,[45] W. Lange,[45] D. Leyva Pernia,[45] K. Lipka,[45,cc] W. Lohmann,[45,dd] R. Mankel,[45] I.-A. Melzer-Pellmann,[45] M. Mendizabal Morentin,[45] J. Metwally,[45] A. B. Meyer,[45] G. Milella,[45] A. Mussgiller,[45] L. P. NAIR,[45] A. Nürnberg,[45] Y. Otarid,[45] J. Park,[45] D. Pérez Adán,[45] E. Ranken,[45] A. Raspereza,[45] B. Ribeiro Lopes,[45] J. Rübenach,[45] A. Saggio,[45] M. Scham,[45,ee,aa] S. Schnake,[45,aa] P. Schütze,[45] C. Schwanenberger,[45,z] D. Selivanova,[45] M. Shchedrolosiev,[45] R. E. Sosa Ricardo,[45] D. Stafford,[45] F. Vazzoler,[45] A. Ventura Barroso,[45] R. Walsh,[45] Q. Wang,[45] Y. Wen,[45] K. Wichmann,[45] L. Wiens,[45,aa] C. Wissing,[45] Y. Yang,[45] A. Zimermmane Castro Santos,[45] A. Albrecht,[46] S. Albrecht,[46] M. Antonello,[46] S. Bein,[46] L. Benato,[46] M. Bonanomi,[46] P. Connor,[46] M. Eich,[46] K. El Morabit,[46] Y. Fischer,[46] A. Fröhlich,[46] C. Garbers,[46] E. Garutti,[46] A. Grohsjean,[46] M. Hajheidari,[46] J. Haller,[46] H. R. Jabusch,[46] G. Kasieczka,[46] P. Keicher,[46] R. Klanner,[46] W. Korcari,[46] T. Kramer,[46] V. Kutzner,[46] F. Labe,[46] J. Lange,[46] A. Lobanov,[46] C. Matthies,[46] A. Mehta,[46] L. Moureaux,[46] M. Mrowietz,[46] A. Nigamova,[46] Y. Nissan,[46] A. Paasch,[46] K. J. Pena Rodriguez,[46] T. Quadfasel,[46] B. Raciti,[46] M. Rieger,[46] D. Savoiu,[46] J. Schindler,[46] P. Schleper,[46] M. Schröder,[46] J. Schwandt,[46] M. Sommerhalder,[46] H. Stadie,[46] G. Steinbrück,[46] A. Tews,[46] M. Wolf,[46] S. Brommer,[47]

M. Burkart,[47] E. Butz,[47] T. Chwalek,[47] A. Dierlamm,[47] A. Droll,[47] N. Faltermann,[47] M. Giffels,[47] A. Gottmann,[47] F. Hartmann,[47,ff] R. Hofsaess,[47] M. Horzela,[47] U. Husemann,[47] J. Kieseler,[47] M. Klute,[47] R. Koppenhöfer,[47] J. M. Lawhorn,[47] M. Link,[47] A. Lintuluoto,[47] S. Maier,[47] S. Mitra,[47] M. Mormile,[47] Th. Müller,[47] M. Neukum,[47] M. Oh,[47] M. Presilla,[47] G. Quast,[47] K. Rabbertz,[47] B. Regnery,[47] N. Shadskiy,[47] I. Shvetsov,[47] H. J. Simonis,[47] N. Trevisani,[47] R. Ulrich,[47] J. van der Linden,[47] R. F. Von Cube,[47] M. Wassmer,[47] S. Wieland,[47] F. Wittig,[47] R. Wolf,[47] S. Wunsch,[47] X. Zuo,[47] G. Anagnostou,[48] P. Assiouras,[48] G. Daskalakis,[48] A. Kyriakis,[48] A. Papadopoulos,[48,ff] A. Stakia,[48] P. Kontaxakis,[49] G. Melachroinos,[49] A. Panagiotou,[49] I. Papavergou,[49] I. Paraskevas,[49] N. Saoulidou,[49] K. Theofilatos,[49] E. Tziaferi,[49] K. Vellidis,[49] I. Zisopoulos,[49] G. Bakas,[50] T. Chatzistavrou,[50] G. Karapostoli,[50] K. Kousouris,[50] I. Papakrivopoulos,[50] E. Siamarkou,[50] G. Tsipolitis,[50] A. Zacharopoulou,[50] K. Adamidis,[51] I. Bestintzanos,[51] I. Evangelou,[51] C. Foudas,[51] P. Gianneios,[51] C. Kamtsikis,[51] P. Katsoulis,[51] P. Kokkas,[51] P. G. Kosmoglou Kioseoglou,[51] N. Manthos,[51] I. Papadopoulos,[51] J. Strologas,[51] M. Bartók,[52,gg] C. Hajdu,[52] D. Horvath,[52,hh,ii] F. Sikler,[52] V. Veszpremi,[52] M. Csanád,[53] K. Farkas,[53] M. M. A. Gadallah,[53,jj] Á. Kadlecsik,[53] P. Major,[53] K. Mandal,[53] G. Pásztor,[53] A. J. Rádl,[53,kk] G. I. Veres,[53] P. Raics,[54] B. Ujvari,[54,ll] G. Zilizi,[54] G. Bencze,[55] S. Czellar,[55] J. Karancsi,[55,gg] J. Molnar,[55] Z. Szillasi,[55] T. Csorgo,[56,kk] F. Nemes,[56,kk] T. Novak,[56] J. Babbar,[57] S. Bansal,[57] S. B. Beri,[57] V. Bhatnagar,[57] G. Chaudhary,[57] S. Chauhan,[57] N. Dhingra,[57,mm] A. Kaur,[57] A. Kaur,[57] H. Kaur,[57] M. Kaur,[57] S. Kumar,[57] M. Meena,[57] K. Sandeep,[57] T. Sheokand,[57] J. B. Singh,[57] A. Singla,[57] A. Ahmed,[58] A. Bhardwaj,[58] A. Chhetri,[58] B. C. Choudhary,[58] A. Kumar,[58] M. Naimuddin,[58] K. Ranjan,[58] S. Saumya,[58] S. Acharya,[59,nn] S. Baradia,[59] S. Barman,[59,oo] S. Bhattacharya,[59] D. Bhowmik,[59] S. Dutta,[59] S. Dutta,[59] B. Gomber,[59,nn] P. Palit,[59] B. Sahu,[59,nn] S. Sarkar,[59] M. M. Ameen,[60] P. K. Behera,[60] S. C. Behera,[60] S. Chatterjee,[60] P. Jana,[60] P. Kalbhor,[60] J. R. Komaragiri,[60,pp] D. Kumar,[60,pp] L. Panwar,[60,pp] R. Pradhan,[60] P. R. Pujahari,[60] N. R. Saha,[60] A. Sharma,[60] A. K. Sikdar,[60] S. Verma,[60] T. Aziz,[61] I. Das,[61] S. Dugad,[61] M. Kumar,[61] G. B. Mohanty,[61] P. Suryadevara,[61] A. Bala,[62] S. Banerjee,[62] R. M. Chatterjee,[62] M. Guchait,[62] Sh. Jain,[62] S. Karmakar,[62] S. Kumar,[62] G. Majumder,[62] K. Mazumdar,[62] S. Mukherjee,[62] S. Parolia,[62] A. Thachayath,[62] S. Bahinipati,[63,qq] A. K. Das,[63] C. Kar,[63] D. Maity,[63,rr] P. Mal,[63] T. Mishra,[63] V. K. Muraleedharan Nair Bindhu,[63,rr] K. Naskar,[63,rr] A. Nayak,[63,rr] P. Sadangi,[63] P. Saha,[63] S. K. Swain,[63] S. Varghese,[63,rr] D. Vats,[63,rr] A. Alpana,[64] S. Dube,[64] B. Kansal,[64] A. Laha,[64] A. Rastogi,[64] S. Sharma,[64] H. Bakhshiansohi,[65,ss] E. Khazaie,[65,tt] M. Zeinali,[65,uu] S. Chenarani,[66,vv] S. M. Etesami,[66] M. Khakzad,[66] M. Mohammadi Najafabadi,[66] M. Grunewald,[67] M. Abbrescia,[68a,68b] R. Aly,[68a,68c,ww] A. Colaleo,[68a,68b] D. Creanza,[68a,68c] B. D'Anzi,[68a,68b] N. De Filippis,[68a,68c] M. De Palma,[68a,68b] A. Di Florio,[68a,68c] W. Elmetenawee,[68a,68b,ww] L. Fiore,[68a] G. Iaselli,[68a,68c] M. Louka,[68a,68b] G. Maggi,[68a,68c] M. Maggi,[68a] I. Margjeka,[68a,68b] V. Mastrapasqua,[68a,68b] S. My,[68a,68b] S. Nuzzo,[68a,68b] A. Pellecchia,[68a,68b] A. Pompili,[68a,68b] G. Pugliese,[68a,68c] R. Radogna,[68a] G. Ramirez-Sanchez,[68a,68c] D. Ramos,[68a] A. Ranieri,[68a] L. Silvestris,[68a] F. M. Simone,[68a,68b] Ü. Sözbilir,[68a] A. Stamerra,[68a] R. Venditti,[68a] P. Verwilligen,[68a] A. Zaza,[68a,68b] G. Abbiendi,[69a] C. Battilana,[69a,69b] D. Bonacorsi,[69a,69b] L. Borgonovi,[69a] P. Capiluppi,[69a,69b] A. Castro,[69a,69b] F. R. Cavallo,[69a] M. Cuffiani,[69a,69b] G. M. Dallavalle,[69a] T. Diotalevi,[69a,69b] F. Fabbri,[69a] A. Fanfani,[69a,69b] D. Fasanella,[69a,69b] P. Giacomelli,[69a] L. Giommi,[69a,69b] C. Grandi,[69a] L. Guiducci,[69a,69b] S. Lo Meo,[69a,xx] L. Lunerti,[69a,69b] S. Marcellini,[69a] G. Masetti,[69a] F. L. Navarria,[69a,69b] A. Perrotta,[69a] F. Primavera,[69a,69b] A. M. Rossi,[69a,69b] T. Rovelli,[69a,69b] G. P. Siroli,[69a,69b] S. Costa,[70a,70b,yy] A. Di Mattia,[70a] R. Potenza,[70a,70b] A. Tricomi,[70a,70b,yy] C. Tuve,[70a,70b] G. Barbagli,[71a] G. Bardelli,[71a,71b] B. Camaiani,[71a,71b] A. Cassese,[71a] R. Ceccarelli,[71a] V. Ciulli,[71a,71b] C. Civinini,[71a] R. D'Alessandro,[71a,71b] E. Focardi,[71a,71b] T. Kello,[71a] G. Latino,[71a,71b] P. Lenzi,[71a,71b] M. Lizzo,[71a] M. Meschini,[71a] S. Paoletti,[71a] A. Papanastassiou,[71a,71b] G. Sguazzoni,[71a] L. Viliani,[71a] L. Benussi,[72] S. Bianco,[72] S. Meola,[72,zz] D. Piccolo,[72] P. Chatagnon,[73a] F. Ferro,[73a] E. Robutti,[73a] S. Tosi,[73a,73b] A. Benaglia,[74a] G. Boldrini,[74a,74b] F. Brivio,[74a] F. Cetorelli,[74a] F. De Guio,[74a,74b] M. E. Dinardo,[74a,74b] P. Dini,[74a] S. Gennai,[74a] R. Gerosa,[74a,74b] A. Ghezzi,[74a,74b] P. Govoni,[74a,74b] L. Guzzi,[74a] M. T. Lucchini,[74a,74b] M. Malberti,[74a] S. Malvezzi,[74a] A. Massironi,[74a] D. Menasce,[74a] L. Moroni,[74a] M. Paganoni,[74a,74b] D. Pedrini,[74a] B. S. Pinolini,[74a] S. Ragazzi,[74a,74b] T. Tabarelli de Fatis,[74a,74b] D. Zuolo,[74a] S. Buontempo,[75a] A. Cagnotta,[75a,75b] F. Carnevali,[75a,75b] N. Cavallo,[75a,75c] A. De Iorio,[75a,75b] F. Fabozzi,[75a,75c] A. O. M. Iorio,[75a,75b] L. Lista,[75a,75b,aaa] P. Paolucci,[75a,ff] B. Rossi,[75a] C. Sciacca,[75a,75b] R. Ardino,[76a] P. Azzi,[76a] N. Bacchetta,[76a,bbb] D. Bisello,[76a,76b] P. Bortignon,[76a]

A. Bragagnolo,[76a,76b] R. Carlin,[76a,76b] P. Checchia,[76a] T. Dorigo,[76a] F. Gasparini,[76a,76b] U. Gasparini,[76a,76b] G. Grosso,[76a] L. Layer,[76a,ccc] E. Lusiani,[76a] M. Margoni,[76a,76b] M. Migliorini,[76a,76b] F. Montecassiano,[76a] J. Pazzini,[76a,76b] P. Ronchese,[76a,76b] R. Rossin,[76a,76b] F. Simonetto,[76a,76b] G. Strong,[76a] M. Tosi,[76a,76b] A. Triossi,[76a,76b] S. Ventura,[76a] H. Yarar,[76a,76b] M. Zanetti,[76a,76b] P. Zotto,[76a,76b] A. Zucchetta,[76a,76b] G. Zumerle,[76a,76b] S. Abu Zeid,[77a,ddd] C. Aimè,[77a,77b] A. Braghieri,[77a] S. Calzaferri,[77a,77b] D. Fiorina,[77a,77b] P. Montagna,[77a,77b] V. Re,[77a] C. Riccardi,[77a,77b] P. Salvini,[77a] I. Vai,[77a,77b] P. Vitulo,[77a,77b] S. Ajmal,[78a,78b] P. Asenov,[78a,eee] G. M. Bilei,[78a] D. Ciangottini,[78a,78b] L. Fanò,[78a,78b] M. Magherini,[78a,78b] G. Mantovani,[78a,78b] V. Mariani,[78a,78b] M. Menichelli,[78a] F. Moscatelli,[78a,eee] A. Rossi,[78a,78b] A. Santocchia,[78a,78b] D. Spiga,[78a] T. Tedeschi,[78a,78b] P. Azzurri,[79a] G. Bagliesi,[79a] R. Bhattacharya,[79a] L. Bianchini,[79a,79b] T. Boccali,[79a] E. Bossini,[79a] D. Bruschini,[79a,79c] R. Castaldi,[79a] M. A. Ciocci,[79a,79b] M. Cipriani,[79a,79b] V. D'Amante,[79a,79d] R. Dell'Orso,[79a] S. Donato,[79a] A. Giassi,[79a] F. Ligabue,[79a,79c] D. Matos Figueiredo,[79a] A. Messineo,[79a,79b] M. Musich,[79a,79b] F. Palla,[79a] A. Rizzi,[79a,79b] G. Rolandi,[79a,79c] S. Roy Chowdhury,[79a] T. Sarkar,[79a] A. Scribano,[79a] P. Spagnolo,[79a] R. Tenchini,[79a,79b] G. Tonelli,[79a,79b] N. Turini,[79a,79d] A. Venturi,[79a] P. G. Verdini,[79a] P. Barria,[80a] M. Campana,[80a,80b] F. Cavallari,[80a] L. Cunqueiro Mendez,[80a,80b] D. Del Re,[80a,80b] E. Di Marco,[80a] M. Diemoz,[80a] F. Errico,[80a,80b] E. Longo,[80a,80b] P. Meridiani,[80a] J. Mijuskovic,[80a,80b] G. Organtini,[80a,80b] F. Pandolfi,[80a] R. Paramatti,[80a,80b] C. Quaranta,[80a,80b] S. Rahatlou,[80a,80b] C. Rovelli,[80a] F. Santanastasio,[80a,80b] L. Soffi,[80a] N. Amapane,[81a,81b] R. Arcidiacono,[81a,81c] S. Argiro,[81a,81b] M. Arneodo,[81a,81c] N. Bartosik,[81a] R. Bellan,[81a,81b] A. Bellora,[81a,81b] C. Biino,[81a] N. Cartiglia,[81a] M. Costa,[81a,81b] R. Covarelli,[81a,81b] N. Demaria,[81a] L. Finco,[81a] M. Grippo,[81a,81b] B. Kiani,[81a,81b] F. Legger,[81a] F. Luongo,[81a,81b] C. Mariotti,[81a] S. Maselli,[81a] A. Mecca,[81a,81b] E. Migliore,[81a,81b] M. Monteno,[81a] R. Mulargia,[81a] M. M. Obertino,[81a,81b] G. Ortona,[81a] L. Pacher,[81a,81b] N. Pastrone,[81a] M. Pelliccioni,[81a] M. Ruspa,[81a,81c] F. Siviero,[81a,81b] V. Sola,[81a,81b] A. Solano,[81a,81b] D. Soldi,[81a,81b] A. Staiano,[81a] C. Tarricone,[81a,81b] D. Trocino,[81a] G. Umoret,[81a,81b] E. Vlasov,[81a,81b] S. Belforte,[82a] V. Candelise,[82a,82b] M. Casarsa,[82a] F. Cossutti,[82a] K. De Leo,[82a,82b] G. Della Ricca,[82a,82b] S. Dogra,[83] J. Hong,[83] C. Huh,[83] B. Kim,[83] D. H. Kim,[83] J. Kim,[83] H. Lee,[83] S. W. Lee,[83] C. S. Moon,[83] Y. D. Oh,[83] S. I. Pak,[83] M. S. Ryu,[83] S. Sekmen,[83] Y. C. Yang,[83] M. S. Kim,[84] G. Bak,[85] P. Gwak,[85] H. Kim,[85] D. H. Moon,[85] E. Asilar,[86] D. Kim,[86] T. J. Kim,[86] J. A. Merlin,[86] S. Choi,[87] S. Han,[87] B. Hong,[87] K. Lee,[87] K. S. Lee,[87] S. Lee,[87] J. Park,[87] S. K. Park,[87] J. Yoo,[87] J. Goh,[88] H. S. Kim,[89] Y. Kim,[89] S. Lee,[89] J. Almond,[90] J. H. Bhyun,[90] J. Choi,[90] W. Jun,[90] J. Kim,[90] J. S. Kim,[90] S. Ko,[90] H. Kwon,[90] H. Lee,[90] J. Lee,[90] J. Lee,[90] B. H. Oh,[90] S. B. Oh,[90] H. Seo,[90] U. K. Yang,[90] I. Yoon,[90] W. Jang,[91] D. Y. Kang,[91] Y. Kang,[91] S. Kim,[91] B. Ko,[91] J. S. H. Lee,[91] Y. Lee,[91] I. C. Park,[91] Y. Roh,[91] I. J. Watson,[91] S. Yang,[91] S. Ha,[92] H. D. Yoo,[92] M. Choi,[93] M. R. Kim,[93] H. Lee,[93] Y. Lee,[93] I. Yu,[93] T. Beyrouthy,[94] Y. Maghrbi,[94] K. Dreimanis,[95] A. Gaile,[95] G. Pikurs,[95] A. Potrebko,[95] M. Seidel,[95] V. Veckalns,[95,fff] N. R. Strautnieks,[96] M. Ambrozas,[97] A. Juodagalvis,[97] A. Rinkevicius,[97] G. Tamulaitis,[97] N. Bin Norjoharuddeen,[98] I. Yusuff,[98,ggg] Z. Zolkapli,[98] J. F. Benitez,[99] A. Castaneda Hernandez,[99] H. A. Encinas Acosta,[99] L. G. Gallegos Maríñez,[99] M. León Coello,[99] J. A. Murillo Quijada,[99] A. Sehrawat,[99] L. Valencia Palomo,[99] G. Ayala,[100] H. Castilla-Valdez,[100] E. De La Cruz-Burelo,[100] I. Heredia-De La Cruz,[100,hhh] R. Lopez-Fernandez,[100] C. A. Mondragon Herrera,[100] A. Sánchez Hernández,[100] C. Oropeza Barrera,[101] M. Ramírez García,[101] I. Bautista,[102] I. Pedraza,[102] H. A. Salazar Ibarguen,[102] C. Uribe Estrada,[102] I. Bubanja,[103] N. Raicevic,[103] P. H. Butler,[104] A. Ahmad,[105] M. I. Asghar,[105] A. Awais,[105] M. I. M. Awan,[105] H. R. Hoorani,[105] W. A. Khan,[105] V. Avati,[106] L. Grzanka,[106] M. Malawski,[106] H. Bialkowska,[107] M. Bluj,[107] B. Boimska,[107] M. Górski,[107] M. Kazana,[107] M. Szleper,[107] P. Zalewski,[107] K. Bunkowski,[108] K. Doroba,[108] A. Kalinowski,[108] M. Konecki,[108] J. Krolikowski,[108] A. Muhammad,[108] K. Pozniak,[109] W. Zabolotny,[109] M. Araujo,[110] D. Bastos,[110] C. Beirão Da Cruz E Silva,[110] A. Boletti,[110] M. Bozzo,[110] G. Da Molin,[110] P. Faccioli,[110] M. Gallinaro,[110] J. Hollar,[110] N. Leonardo,[110] T. Niknejad,[110] A. Petrilli,[110] M. Pisano,[110] J. Seixas,[110] J. Varela,[110] J. W. Wulff,[110] P. Adzic,[111] P. Milenovic,[111] M. Dordevic,[112] J. Milosevic,[112] V. Rekovic,[112] M. Aguilar-Benitez,[113] J. Alcaraz Maestre,[113] Cristina F. Bedoya,[113] M. Cepeda,[113] M. Cerrada,[113] N. Colino,[113] B. De La Cruz,[113] A. Delgado Peris,[113] D. Fernández Del Val,[113] J. P. Fernández Ramos,[113] J. Flix,[113] M. C. Fouz,[113] O. Gonzalez Lopez,[113] S. Goy Lopez,[113] J. M. Hernandez,[113] M. I. Josa,[113] J. León Holgado,[113] D. Moran,[113] C. M. Morcillo Perez,[113] Á. Navarro Tobar,[113] C. Perez Dengra,[113] A. Pérez-Calero Yzquierdo,[113] J. Puerta Pelayo,[113] I. Redondo,[113] D. D. Redondo Ferrero,[113]

L. Romero,[113] S. Sánchez Navas,[113] L. Urda Gómez,[113] J. Vazquez Escobar,[113] C. Willmott,[113] J. F. de Trocóniz,[114] B. Alvarez Gonzalez,[115] J. Cuevas,[115] J. Fernandez Menendez,[115] S. Folgueras,[115] I. Gonzalez Caballero,[115] J. R. González Fernández,[115] E. Palencia Cortezon,[115] C. Ramón Álvarez,[115] V. Rodríguez Bouza,[115] A. Soto Rodríguez,[115] A. Trapote,[115] C. Vico Villalba,[115] P. Vischia,[115] S. Bhowmik,[116] S. Blanco Fernández,[116] J. A. Brochero Cifuentes,[116] I. J. Cabrillo,[116] A. Calderon,[116] J. Duarte Campderros,[116] M. Fernandez,[116] C. Fernandez Madrazo,[116] G. Gomez,[116] C. Lasaosa García,[116] C. Martinez Rivero,[116] P. Martinez Ruiz del Arbol,[116] F. Matorras,[116] P. Matorras Cuevas,[116] E. Navarrete Ramos,[116] J. Piedra Gomez,[116] L. Scodellaro,[116] I. Vila,[116] J. M. Vizan Garcia,[116] M. K. Jayananda,[117] B. Kailasapathy,[117,iii] D. U. J. Sonnadara,[117] D. D. C. Wickramarathna,[117] W. G. D. Dharmaratna,[118] K. Liyanage,[118] N. Perera,[118] N. Wickramage,[118] D. Abbaneo,[119] C. Amendola,[119] E. Auffray,[119] G. Auzinger,[119] J. Baechler,[119] D. Barney,[119] A. Bermúdez Martínez,[119] M. Bianco,[119] B. Bilin,[119] A. A. Bin Anuar,[119] A. Bocci,[119] E. Brondolin,[119] C. Caillol,[119] T. Camporesi,[119] G. Cerminara,[119] N. Chernyavskaya,[119] D. d'Enterria,[119] A. Dabrowski,[119] A. David,[119] A. De Roeck,[119] M. M. Defranchis,[119] M. Deile,[119] M. Dobson,[119] F. Fallavollita,[119,jjj] L. Forthomme,[119] G. Franzoni,[119] W. Funk,[119] S. Giani,[119] D. Gigi,[119] K. Gill,[119] F. Glege,[119] L. Gouskos,[119] M. Haranko,[119] J. Hegeman,[119] B. Huber,[119] V. Innocente,[119] T. James,[119] P. Janot,[119] S. Laurila,[119] P. Lecoq,[119] E. Leutgeb,[119] C. Lourenço,[119] B. Maier,[119] L. Malgeri,[119] M. Mannelli,[119] A. C. Marini,[119] M. Matthewman,[119] F. Meijers,[119] S. Mersi,[119] E. Meschi,[119] V. Milosevic,[119] F. Moortgat,[119] M. Mulders,[119] S. Orfanelli,[119] F. Pantaleo,[119] G. Petrucciani,[119] A. Pfeiffer,[119] M. Pierini,[119] D. Piparo,[119] H. Qu,[119] D. Rabady,[119] G. Reales Gutiérrez,[119] M. Rovere,[119] H. Sakulin,[119] S. Scarfi,[119] C. Schwick,[119] M. Selvaggi,[119] A. Sharma,[119] K. Shchelina,[119] P. Silva,[119] P. Sphicas,[119,kkk] A. G. Stahl Leiton,[119] A. Steen,[119] S. Summers,[119] D. Treille,[119] P. Tropea,[119] A. Tsirou,[119] D. Walter,[119] J. Wanczyk,[119,lll] K. A. Wozniak,[119,mmm] S. Wuchterl,[119] P. Zehetner,[119] P. Zejdl,[119] W. D. Zeuner,[119] T. Bevilacqua,[120,nnn] L. Caminada,[120,nnn] A. Ebrahimi,[120] W. Erdmann,[120] R. Horisberger,[120] Q. Ingram,[120] H. C. Kaestli,[120] D. Kotlinski,[120] C. Lange,[120] M. Missiroli,[120,nnn] L. Noehte,[120,nnn] T. Rohe,[120] T. K. Aarrestad,[121] K. Androsov,[121,lll] M. Backhaus,[121] A. Calandri,[121] C. Cazzaniga,[121] K. Datta,[121] A. De Cosa,[121] G. Dissertori,[121] M. Dittmar,[121] M. Donegà,[121] F. Eble,[121] M. Galli,[121] K. Gedia,[121] F. Glessgen,[121] C. Grab,[121] D. Hits,[121] W. Lustermann,[121] A.-M. Lyon,[121] R. A. Manzoni,[121] M. Marchegiani,[121] L. Marchese,[121] C. Martin Perez,[121] A. Mascellani,[121,lll] F. Nessi-Tedaldi,[121] F. Pauss,[121] V. Perovic,[121] S. Pigazzini,[121] M. G. Ratti,[121] M. Reichmann,[121] C. Reissel,[121] T. Reitenspiess,[121] B. Ristic,[121] F. Riti,[121] D. Ruini,[121] D. A. Sanz Becerra,[121] R. Seidita,[121] J. Steggemann,[121,lll] D. Valsecchi,[121] R. Wallny,[121] C. Amsler,[122,ooo] P. Bärtschi,[122] C. Botta,[122] D. Brzhechko,[122] M. F. Canelli,[122] K. Cormier,[122] R. Del Burgo,[122] J. K. Heikkilä,[122] M. Huwiler,[122] W. Jin,[122] A. Jofrehei,[122] B. Kilminster,[122] S. Leontsinis,[122] S. P. Liechti,[122] A. Macchiolo,[122] P. Meiring,[122] V. M. Mikuni,[122] U. Molinatti,[122] I. Neutelings,[122] A. Reimers,[122] P. Robmann,[122] S. Sanchez Cruz,[122] K. Schweiger,[122] M. Senger,[122] Y. Takahashi,[122] R. Tramontano,[122] C. Adloff,[123,ppp] C. M. Kuo,[123] W. Lin,[123] P. K. Rout,[123] P. C. Tiwari,[123,pp] S. S. Yu,[123] L. Ceard,[124] Y. Chao,[124] K. F. Chen,[124] P. s. Chen,[124] Z. g. Chen,[124] W.-S. Hou,[124] T. h. Hsu,[124] Y. w. Kao,[124] R. Khurana,[124] G. Kole,[124] Y. y. Li,[124] R.-S. Lu,[124] E. Paganis,[124] A. Psallidas,[124] X. f. Su,[124] J. Thomas-Wilsker,[124] L. s. Tsai,[124] H. y. Wu,[124] E. Yazgan,[124] C. Asawatangtrakuldee,[125] N. Srimanobhas,[125] V. Wachirapusitanand,[125] D. Agyel,[126] F. Boran,[126] Z. S. Demiroglu,[126] F. Dolek,[126] I. Dumanoglu,[126,qqq] E. Eskut,[126] Y. Guler,[126,rrr] E. Gurpinar Guler,[126,rrr] C. Isik,[126] O. Kara,[126] A. Kayis Topaksu,[126] U. Kiminsu,[126] G. Onengut,[126] K. Ozdemir,[126,sss] A. Polatoz,[126] B. Tali,[126,ttt] U. G. Tok,[126] S. Turkcapar,[126] E. Uslan,[126] I. S. Zorbakir,[126] M. Yalvac,[127,uuu] B. Akgun,[128] I. O. Atakisi,[128] E. Gülmez,[128] M. Kaya,[128,vvv] O. Kaya,[128,www] S. Tekten,[128,xxx] A. Cakir,[129] K. Cankocak,[129,qqq,yyy] Y. Komurcu,[129] S. Sen,[129,zzz] O. Aydilek,[130] S. Cerci,[130,ttt] V. Epshteyn,[130] B. Hacisahinoglu,[130] I. Hos,[130,aaaa] B. Isildak,[130,bbbb] B. Kaynak,[130] S. Ozkorucuklu,[130] O. Potok,[130] H. Sert,[130] C. Simsek,[130] D. Sunar Cerci,[130,ttt] C. Zorbilmez,[130] A. Boyaryntsev,[131] B. Grynyov,[131] L. Levchuk,[132] D. Anthony,[133] J. J. Brooke,[133] A. Bundock,[133] F. Bury,[133] E. Clement,[133] D. Cussans,[133] H. Flacher,[133] M. Glowacki,[133] J. Goldstein,[133] H. F. Heath,[133] L. Kreczko,[133] B. Krikler,[133] S. Paramesvaran,[133] S. Seif El Nasr-Storey,[133] V. J. Smith,[133] N. Stylianou,[133,cccc] K. Walkingshaw Pass,[133] R. White,[133] A. H. Ball,[134] K. W. Bell,[134] A. Belyaev,[134,dddd] C. Brew,[134] R. M. Brown,[134] D. J. A. Cockerill,[134] C. Cooke,[134] K. V. Ellis,[134] K. Harder,[134] S. Harper,[134] M.-L. Holmberg,[134,eeee] J. Linacre,[134] K. Manolopoulos,[134] D. M. Newbold,[134]

E. Olaiya,[134] D. Petyt,[134] T. Reis,[134] G. Salvi,[134] T. Schuh,[134] C. H. Shepherd-Themistocleous,[134] I. R. Tomalin,[134] T. Williams,[134] R. Bainbridge,[135] P. Bloch,[135] C. E. Brown,[135] O. Buchmuller,[135] V. Cacchio,[135] C. A. Carrillo Montoya,[135] G. S. Chahal,[135,ffff] D. Colling,[135] J. S. Dancu,[135] P. Dauncey,[135] G. Davies,[135] J. Davies,[135] M. Della Negra,[135] S. Fayer,[135] G. Fedi,[135] G. Hall,[135] M. H. Hassanshahi,[135] A. Howard,[135] G. Iles,[135] M. Knight,[135] J. Langford,[135] L. Lyons,[135] A.-M. Magnan,[135] S. Malik,[135] A. Martelli,[135] M. Mieskolainen,[135] J. Nash,[135,gggg] M. Pesaresi,[135] B. C. Radburn-Smith,[135] A. Richards,[135] A. Rose,[135] C. Seez,[135] R. Shukla,[135] A. Tapper,[135] K. Uchida,[135] G. P. Uttley,[135] L. H. Vage,[135] T. Virdee,[135,ff] M. Vojinovic,[135] N. Wardle,[135] D. Winterbottom,[135] K. Coldham,[136] J. E. Cole,[136] A. Khan,[136] P. Kyberd,[136] I. D. Reid,[136] S. Abdullin,[137] A. Brinkerhoff,[137] B. Caraway,[137] J. Dittmann,[137] K. Hatakeyama,[137] J. Hiltbrand,[137] A. R. Kanuganti,[137] B. McMaster,[137] M. Saunders,[137] S. Sawant,[137] C. Sutantawibul,[137] M. Toms,[137,q] J. Wilson,[137] R. Bartek,[138] A. Dominguez,[138] C. Huerta Escamilla,[138] A. E. Simsek,[138] R. Uniyal,[138] A. M. Vargas Hernandez,[138] R. Chudasama,[139] S. I. Cooper,[139] S. V. Gleyzer,[139] C. U. Perez,[139] P. Rumerio,[139,hhhh] E. Usai,[139] C. West,[139] R. Yi,[139] A. Akpinar,[140] A. Albert,[140] D. Arcaro,[140] C. Cosby,[140] Z. Demiragli,[140] C. Erice,[140] E. Fontanesi,[140] D. Gastler,[140] S. Jeon,[140] J. Rohlf,[140] K. Salyer,[140] D. Sperka,[140] D. Spitzbart,[140] I. Suarez,[140] A. Tsatsos,[140] S. Yuan,[140] G. Benelli,[141] X. Coubez,[141,aa] D. Cutts,[141] M. Hadley,[141] U. Heintz,[141] J. M. Hogan,[141,iiii] T. Kwon,[141] G. Landsberg,[141] K. T. Lau,[141] D. Li,[141] J. Luo,[141] S. Mondal,[141] M. Narain,[141,a] N. Pervan,[141] S. Sagir,[141,jjjj] F. Simpson,[141] M. Stamenkovic,[141] W. Y. Wong,[141] X. Yan,[141] W. Zhang,[141] S. Abbott,[142] J. Bonilla,[142] C. Brainerd,[142] R. Breedon,[142] M. Calderon De La Barca Sanchez,[142] M. Chertok,[142] M. Citron,[142] J. Conway,[142] P. T. Cox,[142] R. Erbacher,[142] F. Jensen,[142] O. Kukral,[142] G. Mocellin,[142] M. Mulhearn,[142] D. Pellett,[142] W. Wei,[142] Y. Yao,[142] F. Zhang,[142] M. Bachtis,[143] R. Cousins,[143] A. Datta,[143] J. Hauser,[143] M. Ignatenko,[143] M. A. Iqbal,[143] T. Lam,[143] E. Manca,[143] D. Saltzberg,[143] V. Valuev,[143] R. Clare,[144] J. W. Gary,[144] M. Gordon,[144] G. Hanson,[144] W. Si,[144] S. Wimpenny,[144,a] J. G. Branson,[145] S. Cittolin,[145] S. Cooperstein,[145] D. Diaz,[145] J. Duarte,[145] L. Giannini,[145] J. Guiang,[145] R. Kansal,[145] V. Krutelyov,[145] R. Lee,[145] J. Letts,[145] M. Masciovecchio,[145] F. Mokhtar,[145] M. Pieri,[145] M. Quinnan,[145] B. V. Sathia Narayanan,[145] V. Sharma,[145] M. Tadel,[145] E. Vourliotis,[145] F. Würthwein,[145] Y. Xiang,[145] A. Yagil,[145] A. Barzdukas,[146] L. Brennan,[146] C. Campagnari,[146] G. Collura,[146] A. Dorsett,[146] J. Incandela,[146] M. Kilpatrick,[146] J. Kim,[146] A. J. Li,[146] P. Masterson,[146] H. Mei,[146] M. Oshiro,[146] J. Richman,[146] U. Sarica,[146] R. Schmitz,[146] F. Setti,[146] J. Sheplock,[146] D. Stuart,[146] S. Wang,[146] A. Bornheim,[147] O. Cerri,[147] A. Latorre,[147] J. Mao,[147] H. B. Newman,[147] T. Q. Nguyen,[147] M. Spiropulu,[147] J. R. Vlimant,[147] C. Wang,[147] S. Xie,[147] R. Y. Zhu,[147] J. Alison,[148] S. An,[148] M. B. Andrews,[148] P. Bryant,[148] V. Dutta,[148] T. Ferguson,[148] A. Harilal,[148] C. Liu,[148] T. Mudholkar,[148] S. Murthy,[148] M. Paulini,[148] A. Roberts,[148] A. Sanchez,[148] W. Terrill,[148] J. P. Cumalat,[149] W. T. Ford,[149] A. Hassani,[149] G. Karathanasis,[149] E. MacDonald,[149] N. Manganelli,[149] F. Marini,[149] A. Perloff,[149] C. Savard,[149] N. Schonbeck,[149] K. Stenson,[149] K. A. Ulmer,[149] S. R. Wagner,[149] N. Zipper,[149] J. Alexander,[150] S. Bright-Thonney,[150] X. Chen,[150] D. J. Cranshaw,[150] J. Fan,[150] X. Fan,[150] D. Gadkari,[150] S. Hogan,[150] J. Monroy,[150] J. R. Patterson,[150] J. Reichert,[150] M. Reid,[150] A. Ryd,[150] J. Thom,[150] P. Wittich,[150] R. Zou,[150] M. Albrow,[151] M. Alyari,[151] O. Amram,[151] G. Apollinari,[151] A. Apresyan,[151] L. A. T. Bauerdick,[151] D. Berry,[151] J. Berryhill,[151] P. C. Bhat,[151] K. Burkett,[151] J. N. Butler,[151] A. Canepa,[151] G. B. Cerati,[151] H. W. K. Cheung,[151] F. Chlebana,[151] G. Cummings,[151] J. Dickinson,[151] I. Dutta,[151] V. D. Elvira,[151] Y. Feng,[151] J. Freeman,[151] A. Gandrakota,[151] Z. Gecse,[151] L. Gray,[151] D. Green,[151] A. Grummer,[151] S. Grünendahl,[151] D. Guerrero,[151] O. Gutsche,[151] R. M. Harris,[151] R. Heller,[151] T. C. Herwig,[151] J. Hirschauer,[151] L. Horyn,[151] B. Jayatilaka,[151] S. Jindariani,[151] M. Johnson,[151] U. Joshi,[151] T. Klijnsma,[151] B. Klima,[151] K. H. M. Kwok,[151] S. Lammel,[151] D. Lincoln,[151] R. Lipton,[151] T. Liu,[151] C. Madrid,[151] K. Maeshima,[151] C. Mantilla,[151] D. Mason,[151] P. McBride,[151] P. Merkel,[151] S. Mrenna,[151] S. Nahn,[151] J. Ngadiuba,[151] D. Noonan,[151] V. Papadimitriou,[151] N. Pastika,[151] K. Pedro,[151] C. Pena,[151,kkkk] F. Ravera,[151] A. Reinsvold Hall,[151,llll] L. Ristori,[151] E. Sexton-Kennedy,[151] N. Smith,[151] A. Soha,[151] L. Spiegel,[151] S. Stoynev,[151] J. Strait,[151] L. Taylor,[151] S. Tkaczyk,[151] N. V. Tran,[151] L. Uplegger,[151] E. W. Vaandering,[151] I. Zoi,[151] C. Aruta,[152] P. Avery,[152] D. Bourilkov,[152] L. Cadamuro,[152] P. Chang,[152] V. Cherepanov,[152] R. D. Field,[152] E. Koenig,[152] M. Kolosova,[152] J. Konigsberg,[152] A. Korytov,[152] K. H. Lo,[152] K. Matchev,[152] N. Menendez,[152] G. Mitselmakher,[152] K. Mohrman,[152] A. Muthirakalayil Madhu,[152] N. Rawal,[152]

D. Rosenzweig,[152] S. Rosenzweig,[152] K. Shi,[152] J. Wang,[152] T. Adams,[153] A. Al Kadhim,[153] A. Askew,[153] N. Bower,[153] R. Habibullah,[153] V. Hagopian,[153] R. Hashmi,[153] R. S. Kim,[153] S. Kim,[153] T. Kolberg,[153] G. Martinez,[153] H. Prosper,[153] P. R. Prova,[153] O. Viazlo,[153] M. Wulansatiti,[153] R. Yohay,[153] J. Zhang,[153] B. Alsufyani,[154] M. M. Baarmand,[154] S. Butalla,[154] T. Elkafrawy,[154,ddd] M. Hohlmann,[154] R. Kumar Verma,[154] M. Rahmani,[154] M. R. Adams,[155] C. Bennett,[155] R. Cavanaugh,[155] S. Dittmer,[155] R. Escobar Franco,[155] O. Evdokimov,[155] C. E. Gerber,[155] D. J. Hofman,[155] J. h. Lee,[155] D. S. Lemos,[155] A. H. Merrit,[155] C. Mills,[155] S. Nanda,[155] G. Oh,[155] B. Ozek,[155] D. Pilipovic,[155] T. Roy,[155] S. Rudrabhatla,[155] M. B. Tonjes,[155] N. Varelas,[155] X. Wang,[155] Z. Ye,[155] J. Yoo,[155] M. Alhusseini,[156] D. Blend,[156] K. Dilsiz,[156,mmmm] L. Emediato,[156] G. Karaman,[156] O. K. Köseyan,[156] J.-P. Merlo,[156] A. Mestvirishvili,[156,nnnn] J. Nachtman,[156] O. Neogi,[156] H. Ogul,[156,oooo] Y. Onel,[156] A. Penzo,[156] C. Snyder,[156] E. Tiras,[156,pppp] B. Blumenfeld,[157] L. Corcodilos,[157] J. Davis,[157] A. V. Gritsan,[157] L. Kang,[157] S. Kyriacou,[157] P. Maksimovic,[157] M. Roguljic,[157] J. Roskes,[157] S. Sekhar,[157] M. Swartz,[157] T. Á. Vámi,[157] A. Abreu,[158] L. F. Alcerro Alcerro,[158] J. Anguiano,[158] P. Baringer,[158] A. Bean,[158] Z. Flowers,[158] D. Grove,[158] J. King,[158] G. Krintiras,[158] M. Lazarovits,[158] C. Le Mahieu,[158] C. Lindsey,[158] J. Marquez,[158] N. Minafra,[158] M. Murray,[158] M. Nickel,[158] M. Pitt,[158] S. Popescu,[158,qqqq] C. Rogan,[158] C. Royon,[158] R. Salvatico,[158] S. Sanders,[158] C. Smith,[158] Q. Wang,[158] G. Wilson,[158] B. Allmond,[159] A. Ivanov,[159] K. Kaadze,[159] A. Kalogeropoulos,[159] D. Kim,[159] Y. Maravin,[159] K. Nam,[159] J. Natoli,[159] D. Roy,[159] G. Sorrentino,[159] F. Rebassoo,[160] D. Wright,[160] A. Baden,[161] A. Belloni,[161] A. Bethani,[161] Y. M. Chen,[161] S. C. Eno,[161] N. J. Hadley,[161] S. Jabeen,[161] R. G. Kellogg,[161] T. Koeth,[161] Y. Lai,[161] S. Lascio,[161] A. C. Mignerey,[161] S. Nabili,[161] C. Palmer,[161] C. Papageorgakis,[161] M. M. Paranjpe,[161] L. Wang,[161] J. Bendavid,[162] W. Busza,[162] I. A. Cali,[162] Y. Chen,[162] M. D'Alfonso,[162] J. Eysermans,[162] C. Freer,[162] G. Gomez-Ceballos,[162] M. Goncharov,[162] P. Harris,[162] D. Hoang,[162] D. Kovalskyi,[162] J. Krupa,[162] L. Lavezzo,[162] Y.-J. Lee,[162] K. Long,[162] C. Mironov,[162] C. Paus,[162] D. Rankin,[162] C. Roland,[162] G. Roland,[162] S. Rothman,[162] Z. Shi,[162] G. S. F. Stephans,[162] J. Wang,[162] Z. Wang,[162] B. Wyslouch,[162] T. J. Yang,[162] B. Crossman,[163] B. M. Joshi,[163] C. Kapsiak,[163] M. Krohn,[163] D. Mahon,[163] J. Mans,[163] B. Marzocchi,[163] S. Pandey,[163] M. Revering,[163] R. Rusack,[163] R. Saradhy,[163] N. Schroeder,[163] N. Strobbe,[163] M. A. Wadud,[163] L. M. Cremaldi,[164] K. Bloom,[165] M. Bryson,[165] D. R. Claes,[165] C. Fangmeier,[165] F. Golf,[165] G. Haza,[165] J. Hossain,[165] C. Joo,[165] I. Kravchenko,[165] I. Reed,[165] J. E. Siado,[165] W. Tabb,[165] A. Vagnerini,[165] A. Wightman,[165] F. Yan,[165] D. Yu,[165] A. G. Zecchinelli,[165] G. Agarwal,[166] H. Bandyopadhyay,[166] L. Hay,[166] I. Iashvili,[166] A. Kharchilava,[166] M. Morris,[166] D. Nguyen,[166] S. Rappoccio,[166] H. Rejeb Sfar,[166] A. Williams,[166] E. Barberis,[167] Y. Haddad,[167] Y. Han,[167] A. Krishna,[167] J. Li,[167] M. Lu,[167] G. Madigan,[167] R. Mccarthy,[167] D. M. Morse,[167] V. Nguyen,[167] T. Orimoto,[167] A. Parker,[167] L. Skinnari,[167] A. Tishelman-Charny,[167] B. Wang,[167] D. Wood,[167] S. Bhattacharya,[168] J. Bueghly,[168] Z. Chen,[168] K. A. Hahn,[168] Y. Liu,[168] Y. Miao,[168] D. G. Monk,[168] M. H. Schmitt,[168] A. Taliercio,[168] M. Velasco,[168] R. Band,[169] R. Bucci,[169] S. Castells,[169] M. Cremonesi,[169] A. Das,[169] R. Goldouzian,[169] M. Hildreth,[169] K. W. Ho,[169] K. Hurtado Anampa,[169] T. Ivanov,[169] C. Jessop,[169] K. Lannon,[169] J. Lawrence,[169] N. Loukas,[169] L. Lutton,[169] J. Mariano,[169] N. Marinelli,[169] I. Mcalister,[169] T. McCauley,[169] C. Mcgrady,[169] C. Moore,[169] Y. Musienko,[169,q] H. Nelson,[169] M. Osherson,[169] A. Piccinelli,[169] R. Ruchti,[169] A. Townsend,[169] Y. Wan,[169] M. Wayne,[169] H. Yockey,[169] M. Zarucki,[169] L. Zygala,[169] A. Basnet,[170] B. Bylsma,[170] M. Carrigan,[170] L. S. Durkin,[170] C. Hill,[170] M. Joyce,[170] A. Lesauvage,[170] M. Nunez Ornelas,[170] K. Wei,[170] B. L. Winer,[170] B. R. Yates,[170] F. M. Addesa,[171] H. Bouchamaoui,[171] P. Das,[171] G. Dezoort,[171] P. Elmer,[171] A. Frankenthal,[171] B. Greenberg,[171] N. Haubrich,[171] S. Higginbotham,[171] G. Kopp,[171] S. Kwan,[171] D. Lange,[171] A. Loeliger,[171] D. Marlow,[171] I. Ojalvo,[171] J. Olsen,[171] A. Shevelev,[171] D. Stickland,[171] C. Tully,[171] S. Malik,[172] A. S. Bakshi,[173] V. E. Barnes,[173] S. Chandra,[173] R. Chawla,[173] S. Das,[173] A. Gu,[173] L. Gutay,[173] M. Jones,[173] A. W. Jung,[173] D. Kondratyev,[173] A. M. Koshy,[173] M. Liu,[173] G. Negro,[173] N. Neumeister,[173] G. Paspalaki,[173] S. Piperov,[173] V. Scheurer,[173] J. F. Schulte,[173] M. Stojanovic,[173] J. Thieman,[173] A. K. Virdi,[173] F. Wang,[173] W. Xie,[173] J. Dolen,[174] N. Parashar,[174] A. Pathak,[174] D. Acosta,[175] A. Baty,[175] T. Carnahan,[175] K. M. Ecklund,[175] P. J. Fernández Manteca,[175] S. Freed,[175] P. Gardner,[175] F. J. M. Geurts,[175] A. Kumar,[175] W. Li,[175] O. Miguel Colin,[175] B. P. Padley,[175] R. Redjimi,[175] J. Rotter,[175] E. Yigitbasi,[175] Y. Zhang,[175] A. Bodek,[176] P. de Barbaro,[176] R. Demina,[176] J. L. Dulemba,[176] C. Fallon,[176] A. Garcia-Bellido,[176] O. Hindrichs,[176]

A. Khukhunaishvili,[176] P. Parygin,[176,q] E. Popova,[176,q] R. Taus,[176] G. P. Van Onsem,[176] K. Goulianos,[177] B. Chiarito,[178] J. P. Chou,[178] Y. Gershtein,[178] E. Halkiadakis,[178] A. Hart,[178] M. Heindl,[178] D. Jaroslawski,[178] O. Karacheban,[178,dd] I. Laflotte,[178] A. Lath,[178] R. Montalvo,[178] K. Nash,[178] H. Routray,[178] S. Salur,[178] S. Schnetzer,[178] S. Somalwar,[178] R. Stone,[178] S. A. Thayil,[178] S. Thomas,[178] J. Vora,[178] H. Wang,[178] H. Acharya,[179] D. Ally,[179] A. G. Delannoy,[179] S. Fiorendi,[179] T. Holmes,[179] N. Karunarathna,[179] L. Lee,[179] E. Nibigira,[179] S. Spanier,[179] D. Aebi,[180] M. Ahmad,[180] O. Bouhali,[180,rrrr] M. Dalchenko,[180] R. Eusebi,[180] J. Gilmore,[180] T. Huang,[180] T. Kamon,[180,ssss] H. Kim,[180] S. Luo,[180] S. Malhotra,[180] R. Mueller,[180] D. Overton,[180] D. Rathjens,[180] A. Safonov,[180] N. Akchurin,[181] J. Damgov,[181] V. Hegde,[181] A. Hussain,[181] Y. Kazhykarim,[181] K. Lamichhane,[181] S. W. Lee,[181] A. Mankel,[181] T. Mengke,[181] S. Muthumuni,[181] T. Peltola,[181] I. Volobouev,[181] A. Whitbeck,[181] E. Appelt,[182] S. Greene,[182] A. Gurrola,[182] W. Johns,[182] R. Kunnawalkam Elayavalli,[182] A. Melo,[182] F. Romeo,[182] P. Sheldon,[182] S. Tuo,[182] J. Velkovska,[182] J. Viinikainen,[182] B. Cardwell,[183] B. Cox,[183] J. Hakala,[183] R. Hirosky,[183] A. Ledovskoy,[183] A. Li,[183] C. Neu,[183] C. E. Perez Lara,[183] P. E. Karchin,[184] A. Aravind,[185] S. Banerjee,[185] K. Black,[185] T. Bose,[185] S. Dasu,[185] I. De Bruyn,[185] P. Everaerts,[185] C. Galloni,[185] H. He,[185] M. Herndon,[185] A. Herve,[185] C. K. Koraka,[185] A. Lanaro,[185] R. Loveless,[185] J. Madhusudanan Sreekala,[185] A. Mallampalli,[185] A. Mohammadi,[185] S. Mondal,[185] G. Parida,[185] D. Pinna,[185] A. Savin,[185] V. Shang,[185] V. Sharma,[185] W. H. Smith,[185] D. Teague,[185] H. F. Tsoi,[185] W. Vetens,[185] A. Warden,[185] S. Afanasiev,[186] V. Andreev,[186] Yu. Andreev,[186] T. Aushev,[186] M. Azarkin,[186] I. Azhgirey,[186] A. Babaev,[186] A. Belyaev,[186] V. Blinov,[186,q] E. Boos,[186] V. Borshch,[186] D. Budkouski,[186] V. Bunichev,[186] M. Chadeeva,[186,q] V. Chekhovsky,[186] M. Danilov,[186,q] A. Dermenev,[186] T. Dimova,[186,q] D. Druzhkin,[186,tttt] M. Dubinin,[186,kkkk] L. Dudko,[186] A. Ershov,[186] G. Gavrilov,[186] V. Gavrilov,[186] S. Gninenko,[186] V. Golovtcov,[186] N. Golubev,[186] I. Golutvin,[186] I. Gorbunov,[186] A. Gribushin,[186] Y. Ivanov,[186] V. Kachanov,[186] L. Kardapoltsev,[186,q] V. Karjavine,[186] A. Karneyeu,[186] V. Kim,[186,q] M. Kirakosyan,[186] D. Kirpichnikov,[186] M. Kirsanov,[186] V. Klyukhin,[186] O. Kodolova,[186,uuuu] D. Konstantinov,[186] V. Korenkov,[186] A. Kozyrev,[186,q] N. Krasnikov,[186] A. Lanev,[186] P. Levchenko,[186,vvvv] N. Lychkovskaya,[186] V. Makarenko,[186] A. Malakhov,[186] V. Matveev,[186,q] V. Murzin,[186] A. Nikitenko,[186,wwww,uuuu] S. Obraztsov,[186] V. Oreshkin,[186] V. Palichik,[186] V. Perelygin,[186] M. Perfilov,[186] S. Petrushanko,[186] S. Polikarpov,[186,q] V. Popov,[186] O. Radchenko,[186,q] R. Ryutin,[186] M. Savina,[186] V. Savrin,[186] V. Shalaev,[186] S. Shmatov,[186] S. Shulha,[186] Y. Skovpen,[186,q] S. Slabospitskii,[186] V. Smirnov,[186] D. Sosnov,[186] V. Sulimov,[186] E. Tcherniaev,[186] A. Terkulov,[186] O. Teryaev,[186] I. Tlisova,[186] A. Toropin,[186] L. Uvarov,[186] A. Uzunian,[186] A. Volkov,[186] A. Vorobyev,[186,a] N. Voytishin,[186] B. S. Yuldashev,[186,xxxx] A. Zarubin,[186] I. Zhizhin,[186] and A. Zhokin[186]

(CMS Collaboration)

[1]*Yerevan Physics Institute, Yerevan, Armenia*
[2]*Institut für Hochenergiephysik, Vienna, Austria*
[3]*Universiteit Antwerpen, Antwerpen, Belgium*
[4]*Vrije Universiteit Brussel, Brussel, Belgium*
[5]*Université Libre de Bruxelles, Bruxelles, Belgium*
[6]*Ghent University, Ghent, Belgium*
[7]*Université Catholique de Louvain, Louvain-la-Neuve, Belgium*
[8]*Centro Brasileiro de Pesquisas Fisicas, Rio de Janeiro, Brazil*
[9]*Universidade do Estado do Rio de Janeiro, Rio de Janeiro, Brazil*
[10]*Universidade Estadual Paulista, Universidade Federal do ABC, São Paulo, Brazil*
[11]*Institute for Nuclear Research and Nuclear Energy, Bulgarian Academy of Sciences, Sofia, Bulgaria*
[12]*University of Sofia, Sofia, Bulgaria*
[13]*Instituto De Alta Investigación, Universidad de Tarapacá, Casilla 7 D, Arica, Chile*
[14]*Beihang University, Beijing, China*
[15]*Department of Physics, Tsinghua University, Beijing, China*
[16]*Institute of High Energy Physics, Beijing, China*
[17]*State Key Laboratory of Nuclear Physics and Technology, Peking University, Beijing, China*
[18]*Sun Yat-Sen University, Guangzhou, China*
[19]*University of Science and Technology of China, Hefei, China*

[20]*Institute of Modern Physics and Key Laboratory of Nuclear Physics and Ion-beam Application (MOE)—Fudan University, Shanghai, China*
[21]*Zhejiang University, Hangzhou, Zhejiang, China*
[22]*Universidad de Los Andes, Bogota, Colombia*
[23]*Universidad de Antioquia, Medellin, Colombia*
[24]*University of Split, Faculty of Electrical Engineering, Mechanical Engineering and Naval Architecture, Split, Croatia*
[25]*University of Split, Faculty of Science, Split, Croatia*
[26]*Institute Rudjer Boskovic, Zagreb, Croatia*
[27]*University of Cyprus, Nicosia, Cyprus*
[28]*Charles University, Prague, Czech Republic*
[29]*Escuela Politecnica Nacional, Quito, Ecuador*
[30]*Universidad San Francisco de Quito, Quito, Ecuador*
[31]*Academy of Scientific Research and Technology of the Arab Republic of Egypt, Egyptian Network of High Energy Physics, Cairo, Egypt*
[32]*Center for High Energy Physics (CHEP-FU), Fayoum University, El-Fayoum, Egypt*
[33]*National Institute of Chemical Physics and Biophysics, Tallinn, Estonia*
[34]*Department of Physics, University of Helsinki, Helsinki, Finland*
[35]*Helsinki Institute of Physics, Helsinki, Finland*
[36]*Lappeenranta-Lahti University of Technology, Lappeenranta, Finland*
[37]*IRFU, CEA, Université Paris-Saclay, Gif-sur-Yvette, France*
[38]*Laboratoire Leprince-Ringuet, CNRS/IN2P3, Ecole Polytechnique, Institut Polytechnique de Paris, Palaiseau, France*
[39]*Université de Strasbourg, CNRS, IPHC UMR 7178, Strasbourg, France*
[40]*Institut de Physique des 2 Infinis de Lyon (IP2I), Villeurbanne, France*
[41]*Georgian Technical University, Tbilisi, Georgia*
[42]*RWTH Aachen University, I. Physikalisches Institut, Aachen, Germany*
[43]*RWTH Aachen University, III. Physikalisches Institut A, Aachen, Germany*
[44]*RWTH Aachen University, III. Physikalisches Institut B, Aachen, Germany*
[45]*Deutsches Elektronen-Synchrotron, Hamburg, Germany*
[46]*University of Hamburg, Hamburg, Germany*
[47]*Karlsruher Institut fuer Technologie, Karlsruhe, Germany*
[48]*Institute of Nuclear and Particle Physics (INPP), NCSR Demokritos, Aghia Paraskevi, Greece*
[49]*National and Kapodistrian University of Athens, Athens, Greece*
[50]*National Technical University of Athens, Athens, Greece*
[51]*University of Ioánnina, Ioánnina, Greece*
[52]*HUN-REN Wigner Research Centre for Physics, Budapest, Hungary*
[53]*MTA-ELTE Lendület CMS Particle and Nuclear Physics Group, Eötvös Loránd University, Budapest, Hungary*
[54]*Faculty of Informatics, University of Debrecen, Debrecen, Hungary*
[55]*Institute of Nuclear Research ATOMKI, Debrecen, Hungary*
[56]*Karoly Robert Campus, MATE Institute of Technology, Gyongyos, Hungary*
[57]*Panjab University, Chandigarh, India*
[58]*University of Delhi, Delhi, India*
[59]*Saha Institute of Nuclear Physics, HBNI, Kolkata, India*
[60]*Indian Institute of Technology Madras, Madras, India*
[61]*Tata Institute of Fundamental Research-A, Mumbai, India*
[62]*Tata Institute of Fundamental Research-B, Mumbai, India*
[63]*National Institute of Science Education and Research, An OCC of Homi Bhabha National Institute, Bhubaneswar, Odisha, India*
[64]*Indian Institute of Science Education and Research (IISER), Pune, India*
[65]*Isfahan University of Technology, Isfahan, Iran*
[66]*Institute for Research in Fundamental Sciences (IPM), Tehran, Iran*
[67]*University College Dublin, Dublin, Ireland*
[68a]*INFN Sezione di Bari, Bari, Italy*
[68b]*Università di Bari, Bari, Italy*
[68c]*Politecnico di Bari, Bari, Italy*
[69a]*INFN Sezione di Bologna, Bologna, Italy*
[69b]*Università di Bologna, Bologna, Italy*
[70a]*INFN Sezione di Catania, Catania, Italy*

[70b]Università di Catania, Catania, Italy
[71a]INFN Sezione di Firenze, Firenze, Italy
[71b]Università di Firenze, Firenze, Italy
[72]INFN Laboratori Nazionali di Frascati, Frascati, Italy
[73a]INFN Sezione di Genova, Genova, Italy
[73b]Università di Genova, Genova, Italy
[74a]INFN Sezione di Milano-Bicocca, Milano, Italy
[74b]Università di Milano-Bicocca, Milano, Italy
[75a]INFN Sezione di Napoli, Napoli, Italy
[75b]Università di Napoli 'Federico II', Napoli, Italy
[75c]Università della Basilicata, Potenza, Italy
[75d]Scuola Superiore Meridionale (SSM), Napoli, Italy
[76a]INFN Sezione di Padova, Padova, Italy
[76b]Università di Padova, Padova, Italy
[76c]Università di Trento, Trento, Italy
[77a]INFN Sezione di Pavia, Pavia, Italy
[77b]Università di Pavia, Pavia, Italy
[78a]INFN Sezione di Perugia, Perugia, Italy
[78b]Università di Perugia, Perugia, Italy
[79a]INFN Sezione di Pisa, Pisa, Italy
[79b]Università di Pisa, Pisa, Italy
[79c]Scuola Normale Superiore di Pisa, Pisa, Italy
[79d]Università di Siena, Siena, Italy
[80a]INFN Sezione di Roma, Roma, Italy
[80b]Sapienza Università di Roma, Roma, Italy
[81a]INFN Sezione di Torino, Torino, Italy
[81b]Università di Torino, Torino, Italy
[81c]Università del Piemonte Orientale, Novara, Italy
[82a]INFN Sezione di Trieste, Trieste, Italy
[82b]Università di Trieste, Trieste, Italy
[83]Kyungpook National University, Daegu, Korea
[84]Department of Mathematics and Physics—GWNU, Gangneung, Korea
[85]Chonnam National University, Institute for Universe and Elementary Particles, Kwangju, Korea
[86]Hanyang University, Seoul, Korea
[87]Korea University, Seoul, Korea
[88]Kyung Hee University, Department of Physics, Seoul, Korea
[89]Sejong University, Seoul, Korea
[90]Seoul National University, Seoul, Korea
[91]University of Seoul, Seoul, Korea
[92]Yonsei University, Department of Physics, Seoul, Korea
[93]Sungkyunkwan University, Suwon, Korea
[94]College of Engineering and Technology, American University of the Middle East (AUM), Dasman, Kuwait
[95]Riga Technical University, Riga, Latvia
[96]University of Latvia (LU), Riga, Latvia
[97]Vilnius University, Vilnius, Lithuania
[98]National Centre for Particle Physics, Universiti Malaya, Kuala Lumpur, Malaysia
[99]Universidad de Sonora (UNISON), Hermosillo, Mexico
[100]Centro de Investigacion y de Estudios Avanzados del IPN, Mexico City, Mexico
[101]Universidad Iberoamericana, Mexico City, Mexico
[102]Benemerita Universidad Autonoma de Puebla, Puebla, Mexico
[103]University of Montenegro, Podgorica, Montenegro
[104]University of Canterbury, Christchurch, New Zealand
[105]National Centre for Physics, Quaid-I-Azam University, Islamabad, Pakistan
[106]AGH University of Krakow, Faculty of Computer Science, Electronics and Telecommunications, Krakow, Poland
[107]National Centre for Nuclear Research, Swierk, Poland
[108]Institute of Experimental Physics, Faculty of Physics, University of Warsaw, Warsaw, Poland
[109]Warsaw University of Technology, Warsaw, Poland
[110]Laboratório de Instrumentação e Física Experimental de Partículas, Lisboa, Portugal

[111]*Faculty of Physics, University of Belgrade, Belgrade, Serbia*
[112]*VINCA Institute of Nuclear Sciences, University of Belgrade, Belgrade, Serbia*
[113]*Centro de Investigaciones Energéticas Medioambientales y Tecnológicas (CIEMAT), Madrid, Spain*
[114]*Universidad Autónoma de Madrid, Madrid, Spain*
[115]*Universidad de Oviedo, Instituto Universitario de Ciencias y Tecnologías Espaciales de Asturias (ICTEA), Oviedo, Spain*
[116]*Instituto de Física de Cantabria (IFCA), CSIC-Universidad de Cantabria, Santander, Spain*
[117]*University of Colombo, Colombo, Sri Lanka*
[118]*University of Ruhuna, Department of Physics, Matara, Sri Lanka*
[119]*CERN, European Organization for Nuclear Research, Geneva, Switzerland*
[120]*Paul Scherrer Institut, Villigen, Switzerland*
[121]*ETH Zurich—Institute for Particle Physics and Astrophysics (IPA), Zurich, Switzerland*
[122]*Universität Zürich, Zurich, Switzerland*
[123]*National Central University, Chung-Li, Taiwan*
[124]*National Taiwan University (NTU), Taipei, Taiwan*
[125]*High Energy Physics Research Unit, Department of Physics, Faculty of Science, Chulalongkorn University, Bangkok, Thailand*
[126]*Çukurova University, Physics Department, Science and Art Faculty, Adana, Turkey*
[127]*Middle East Technical University, Physics Department, Ankara, Turkey*
[128]*Bogazici University, Istanbul, Turkey*
[129]*Istanbul Technical University, Istanbul, Turkey*
[130]*Istanbul University, Istanbul, Turkey*
[131]*Institute for Scintillation Materials of National Academy of Science of Ukraine, Kharkiv, Ukraine*
[132]*National Science Centre, Kharkiv Institute of Physics and Technology, Kharkiv, Ukraine*
[133]*University of Bristol, Bristol, United Kingdom*
[134]*Rutherford Appleton Laboratory, Didcot, United Kingdom*
[135]*Imperial College, London, United Kingdom*
[136]*Brunel University, Uxbridge, United Kingdom*
[137]*Baylor University, Waco, Texas, USA*
[138]*Catholic University of America, Washington, DC, USA*
[139]*The University of Alabama, Tuscaloosa, Alabama, USA*
[140]*Boston University, Boston, Massachusetts, USA*
[141]*Brown University, Providence, Rhode Island, USA*
[142]*University of California, Davis, Davis, California, USA*
[143]*University of California, Los Angeles, California, USA*
[144]*University of California, Riverside, Riverside, California, USA*
[145]*University of California, San Diego, La Jolla, California, USA*
[146]*University of California, Santa Barbara—Department of Physics, Santa Barbara, California, USA*
[147]*California Institute of Technology, Pasadena, California, USA*
[148]*Carnegie Mellon University, Pittsburgh, Pennsylvania, USA*
[149]*University of Colorado Boulder, Boulder, Colorado, USA*
[150]*Cornell University, Ithaca, New York, USA*
[151]*Fermi National Accelerator Laboratory, Batavia, Illinois, USA*
[152]*University of Florida, Gainesville, Florida, USA*
[153]*Florida State University, Tallahassee, Florida, USA*
[154]*Florida Institute of Technology, Melbourne, Florida, USA*
[155]*University of Illinois Chicago, Chicago, USA, Chicago, USA*
[156]*The University of Iowa, Iowa City, Iowa, USA*
[157]*Johns Hopkins University, Baltimore, Maryland, USA*
[158]*The University of Kansas, Lawrence, Kansas, USA*
[159]*Kansas State University, Manhattan, Kansas, USA*
[160]*Lawrence Livermore National Laboratory, Livermore, California, USA*
[161]*University of Maryland, College Park, Maryland, USA*
[162]*Massachusetts Institute of Technology, Cambridge, Massachusetts, USA*
[163]*University of Minnesota, Minneapolis, Minnesota, USA*
[164]*University of Mississippi, Oxford, Mississippi, USA*
[165]*University of Nebraska-Lincoln, Lincoln, Nebraska, USA*
[166]*State University of New York at Buffalo, Buffalo, New York, USA*
[167]*Northeastern University, Boston, Massachusetts, USA*
[168]*Northwestern University, Evanston, Illinois, USA*

[169]*University of Notre Dame, Notre Dame, Indiana, USA*
[170]*The Ohio State University, Columbus, Ohio, USA*
[171]*Princeton University, Princeton, New Jersey, USA*
[172]*University of Puerto Rico, Mayaguez, Puerto Rico, USA*
[173]*Purdue University, West Lafayette, Indiana, USA*
[174]*Purdue University Northwest, Hammond, Indiana, USA*
[175]*Rice University, Houston, Texas, USA*
[176]*University of Rochester, Rochester, New York, USA*
[177]*The Rockefeller University, New York, New York, USA*
[178]*Rutgers, The State University of New Jersey, Piscataway, New Jersey, USA*
[179]*University of Tennessee, Knoxville, Tennessee, USA*
[180]*Texas A&M University, College Station, Texas, USA*
[181]*Texas Tech University, Lubbock, Texas, USA*
[182]*Vanderbilt University, Nashville, Tennessee, USA*
[183]*University of Virginia, Charlottesville, Virginia, USA*
[184]*Wayne State University, Detroit, Michigan, USA*
[185]*University of Wisconsin—Madison, Madison, Wisconsin, USA*
[186]*An institute or international laboratory covered by a cooperation agreement with CERN*

[a]Deceased.
[b]Also at Yerevan State University, Yerevan, Armenia.
[c]Also at TU Wien, Vienna, Austria.
[d]Also at Institute of Basic and Applied Sciences, Faculty of Engineering, Arab Academy for Science, Technology and Maritime Transport, Alexandria, Egypt.
[e]Also at Ghent University, Ghent, Belgium.
[f]Also at Universidade Estadual de Campinas, Campinas, Brazil.
[g]Also at Federal University of Rio Grande do Sul, Porto Alegre, Brazil.
[h]Also at UFMS, Nova Andradina, Brazil.
[i]Also at Nanjing Normal University, Nanjing, China.
[j]Also at Henan Normal University, Xinxiang, China.
[k]Also at The University of Iowa, Iowa City, Iowa, USA.
[l]Also at University of Chinese Academy of Sciences, Beijing, China.
[m]Also at China Center of Advanced Science and Technology, Beijing, China.
[n]Also at University of Chinese Academy of Sciences, Beijing, China.
[o]Also at China Spallation Neutron Source, Guangdong, China.
[p]Also at Université Libre de Bruxelles, Bruxelles, Belgium.
[q]Also at Another institute or international laboratory covered by a cooperation agreement with CERN.
[r]Also at British University in Egypt, Cairo, Egypt.
[s]Also at Cairo University, Cairo, Egypt.
[t]Also at Birla Institute of Technology, Mesra, Mesra, India.
[u]Also at Purdue University, West Lafayette, Indiana, USA.
[v]Also at Université de Haute Alsace, Mulhouse, France.
[w]Also at Department of Physics, Tsinghua University, Beijing, China.
[x]Also at The University of the State of Amazonas, Manaus, Brazil.
[y]Also at Erzincan Binali Yildirim University, Erzincan, Turkey.
[z]Also at University of Hamburg, Hamburg, Germany.
[aa]Also at RWTH Aachen University, III. Physikalisches Institut A, Aachen, Germany.
[bb]Also at Isfahan University of Technology, Isfahan, Iran.
[cc]Also at Bergische University Wuppertal (BUW), Wuppertal, Germany.
[dd]Also at Brandenburg University of Technology, Cottbus, Germany.
[ee]Also at Forschungszentrum Jülich, Juelich, Germany.
[ff]Also at CERN, European Organization for Nuclear Research, Geneva, Switzerland.
[gg]Also at Institute of Physics, University of Debrecen, Debrecen, Hungary.
[hh]Also at Institute of Nuclear Research ATOMKI, Debrecen, Hungary.
[ii]Also at Universitatea Babes-Bolyai—Facultatea de Fizica, Cluj-Napoca, Romania.
[jj]Also at Physics Department, Faculty of Science, Assiut University, Assiut, Egypt.
[kk]Also at HUN-REN Wigner Research Centre for Physics, Budapest, Hungary.
[ll]Also at Faculty of Informatics, University of Debrecen, Debrecen, Hungary.

[mm]Also at Punjab Agricultural University, Ludhiana, India.
[nn]Also at University of Hyderabad, Hyderabad, India.
[oo]Also at University of Visva-Bharati, Santiniketan, India.
[pp]Also at Indian Institute of Science (IISc), Bangalore, India.
[qq]Also at IIT Bhubaneswar, Bhubaneswar, India.
[rr]Also at Institute of Physics, Bhubaneswar, India.
[ss]Also at Deutsches Elektronen-Synchrotron, Hamburg, Germany.
[tt]Also at Department of Physics, Isfahan University of Technology, Isfahan, Iran.
[uu]Also at Sharif University of Technology, Tehran, Iran.
[vv]Also at Department of Physics, University of Science and Technology of Mazandaran, Behshahr, Iran.
[ww]Also at Helwan University, Cairo, Egypt.
[xx]Also at Italian National Agency for New Technologies, Energy and Sustainable Economic Development, Bologna, Italy.
[yy]Also at Centro Siciliano di Fisica Nucleare e di Struttura Della Materia, Catania, Italy.
[zz]Also at Università degli Studi Guglielmo Marconi, Roma, Italy.
[aaa]Also at Scuola Superiore Meridionale, Università di Napoli 'Federico II', Napoli, Italy.
[bbb]Also at Fermi National Accelerator Laboratory, Batavia, Illinois, USA.
[ccc]Also at Università di Napoli 'Federico II', Napoli, Italy.
[ddd]Also at Ain Shams University, Cairo, Egypt.
[eee]Also at Consiglio Nazionale delle Ricerche—Istituto Officina dei Materiali, Perugia, Italy.
[fff]Also at Riga Technical University, Riga, Latvia.
[ggg]Also at Department of Applied Physics, Faculty of Science and Technology, Universiti Kebangsaan Malaysia, Bangi, Malaysia.
[hhh]Also at Consejo Nacional de Ciencia y Tecnología, Mexico City, Mexico.
[iii]Also at Trincomalee Campus, Eastern University, Sri Lanka, Nilaveli, Sri Lanka.
[jjj]Also at INFN Sezione di Pavia, Università di Pavia, Pavia, Italy.
[kkk]Also at National and Kapodistrian University of Athens, Athens, Greece.
[lll]Also at Ecole Polytechnique Fédérale Lausanne, Lausanne, Switzerland.
[mmm]Also at University of Vienna Faculty of Computer Science, Vienna, Austria.
[nnn]Also at Universität Zürich, Zurich, Switzerland.
[ooo]Also at Stefan Meyer Institute for Subatomic Physics, Vienna, Austria.
[ppp]Also at Laboratoire d'Annecy-le-Vieux de Physique des Particules, IN2P3-CNRS, Annecy-le-Vieux, France.
[qqq]Also at Near East University, Research Center of Experimental Health Science, Mersin, Turkey.
[rrr]Also at Konya Technical University, Konya, Turkey.
[sss]Also at Izmir Bakircay University, Izmir, Turkey.
[ttt]Also at Adiyaman University, Adiyaman, Turkey.
[uuu]Also at Bozok Universitetesi Rektörlügü, Yozgat, Turkey.
[vvv]Also at Marmara University, Istanbul, Turkey.
[www]Also at Milli Savunma University, Istanbul, Turkey.
[xxx]Also at Kafkas University, Kars, Turkey.
[yyy]Also at stanbul Okan University, Istanbul, Turkey.
[zzz]Also at Hacettepe University, Ankara, Turkey.
[aaaa]Also at Istanbul University—Cerrahpasa, Faculty of Engineering, Istanbul, Turkey.
[bbbb]Also at Yildiz Technical University, Istanbul, Turkey.
[cccc]Also at Vrije Universiteit Brussel, Brussel, Belgium.
[dddd]Also at School of Physics and Astronomy, University of Southampton, Southampton, United Kingdom.
[eeee]Also at University of Bristol, Bristol, United Kingdom.
[ffff]Also at IPPP Durham University, Durham, United Kingdom.
[gggg]Also at Monash University, Faculty of Science, Clayton, Australia.
[hhhh]Also at Università di Torino, Torino, Italy.
[iiii]Also at Bethel University, St. Paul, Minnesota, USA.
[jjjj]Also at Karamanoğlu Mehmetbey University, Karaman, Turkey.
[kkkk]Also at California Institute of Technology, Pasadena, California, USA.
[llll]Also at United States Naval Academy, Annapolis, Maryland, USA.
[mmmm]Also at Bingol University, Bingol, Turkey.
[nnnn]Also at Georgian Technical University, Tbilisi, Georgia.
[oooo]Also at Sinop University, Sinop, Turkey.
[pppp]Also at Erciyes University, Kayseri, Turkey.
[qqqq]Also at Horia Hulubei National Institute of Physics and Nuclear Engineering (IFIN-HH), Bucharest, Romania.
[rrrr]Also at Texas A&M University at Qatar, Doha, Qatar.

[ssss]Also at Kyungpook National University, Daegu, Korea.
[tttt]Also at Universiteit Antwerpen, Antwerpen, Belgium.
[uuuu]Also at Yerevan Physics Institute, Yerevan, Armenia.
[vvvv]Also at Northeastern University, Boston, Massachusetts, USA.
[wwww]Also at Imperial College, London, United Kingdom.
[xxxx]Also at Institute of Nuclear Physics of the Uzbekistan Academy of Sciences, Tashkent, Uzbekistan.